



**HAL**  
open science

## Synthesis of glycopolymer architectures by reversible-deactivation radical polymerization

A. Ghabdan, L. Albertin

► **To cite this version:**

A. Ghabdan, L. Albertin. Synthesis of glycopolymer architectures by reversible-deactivation radical polymerization. *Polymers*, 2013, pp.431-526. hal-00825417

**HAL Id: hal-00825417**

**<https://hal.science/hal-00825417>**

Submitted on 23 May 2013

**HAL** is a multi-disciplinary open access archive for the deposit and dissemination of scientific research documents, whether they are published or not. The documents may come from teaching and research institutions in France or abroad, or from public or private research centers.

L'archive ouverte pluridisciplinaire **HAL**, est destinée au dépôt et à la diffusion de documents scientifiques de niveau recherche, publiés ou non, émanant des établissements d'enseignement et de recherche français ou étrangers, des laboratoires publics ou privés.

*Review*

## Synthesis of Glycopolymer Architectures by Reversible-Deactivation Radical Polymerization

Ali Ghadban <sup>1,\*</sup> and Luca Albertin <sup>2,\*</sup><sup>1</sup> Ingénierie des Matériaux Polymères, INSA Lyon, Villeurbanne F-69621, France<sup>2</sup> Centre de Recherches sur les Macromolécules Végétales (CERMAV-CNRS) <sup>†</sup>, BP53, Grenoble cedex 9 38041, France

\* Authors to whom correspondence should be addressed; E-Mails: ghadban.ali@hotmail.com (A.G.); luca.albertin@cermav.cnrs.fr (L.A.); Tel.: +33-4-7603-7660 (L.A.); Fax: +33-4-7654-7203 (L.A.).

<sup>†</sup> Affiliated with Université Joseph Fourier, and member of the Institut de Chimie Moléculaire de Grenoble.

*Received: 22 March 2013; in revised form: 1 May 2013 / Accepted: 3 May 2013 /*

*Published: 21 May 2013*

---

**Abstract:** This review summarizes the state of the art in the synthesis of well-defined glycopolymers by Reversible-Deactivation Radical Polymerization (RDRP) from its inception in 1998 until August 2012. Glycopolymers architectures have been successfully synthesized with four major RDRP techniques: Nitroxide-mediated radical polymerization (NMP), cyanoxyl-mediated radical polymerization (CMRP), atom transfer radical polymerization (ATRP) and reversible addition-fragmentation chain transfer (RAFT) polymerization. Over 140 publications were analyzed and their results summarized according to the technique used and the type of monomer(s) and carbohydrates involved. Particular emphasis was placed on the experimental conditions used, the structure obtained (comonomer distribution, topology), the degree of control achieved and the (potential) applications sought. A list of representative examples for each polymerization process can be found in tables placed at the beginning of each section covering a particular RDRP technique.

**Keywords:** carbohydrate; glycomonomer; glycopolymer; RDRP; NMP; CMRP; ATRP; RAFT

## Symbols and Abbreviations

A $\beta$ peptide	amyloid $\beta$ peptide
AFM	atomic force microscopy
AGET	activator generated by electron transfer
<b>Ai</b>	<b>initiator “i” used in ATRP</b>
AIBN	2,2'-azobis-isobutyronitrile
ATRP	atom transfer radical polymerization
BIEM	2-(2-bromoisobutyryloxy)ethyl methacrylate
BSA	bovine serum albumin
cac	critical association concentration
CD	circular dichroism
CMC	critical micelle concentration
CMPSF	chloromethylated polysulfone
COD	1,5-cyclooctadiene
ConA	Concanavalin A
Conv	conversion
Cp	cyclopentadiene
CTA	chain transfer agent
Ctx	cholera toxin
DCM	dichloromethane
<i>D</i>	molar mass dispersity index
<i>D<sub>a</sub></i>	particle diameter dispersity index
DCP	dicumyl peroxide
DLS	dynamic light scattering
DMAc	dimethyl acetamide
DMF	dimethylformamide
DMPA	2,2-dimethoxy-2-phenylacetophenone
DMSO	dimethyl sulfoxide
DNA	deoxyribonucleic acid
<i>DP</i>	degree of polymerization
DTT	1,4-dithiothreitol
ECA	<i>Erythrina cristagalli</i> agglutinin
EDC	1-ethyl-3-(3-dimethylaminopropyl-carbodiimide)
EWCRDS	evanescent wave cavity ring-down spectroscopy
Fb	Fibrinogen
FCS	fluorescence correlation spectroscopy
FGF	Fibroblast growth factor
FimH	fimbrial lectin
FRET	Förster resonance energy transfer
FTIR	Fourier transform infrared
Gal	galactose

Glc	glucose
GlcNAc	<i>N</i> -acetyl-D-glucosamine
GNP(s)	gold nanoparticle(s)
HDA	hetero-Diels Alder
HEMA	2-hydroxyethyl methacrylate
HIV	human immunodeficiency virus
HOBT	1-hydroxybenzotriazole
homo	homopolymer
HPA	<i>Helix pomatia</i> agglutinin
IC <sub>50</sub>	the half maximal inhibitory concentration, <i>i.e.</i> , the concentration of a particular substance (inhibitor) needed to inhibit a given biological process by half
Lac	lactose
LBL	layer by layer
LCST	lower critical solution temperature
<b>Li</b>	<b>ligand “i” used in ATRP catalyst</b>
<b>MA</b>	methyl acrylate
MALDI-ToF	matrix-assisted laser desorption ionization-time of flight
Man	mannose
<b>MA<sub>nh</sub></b>	maleic anhydride
MHS	Mark-Houwink-Sakurada
<b>Mi</b>	<b>monomer “i”</b>
<b>MMA</b>	methyl methacrylate
$M_n$	number average molar mass
$M_{n,th}$	theoretical number average molar mass
MS	mass spectroscopy
$M_w$	weight average molar mass
MWNT	multiwalled carbon nanotube
NHS	<i>N</i> -hydroxysuccinimide
<b>Ni</b>	<b>initiator/control agent “i” used in NMP</b>
<b>NIPAA<sub>m</sub></b>	<i>N</i> -isopropylacrylamide
NMP	nitroxide mediated polymerization
NMR	nuclear magnetic resonance
<i>p</i>	monomer conversion
PDVB	poly(divinylbenzene)
PEG	polyethylene glycol
PEO	polyethylene oxide
PET	poly(ethyleneterephthalate)
PMMA	poly(methylmethacrylate)
poly <b>Mi</b>	poly( <b>monomer i</b> )
poly <b>Mi-Ni(Ri)</b>	macro-initiator/macro-control agent poly( <b>monomer i</b> ) obtained from the polymerization of <b>monomer “i”</b> with initiator <b>Ni</b> or RAFT agent <b>Ri</b>
PNA	peanut agglutinin

PSF	polysulfone
p-TsCl	p-toluenesulfonyl chloride (Tosyl chloride)
PVDF	poly(vinylidene difluoride)
QCM	quartz crystal microbalance
QD	quatum dots
RAFT	reversible addition-fragmentation chain transfer
RAFTstab	reversible addition-fragmentation chain transfer colloidal stabilizer
RCA	<i>Ricinus communis</i> agglutinin
RDRP	reversible deactivation radical polymerization
<b>Ri</b>	<b>chain transfer agent “i” used in RAFT polymerization</b>
RNA	ribonucleic acid
ROMP	ring Opening Metathesis Polymerization
ROP	ring Opening Polymerization
RT	room temperature
SBA	soybean agglutinin
SCVCP	self-condensing vinyl copolymerization
SEC	size exclusion chromatography
SEM	scanning Electron Microscopy
SG1	<i>N</i> -tert-butyl- <i>N</i> -(1-diethylphosphono-2,2-dimethylpropyl)
siRNA	small interfering RNA
SLS	static light scattering
SPR	surface plasmon resonance
<b>Sty</b>	styrene
TBAF	tetra- <i>n</i> -butylammonium fluoride
TEM	transmission electron microscopy
TEMPO	2,2,6,6-tetramethylpiperidine-1-oxyl
TFA	trifluoroacetic acid
THF	tetrahydrofuran
ThT	thioflavin T
TIPNO	2,2,5-trimethyl-4-phenyl-3-azahexane-3-oxyl
TsCl	<i>p</i> -toluenesulfonyl chloride
VVA	<i>Vicia villosa</i> agglutinin
WFL	<i>Wisteria floribunda</i> lectin
WGA	wheat germ agglutinin

## 1. Introduction

Glycopolymers are synthetic polymers possessing a non-carbohydrate main chain but featuring pendant and/or terminal carbohydrate moieties. Since the pioneering work of Horejsi *et al.* [1], on the precipitation of lectins glycopolymers have raised an ever-increasing interest as artificial materials for

a number of biological and biomedical uses. This is due to the expectation that polymers displaying carbohydrate functionalities, similar to those of natural glycoconjugates, might be able to mimic, or even exceed, their performance in specific applications (biomimetic approach). More in general, studies have been published on their use of as macromolecular drugs [2–8], drug delivery systems [9–12], cell culture substrates [13,14], stationary phase in separation problems [15,16] and bioassays [17]; responsive [18] and catalytic [19] hydrogels, surface modifiers [20–23], artificial tissues and artificial organ substrates [13].

The making of a living cell in nature requires four major classes of molecules: nucleic acids, proteins, lipids and carbohydrates. Researchers in molecular biology have historically devoted much greater attention to nucleic acids and proteins than to lipids and carbohydrates, mostly due to the powerful paradigm that biological information flows from DNA to RNA to proteins via template-based transcription and translation processes. Nonetheless, it is now understood that lipids and carbohydrates are essential for the relatively small number of genes in a typical genome to generate the enormous biological complexity of a living organism [24]. Carbohydrates in particular are present in all cells and in numerous biological macromolecules, where they usually decorate the outer surface. Thus, they are ideally situated to mediate or modulate a variety of cell-cell, cell-matrix and cell-molecule interactions which are critical to the development and function of a complex multicellular organism. Moreover, they can mediate the interaction between different organisms, such as that between a host and a parasite or symbiont [24]. A well-known example of this kind is the attachment of the human influenza virus to the surface of host cells, which is mediated by 5-*N*-acetylneuraminic acid residues on the cell surface and by hemagglutinin trimers on the virus surface [25].

Many of the interactions mediated by carbohydrates involve their specific recognition by Glycan Binding Proteins (GBP), which are broadly classified into lectins and glycosaminoglycan-binding proteins. Lectins are proteins capable to bind the outer end of carbohydrates with high stereospecificity but without catalyzing their modification. Although the affinity of a single carbohydrate-recognition domain (CRD) for its natural ligand is often low (with dissociation constants  $K_d$  in the micro- to millimolar range), high avidity is achieved via multivalent interactions between multiple CRDs and multiple carbohydrate residues. To this end, multiple CRDs are either present within the lectin structure (e.g., the hemagglutinin trimer) [26] or are the result of multiple lectins clustered together (e.g., selectins). In both cases, the predominantly multivalent nature of lectin-ligand recognition processes is a big incentive to the design of glycosylated structures displaying multiple copies of the recognition elements: Hence the interest for the synthesis of well-defined glycopolymer architectures [27].

Besides their signaling and recognition activity, carbohydrates of higher molar mass (polysaccharides) play fundamental structural roles in living organisms thanks to their unique physical properties (chain rigidity, self-assembling capabilities, solvation and complexation properties) [28,29]. For this reason, a number of studies have been published in which natural oligosaccharides are incorporated into glycopolymers to take advantage of their physical properties. For instance, amphiphilic glycopolymers can inducing phase separation in a selective solvent [30–34] or in a film [35], and can stabilize an emulsion or latex [36]. Recently, oligo (1→4)- $\alpha$ -L-guluronan extracted from alginate was incorporated into a biohybrid glycopolymer to bestow it with ionotropic gelation properties in the presence of  $\text{Ca}^{2+}$  ions [37].

The presence of an appropriate carbohydrate in a glycolpolymer is *per se* insufficient to bestow it with the biological and physicochemical properties required by a given application, and control of the macromolecular architecture has proven essential to enable sophisticated functions [4,38,39] and to allow a precise correlation between these functions and the polymer structure. For this reason, over the past twenty years a trend has emerged in which more and more polymer chemists got involved in the synthesis of novel glycopolymers via both traditional and precise polymerization techniques, while a greater number of biochemists and carbohydrate chemists have adopted the techniques of polymer synthesis for designing tailored glycoligands.

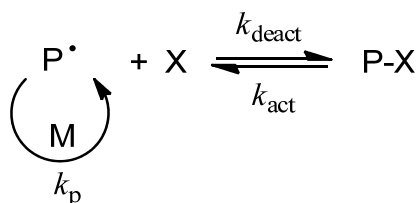
## 2. Glycopolymers and Reversible-Deactivation Radical Polymerization

Beginning in the 1990s and with the advent of Reversible-deactivation Radical Polymerization (RDRP) techniques [40–42], a wealth of new possibilities has been disclosed to those pursuing the synthesis of well-defined glycopolymers and complex glycopolymer architectures. RDRPs are extremely versatile techniques combining the characteristics of a “living” process (*i.e.*, homogeneous macromolecules, predetermined molar masses, dormant chain ends) with the simplicity and robustness of radical polymerization [43]. Above all, RDRPs can be effective under conditions that are important for glycopolymers’ synthesis: In homogeneous aqueous media [44], at ambient temperature [45–47], and with monomers carrying complex functional groups [48–52].

A detailed description of specific RDRP techniques is beyond the scope of this review, and the interested reader can refer to more specialized texts [43,48–51,53]. Here we will simply recall the fundamentals of all RDRP processes. According to IUPAC, a reversible-deactivation radical polymerization is a chain polymerization propagated by radicals that are deactivated reversibly, bringing them into active-dormant equilibria of which there might be more than one [54]. Hence, RDRP processes are distinguished from conventional radical polymerization in that they involve some form of *reversible deactivation (or activation) reaction* [55]. As shown in Scheme 1, the end-capped “dormant” chain P–X is in equilibrium with the polymeric chain carrier P<sup>•</sup>, which undergoes propagation in the presence of monomer until it is deactivated back to its dormant form. The rate constants of activation ( $k_{\text{act}}$ ) and deactivation ( $k_{\text{deact}}$ ) are both defined as pseudo-first order constants, having the unit  $\text{s}^{-1}$ . In this scheme, every dormant chain is activated every  $k_{\text{act}}^{-1}$  seconds (typically  $10\text{--}10^3$ ) and deactivated back to the dormant state after a “transient” lifetime ( $\tau$ ) of  $k_{\text{deact}}^{-1}$  seconds (typically 0.1–10 ms). For the quasi-equilibrium

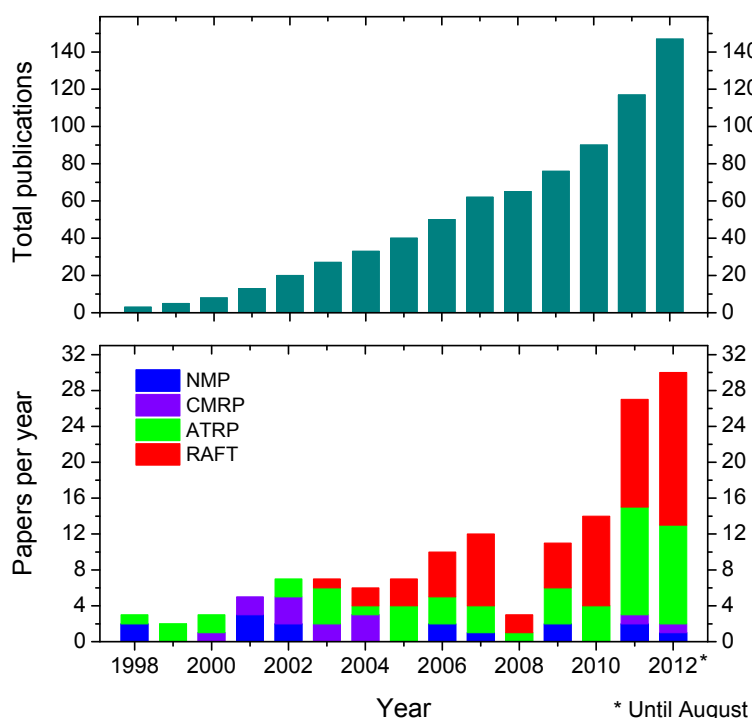
$$k_{\text{deact}} [\text{P}] = k_{\text{act}} [\text{P-X}]$$

to hold, the concentration of chain carriers must be around  $10^{-2}\text{--}10^{-4}$  that of the dormant chains. As a result, the total number of chains will be practically identical to the number of dormant chains. In general, after each activation-deactivation cycle the chain length of P–X will have increased, and if the frequency of these cycles is high compared to the polymerization time, every chain will nearly have an equal chance to grow, resulting in a linear increase of molar mass with conversion. Moreover, if the equilibrium is established at low monomer conversion and only a small amount of chain-terminating reactions take place, uniform polymers will be obtained and the dispersity index will decrease with conversion [56].

**Scheme 1.** Reversible deactivation mechanism.

A number of review articles have already been published on the synthesis and application of glycopolymers at large [22,57–68] and the interested reader can refer to them for a broader perspective. Here we report an exhaustive compilation (up to August 2012) of the glycopolymers prepared by reversible-deactivation radical polymerization, with particular emphasis on the experimental conditions used, the structure obtained (comonomer distribution, topology), the degree of control achieved and the (potential) applications sought.

**Scheme 2.** Number of publications per year (bottom) and total number of publications (top) on the synthesis of glycopolymers by nitroxide mediated polymerization (NMP), cyanoxyl-mediated radical polymerization (CMRP), atom transfer radical polymerization (ATRP), and reversible addition-fragmentation chain transfer (RAFT) polymerization in the period from 1998 (first report appeared) to August 2012 (end of our survey).



Although the number of successful RDRP techniques has steadily increased throughout the years and now includes Nitroxide Mediated Polymerization (NMP) [52], Cyanoxyl-Mediated Radical Polymerization (CMRP) [69–71], Atom Transfer Radical Polymerization (ATRP) [51], Reversible Addition-Fragmentation chain Transfer (RAFT) polymerization [48–50], Iodine-Transfer Polymerization (ITP) [72], Telluride-Mediated Polymerization (TERP) [73], Stibine-Mediated Polymerization [73] and Reversible Chain Transfer Catalyzed Living Radical Polymerization (RTCP) [74], only NMP,



CMRP, ATRP and RAFT have been applied to glycopolymers' synthesis. As shown in Scheme 2, in the period 1998–2004 the number of publications on the subject did not exceed 5 per year. From 2005 onward that number increased steadily though, and 29 reports were published in the first 8 months of 2012 alone. Also, whereas NMP was well represented up to 2002, it has been later outnumbered by studies using ATRP or RAFT, which now account for ~90% of the articles on the subject.

### 3. How to Consult the Review

The review is divided in three sections, each detailing the results obtained by Stable Free Radical polymerization (*i.e.*, NMP and CMRP), ATRP or RAFT. To facilitate consultation, the structure of all (glycol)monomers cited is shown in Scheme 3 and a list of representative examples for each polymerization process can be found in a table at the beginning of each section. Entries to these tables are listed in ascending alphabetical order of (i) the monomer type (e.g., styrenic) and (ii) the carbohydrate residue (e.g., lactose). Concerning the later, the anomeric configuration ( $\alpha$  or  $\beta$ ), the position of connection to the rest of the polymer, the nature of the heteroatom involved as well as any further functionalization (e.g., sulfation) of the carbohydrate(s) featured by a glycopolymer are specified in parenthesis. When protected carbohydrates were used for polymer synthesis, this information refers to the glycopolymer after deprotection. Unless otherwise stated, each carbohydrate should be assumed to have its most common configuration (e.g., D or L) and ring size (e.g., pyranose). For instance, “glucose ( $\beta$ -N)” indicates a  $\beta$ -D-glucopyranosylamine linked to the polymer via the nitrogen atom and “N-acetylglucosamine (6-sulfo,  $\beta$ -O)” indicates 2-acetylamino-2-deoxy-6-O-sulfo- $\beta$ -D-glucopyranoside linked to the polymer via the anomeric oxygen.

Also, the formula of ATRP catalysts is reported as “MX(Li)”, where M is the metal, X is a halide and Li is “ligand i” (see Section 4.3). This formula simply indicates the metal halide and ligand used for polymerization and does not imply a specific stoichiometry or structure for the resulting complex [75].

### 4. Synthesis of Glycopolymers by Stable Free Radical Polymerization (SFRP)

The structures of the initiators/control agents used for the synthesis of glycopolymers by SFRP are reported in Scheme 4.

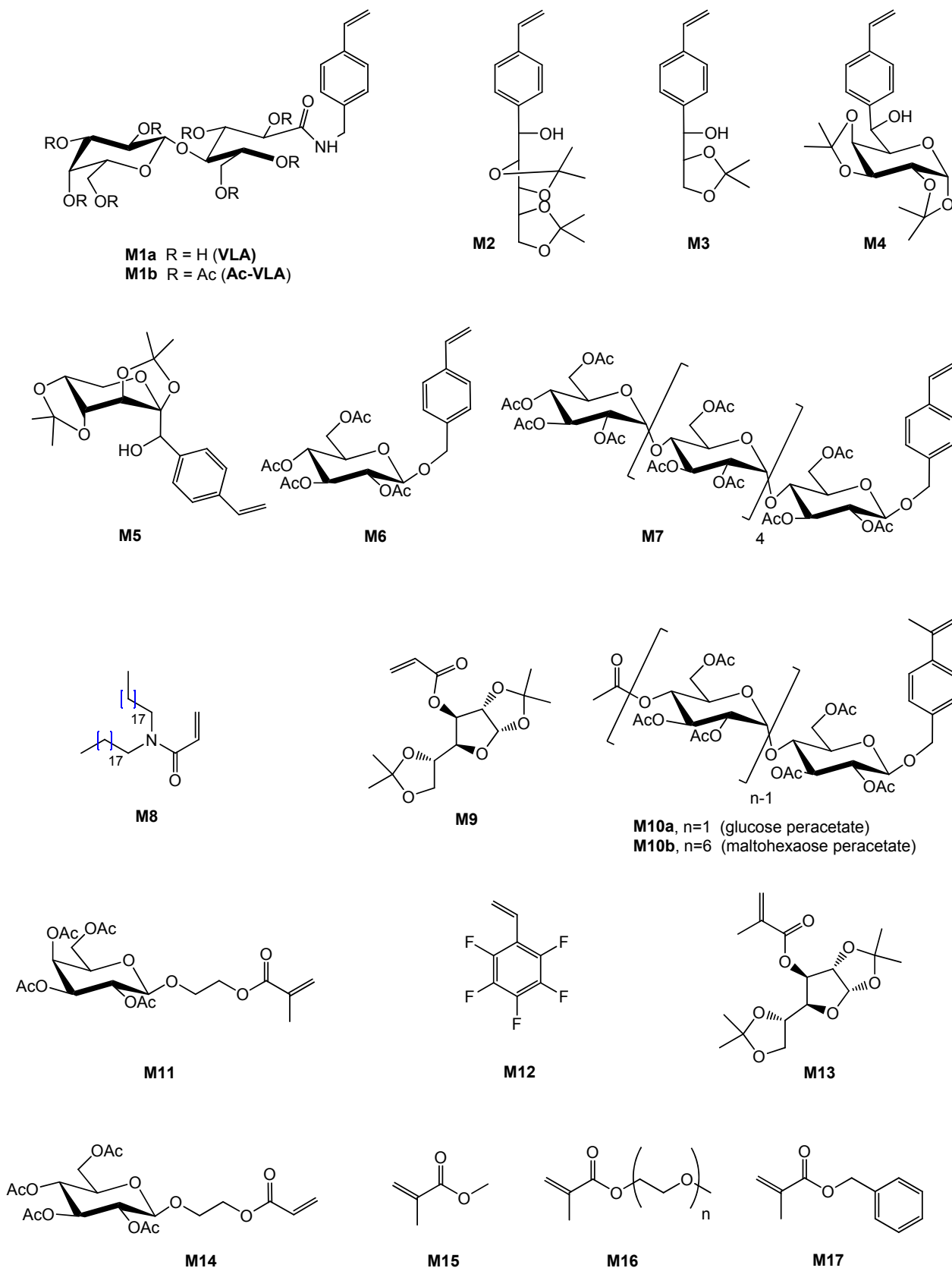
#### 4.1. SFRP Starting from Protected Glycomonomers/Control Agents

##### 4.1.1. (Meth)acrylate Monomers

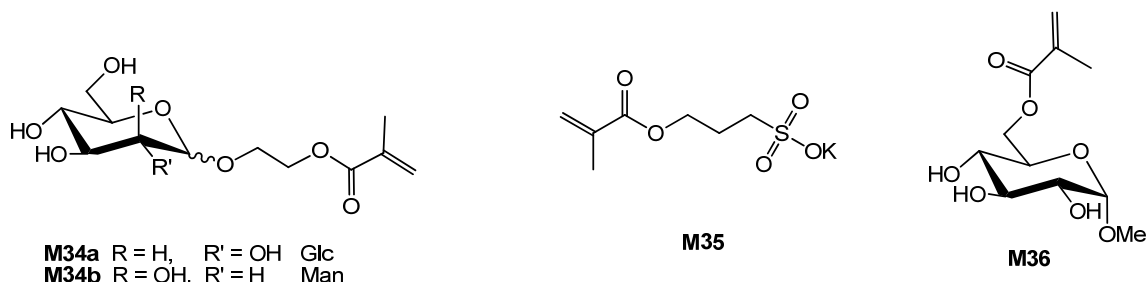
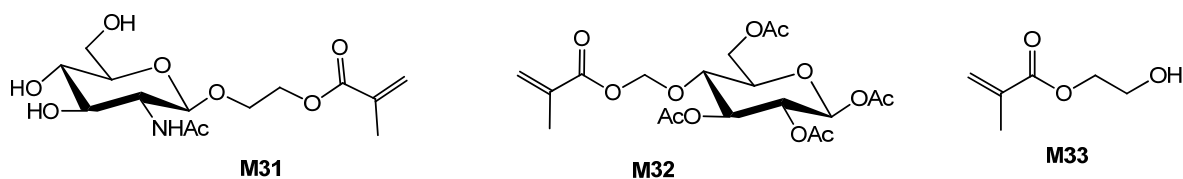
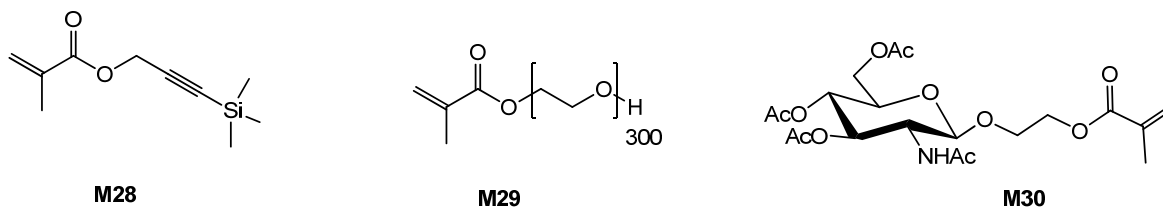
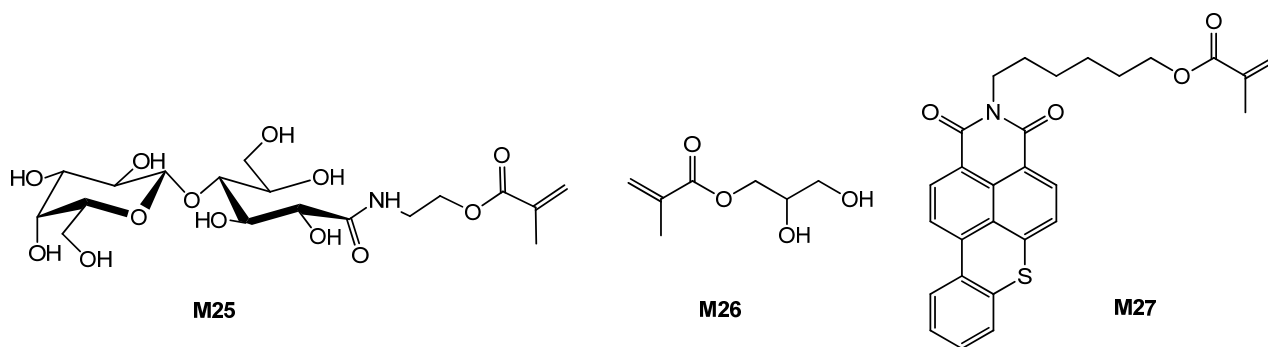
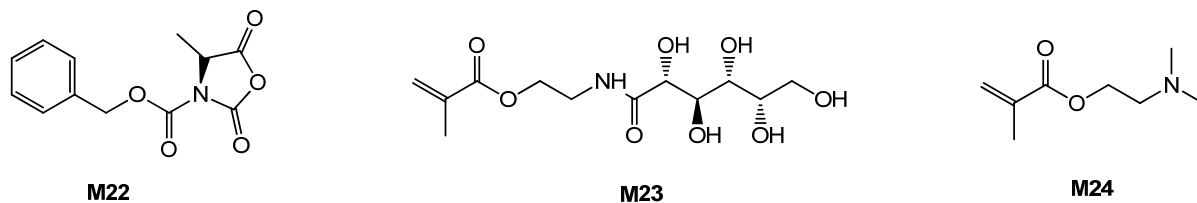
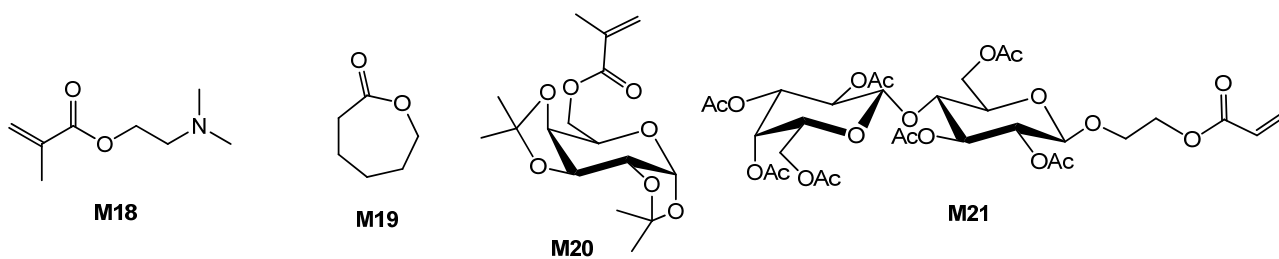
Table 1 summarizes the results obtained for the synthesis of glycopolymers by SFRP [76–100]. Hawker *et al.* [87] examined the polymerization of isopropylidene protected glucofuranose acrylate **M9** in the presence of a lipid functionalized alkoxyamine **N7** and 4% mole equivalents of the corresponding nitroxide (DMF, 105 °C). The polymerization rate was slow ( $p = 60\%$  after 50 h) but a fairly uniform lipo-glycopolymer was obtained (Entry 13, Table 1). A statistical copolymer of **M9** with *N,N'*-di(octadecyl)acrylamide **M8** was also prepared under similar conditions and with similar results ( $p = 55\%$  after 40 h,  $D = 1.2$ ; Entry 14, Table 1). Amphiphilic lipo-glycopolymers were obtained after

the removal of the alkoxy amine end chain with tributyltin hydride ( $\text{Bu}_3\text{SnH}$ ) and deprotection of the glucose residue with 9/1 trifluoroacetic acid/water.

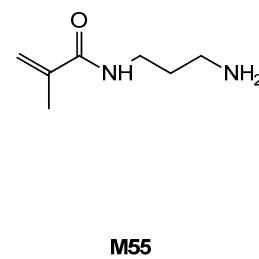
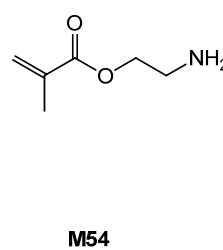
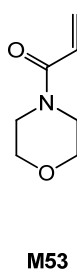
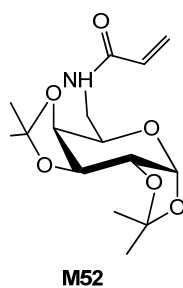
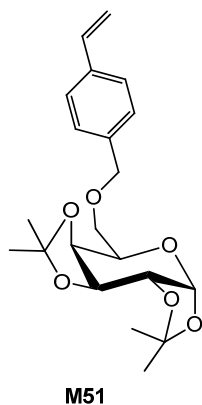
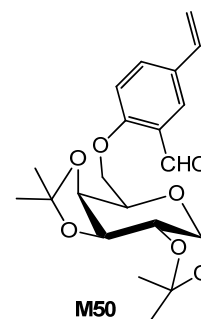
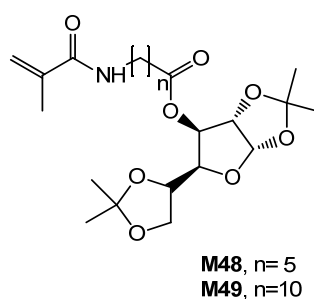
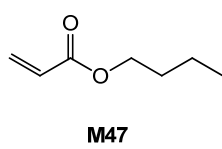
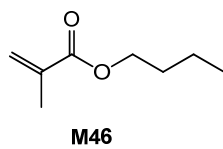
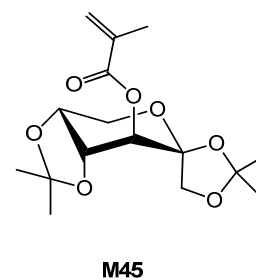
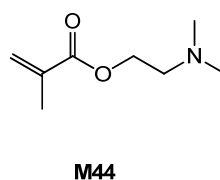
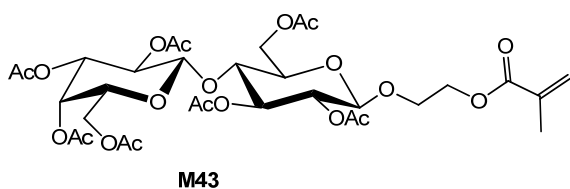
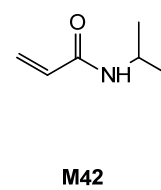
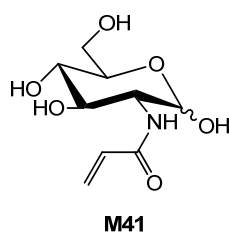
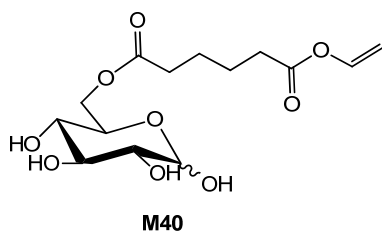
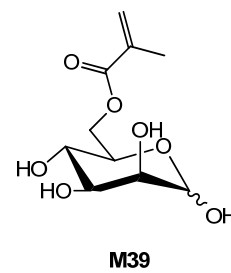
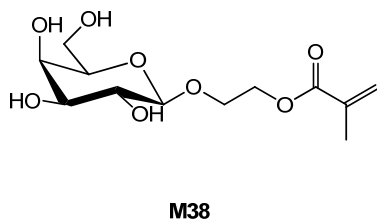
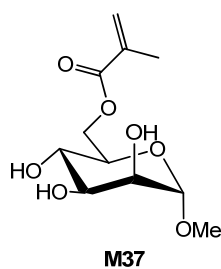
**Scheme 3.** Glycomonomers and related co-monomers polymerized by Reversible-Deactivation Radical Polymerization (RDRP).



Scheme 3. Cont.

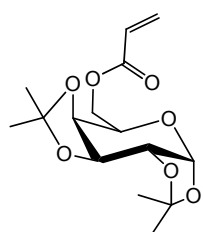


Scheme 3. Cont.

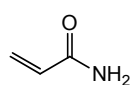




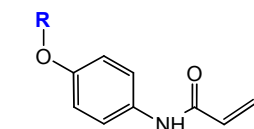
Scheme 3. Cont.



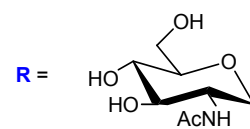
M74



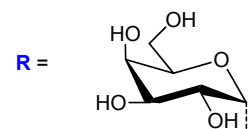
M75

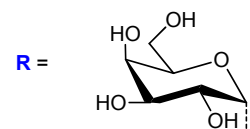


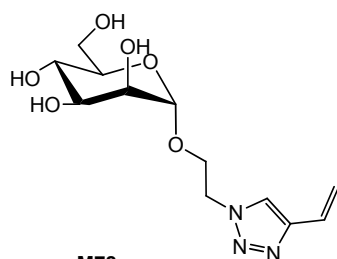
R =  M76



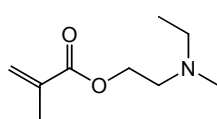
R =  M77



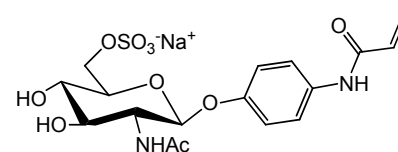
R =  M77b



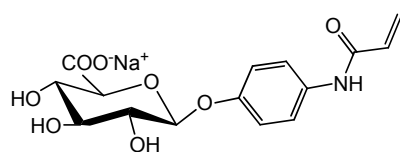
M78



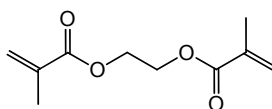
M79



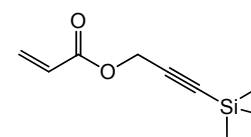
M80



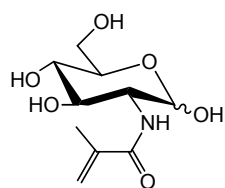
M81



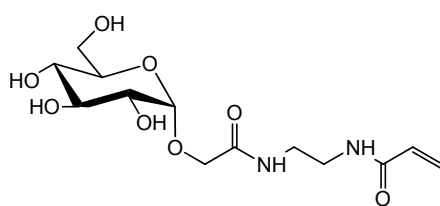
M82



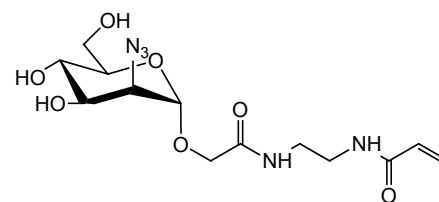
M83



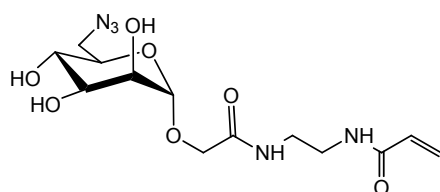
M84



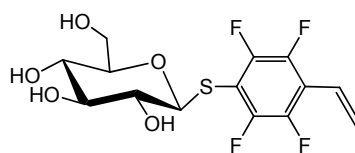
M85



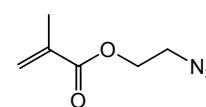
M86



M87

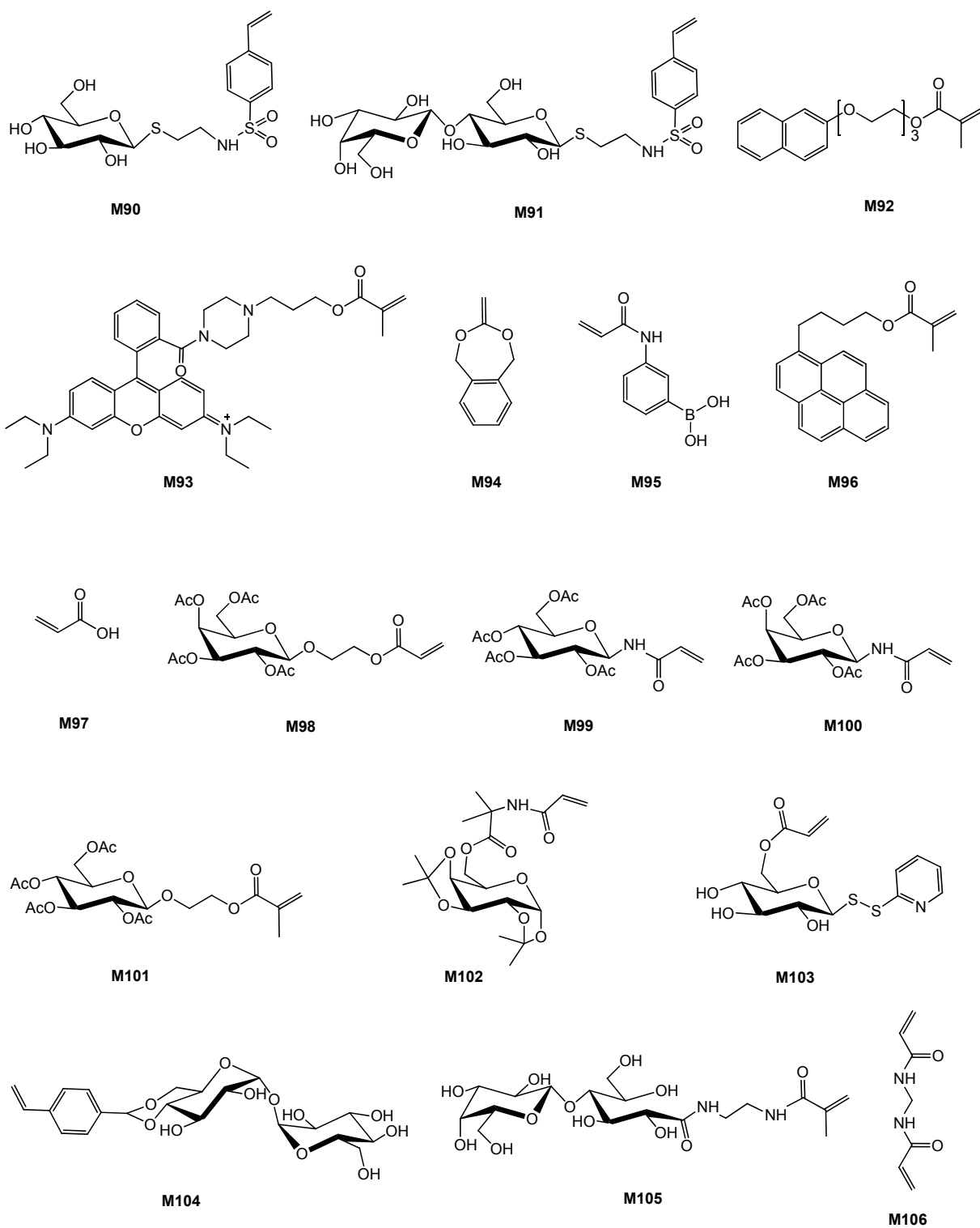


M88

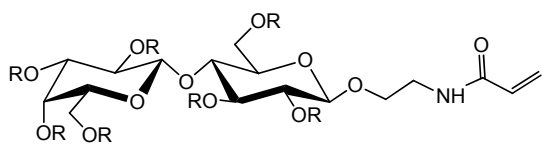


M89

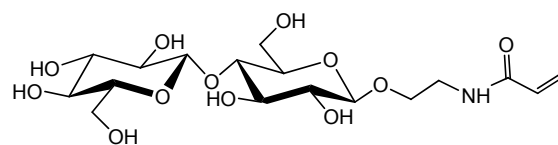
Scheme 3. Cont.



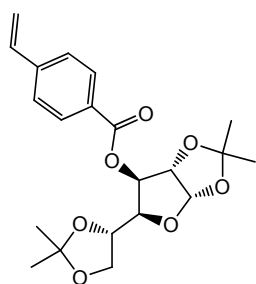
Scheme 3. Cont.



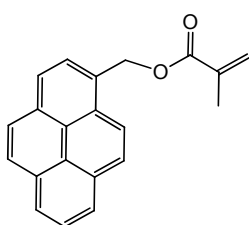
**M107a**, R = H  
**M107b**, R = SO<sub>3</sub><sup>-</sup>Na<sup>+</sup>



**M108**



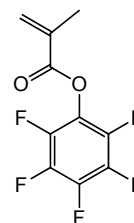
**M109**



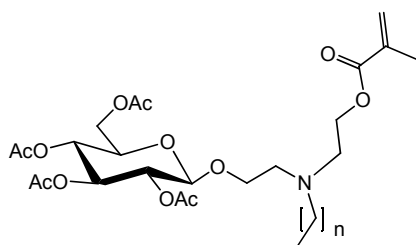
**M110**



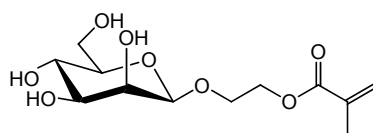
**M111**



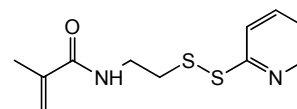
**M112**



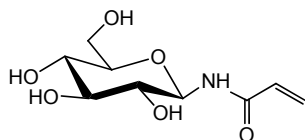
**M113a**, n=5  
**M113b**, n=7



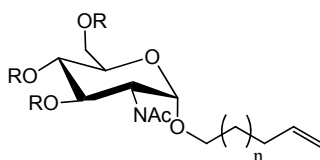
**M114**



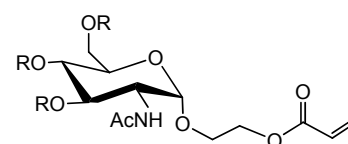
**M115**



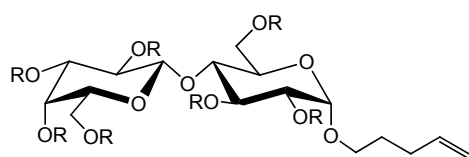
**M116**



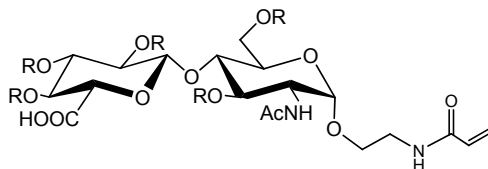
**M117a**, R = H n = 0  
**M117b**, R = SO<sub>3</sub><sup>-</sup>Na<sup>+</sup> n = 0  
**M117c**, R = H n = 7  
**M117d**, R = SO<sub>3</sub><sup>-</sup>Na<sup>+</sup> n = 7



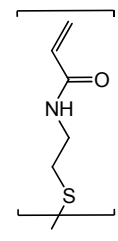
**M118a**, R = H  
**M118b**, R = SO<sub>3</sub><sup>-</sup>Na<sup>+</sup>



**M119a**, R = H  
**M119b**, R = SO<sub>3</sub><sup>-</sup>Na<sup>+</sup>



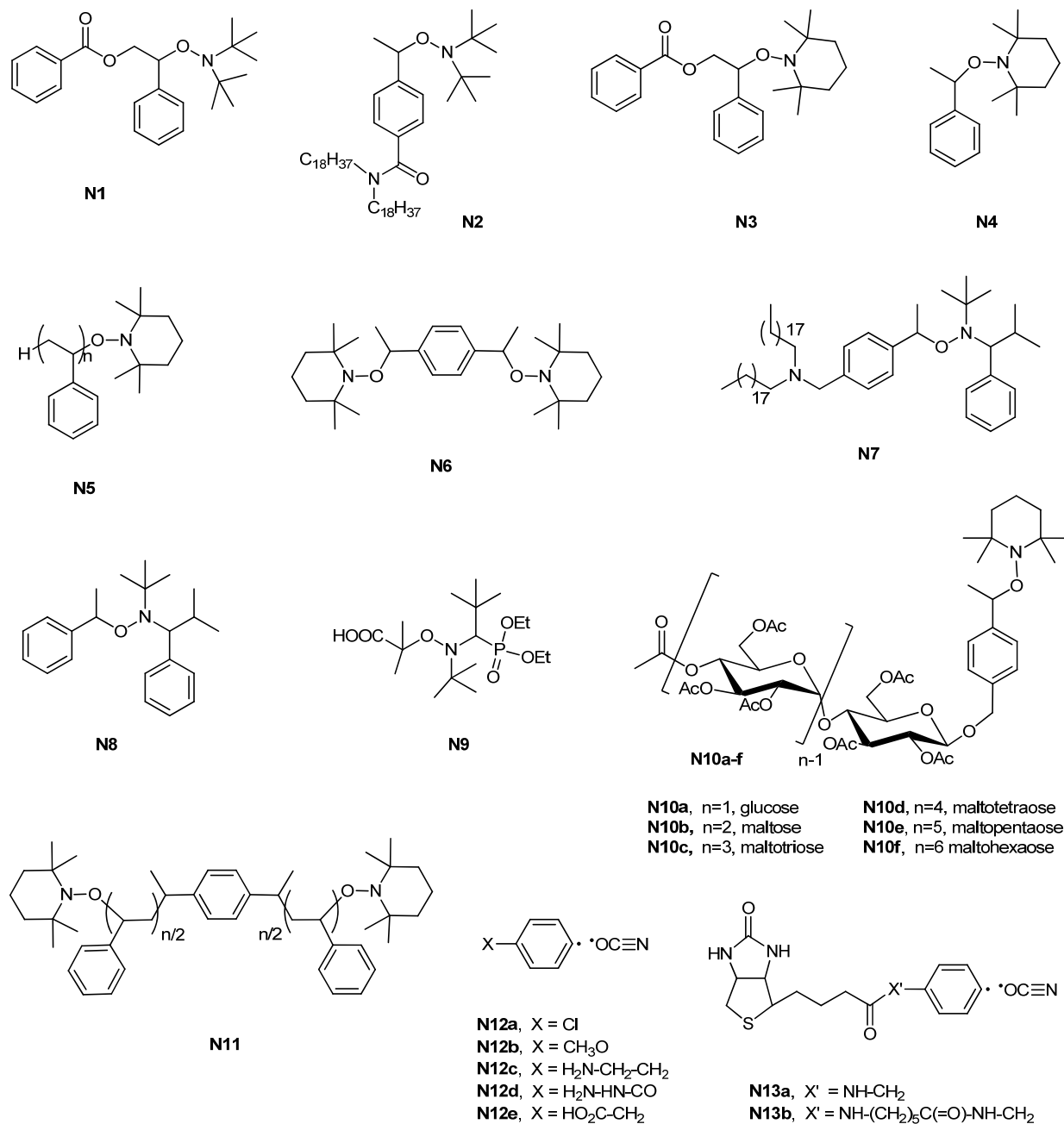
**M120a**, R = H  
**M120b**, R = SO<sub>3</sub><sup>-</sup>Na<sup>+</sup>



**M121**



**Scheme 4.** Initiators/control agents used for the synthesis of glycopolymers by Stable Free Radical Polymerization (SFRP).



Ting *et al.* [86] reported the synthesis of an amphiphilic glycopolymer bearing  $\alpha$ -galactoside residues (Entry 11–12, Table 1). Initially, methacrylate glycomonomer **M11** was copolymerized with styrene in the presence of **N9** as the initiator to afford fairly uniform poly(**M11**<sub>0.9</sub>-*stat*-**St**<sub>0.1</sub>) (1,4-dioxane, 85 °C, 2.7 h). The latter polymer contained only 81% of dormant chains though, and the study was continued by inverting the polymerization sequence. Hence, a 9:1 mixture of **M11**/**St** was used to chain extend a poly**St**·**N9** macro-alkoxyamine (1,4-dioxane, 120 °C for 0.5 h, then 85 °C for ~2.5 h) to obtain reasonably uniform diblock copolymers with structure poly**St**-*block*-poly(**M11**<sub>0.9</sub>-*stat*-**St**<sub>0.1</sub>). Deprotection of the latter with sodium methoxide in MeOH/DCM yielded amphiphilic glycopolymers that self-assembled into micelles in water and formed honeycomb structured porous films via the “breath figure” technique. Both materials could bind to PNA lectin.

**Table 1.** Glycopolymers by Stable Free Radical Polymerization (SFRP).

Entry	Carbohydrate	Monomer(s)	Initiator	Additive	Conv. <sup>a</sup> %	$M_n (\times 10^{-3})$	$M_n/M_{n,th}$ <sup>b</sup>	$\bar{D}$ <sup>c</sup>	Structure	Application sought/test	Reference
<b>Alkene monomers (unprotected)</b>											
1	lactose ( $\alpha$ -O)	M119a/M75	N12a	–	15	28.8	–	1.31	A-stat-B	promoter of binding of dFGF-2 to FGF receptor-1	Baskaran <i>et al.</i> [76]
2	lactose (persulfated, $\alpha$ -O)	M119b/M75	N12a	–	30	38.0	–	1.50	A-stat-B	promoter of binding of dFGF-2 to FGF receptor-1	Baskaran <i>et al.</i> [76]
3	N-acetylglucosamine ( $\alpha$ -O)	M117a/M75	N12a	–	30	43.0	–	1.47	A-stat-B	–	Chaikof <i>et al.</i> [77,78]
4	N-acetylglucosamine ( $\alpha$ -O)	M117c/M75	N12a	–	20	99.3	–	1.45	A-stat-B	–	Chaikof <i>et al.</i> [77,78]
5	N-acetylglucosamine (persulfated, $\alpha$ -O)	M117b/M75	N12a	–	35	57.3	–	1.37	A-stat-B	–	Chaikof <i>et al.</i> [77,78]
6	N-acetylglucosamine (persulfated, $\alpha$ -O)	M117d/M75	N12a	–	26	57.2	–	1.20	A-stat-B	–	Chaikof <i>et al.</i> [77,78]
<b>(Meth)acrylamide monomers (unprotected)</b>											
7	lactose ( $\beta$ -O)	M107a/M75	N12a	–	71	9.0	–	1.30	A-stat-B	anticoagulant, antithrombin	Sun <i>et al.</i> [79]
8	lactose (persulfated, $\beta$ -O)	M107b	N12a	–	55	7.5	–	1.19	homo	anticoagulant, antithrombin	Chaikof <i>et al.</i> [79,80]
9	lactose (persulfated, $\beta$ -O)	M107b/M75	N12a	–	67	33.4	–	1.47	homo	anticoagulant/antithrombin, promoter of binding of dFGF-2 to FGF receptor-1	Chaikof <i>et al.</i> [79,80]
10	lactose ( $\beta$ -O)	M107a/M75	N13a	–	75	12.0	–	1.30	A-stat-B	surface modification, lectin interaction	Chaikof <i>et al.</i> [81–85]
<b>(Meth)acrylate monomers (protected)</b>											
11	galactose ( $\beta$ -O)	M11/St	N9	–	45	40.6	–	1.26	A-stat-B	–	Ting <i>et al.</i> [86]
12	galactose ( $\beta$ -O)	M11/St	polySt-N9	–	48–79	21.7–79.9	–	1.34–1.50	(A-stat-B)-block-C	micelles and structured films for lectin recognition	Ting <i>et al.</i> [86]
13	glucose ( $\alpha/\beta$ , 3-O)	M9	N7	–	58	9.0	–	1.17	homo	film synthesis	Gotz <i>et al.</i> [87]
14	glucose ( $\alpha/\beta$ , 3-O)	M9/M8	N8	–	55	13.8	–	1.20	A-stat-B	film synthesis	Gotz <i>et al.</i> [87]

Table 1. Cont.

Entry	Carbohydrate	Monomer(s)	Initiator	Additive	Conv. <sup>a</sup> %	$M_n (\times 10^{-3})$	$M_n/M_{n,th}$ <sup>b</sup>	$\bar{D}$ <sup>c</sup>	Structure	Application sought/test	Reference
<b>(Meth)acrylate monomers (unprotected)</b>											
15	<i>N</i> -acetylglucosamine ( $\alpha$ - <i>O</i> )	M118a	N12a	–	25	15.4	–	1.26	homo	–	Grande <i>et al.</i> [78]
16	<i>N</i> -acetylglucosamine ( $\alpha$ - <i>O</i> )	M118a/M75	N12a	–	33	30.6	–	1.35	<i>A</i> - <i>stat</i> - <i>B</i>	–	Grande <i>et al.</i> [78]
17	<i>N</i> -acetylglucosamine (persulfated, $\alpha$ - <i>O</i> )	M118b	N12a	–	35	9.9	–	1.13	homo	–	Grande <i>et al.</i> [78]
18	<i>N</i> -acetylglucosamine (persulfated, $\alpha$ - <i>O</i> )	M118b/M75	N12a	–	–	21.7	–	1.20	<i>A</i> - <i>stat</i> - <i>B</i>	anticoagulant, antithrombin, promoter of binding of dFGF-2 to FGF receptor-1	Chaikof <i>et al.</i> [79,80]
<b>Styrenic monomers (protected)</b>											
19	fructose (pyranose, 1- <i>C</i> )	M5	N4	DCP	79	16.7	0.58	2.00	homo	–	Chen <i>et al.</i> [88]
20	galactose ( $\alpha/\beta$ , 6- <i>O</i> )	M4	N4	DCP	56	11.0	0.54	1.36	homo	–	Chen <i>et al.</i> [88]
21	glucitol/mannitol	M2	N4	DCP	82	16.8	0.61	1.37	homo	–	Chen <i>et al.</i> [88]
22	glucitol/mannitol	M2	polySt-N4	–	–	38.0	–	1.54	block AB	film synthesis, surface modification	Chen <i>et al.</i> [89]
23	glucitol/mannitol	St	polyM2-N4	–	–	96.5	–	1.37	block AB	film synthesis, surface modification	Chen <i>et al.</i> [89]
24	glucose ( $\beta$ - <i>O</i> )	M6	N5	–	~50	12.7	–	1.13	block AB	–	Narumi <i>et al.</i> [90]
25	glucose ( $\beta$ - <i>O</i> )	M6	N6	CSA	21	4.20	–	1.09	homo	–	Narumi <i>et al.</i> [91]
26	glucose ( $\beta$ - <i>O</i> )	St	polyM6-N6	–	10	12.5	–	1.14	block ABA	–	Narumi <i>et al.</i> [91]
27	glucose ( $\beta$ - <i>O</i> )	St	polyM6-N6	–	18	17.9	–	1.12	block ABA	–	Narumi <i>et al.</i> [91]
28	glucose ( $\beta$ - <i>O</i> )	St	polyM6-N6	–	17	29.4	–	1.17	block ABA	–	Narumi <i>et al.</i> [91]
29	glucose ( $\beta$ - <i>O</i> )	M10a	N10a	DCP	73	21.0	–	1.16	block ABA	–	Narumi <i>et al.</i> [92]
30	glucose to maltohexaose ( $\beta$ - <i>O</i> )	St	N10a-f	–	~40	5–25	–	1.07–1.14	homo	–	Narumi <i>et al.</i> [33]
31	glyceraldehyde (1- <i>C</i> )	M3	N4	DCP	88	13.1	0.63	1.26	homo	–	Chen <i>et al.</i> [88]
32	lactobionic acid (amide)	M1a	N1	DCP	35	7.50	–	1.30	homo	–	Ohno <i>et al.</i> [93]
33	lactobionic acid (amide)	M1b	N1	DCP	90	12.5	–	1.10	homo	–	Ohno <i>et al.</i> [93]
34	lactobionic acid (amide)	M1b	N2	DCP	90	12.0	–	≤1.20	homo	lectin recognition	Ohno <i>et al.</i> [94]

Table 1. Cont.

Entry	Carbohydrate	Monomer(s)	Initiator	Additive	Conv. <sup>a</sup> %	$M_n (\times 10^{-3})$	$M_n/M_{n,th}$ <sup>b</sup>	$\bar{D}$ <sup>c</sup>	Structure	Application sought/test	Reference
35	lactobionic acid (amide)	M1b	N3	–	36	17.5	–	1.36	homo	lectin recognition	Miura <i>et al.</i> [95]
36	maltotetraose ( $\beta$ -O)	M7	N5	–	$\approx 50$	16.2	–	1.21	block AB	–	Narumi <i>et al.</i> [90]
37	maltotetraose ( $\beta$ -O)	M10b	N11	DCP	84	31.8	–	1.11	block ABA	–	Narumi <i>et al.</i> [92]
<b>Styrenic monomers (unprotected)</b>											
38	glucose ( $\beta$ -S)	M88	N9	–	70	24.0	–	1.16	homo	cytotoxicity	Babiuch <i>et al.</i> [96]
<b>Glycopolymers from post-polymerization reactions</b>											
39	galactose ( $\beta$ -S)	M12	N9	–	78	5.7	0.79	1.06	homo	–	Babiuch <i>et al.</i> [97]
40	galactose ( $\beta$ -S)	M12	polySt·N9	–	52	14.3	1.15	1.16	block BA	biocompatible films and nanoparticles	Babiuch <i>et al.</i> [97]
41	galactose ( $\beta$ -S)	M12	N9	–	–	6.3	–	1.07	homo	–	Wild <i>et al.</i> [98]
42	glucose ( $\beta$ -S)	M12	N9	–	78	3.5	0.44	1.03	homo	–	Becer <i>et al.</i> [99]
43	glucose ( $\beta$ -S)	St	polyM12·N9	–	66	17.8	1.02	1.21	block AB	biocompatible films and nanoparticles	Becer <i>et al.</i> [99]
44	glucose ( $\beta$ -S)	M12	polySt·N9	–	76	7.1	0.56	1.16	block AB	biocompatible films and nanoparticles	Becer <i>et al.</i> [99]
45	$\alpha$ 2,3-sialyllactose ( $\beta$ -O)	M107a	N12a	–	60	7.0	–	–	A-stat-B	SPR, lectin binding	Narla <i>et al.</i> [100]
46	$\alpha$ 2,6-sialyllactose ( $\beta$ -O)	M107a	N12a	–	60	7.0	–	–	A-stat-B	SPR, lectin binding	Narla <i>et al.</i> [100]

<sup>a</sup> Conv. = conversion; <sup>b</sup> Degree of control,  $M_{n,th}$  is the number average theoretical molar mass; <sup>c</sup>  $\bar{D} = M_w/M_n$ , dispersity index.

#### 4.1.2. Styrenic Monomers

Fukuda's group first described in 1998 the nitroxide mediated polymerization of styrenic glycomonomers **M1a–b** in DMF at 90 °C using **N1** (Scheme 4) as control agent and DCP (dicumyl peroxide) as an accelerator [93]. When the unprotected monomer was used, conversion was low and only low molar mass polymers were obtained. By contrast, polymerization of the protected monomer **M1b** under the same conditions proceeded to higher conversion and afforded uniform polymers with  $M_n$  ranging from 2000 Da to 40,000 Da (Entry 32–33, Table 1). The same polymerization was successfully repeated in 1,2-dichloroethane using the dioctadecyl-functionalized alkoxyamine **N2** as initiator (Entry 34, Table 1) [94]: a uniform **DODA-pM1b** polymer was obtained ( $1.1 \leq D \leq 1.2$ ) with average mass in the range 3000–12,000 Da. Deprotection of the lactobionic acid residues afforded an amphiphilic polymer that formed liposomes in aqueous solution and showed specific recognition by *Ricinus communis* agglutinin 120 (RCA<sub>120</sub>), a  $\beta$ -D-galactose binding lectin. More recently, the NMP of **M1a–b** in DMF was revisited by Miura *et al.*, using **N3** as initiator (Entry 35, Table 1) [95]. The results were similar to the previous studies though, with the unprotected monomer **M1a** leading to non-uniform glycopolymers ( $D \cong 1.7$ ) and its protected analogue **M1b** affording more uniform macromolecules ( $D < 1.36$ ). Also, the authors found that the affinity for RCA<sub>120</sub> of the deprotected polymers increased with their *DP*, as normally observed for a multivalent interaction [101].

Chen and Wulff reported two studies [88,89] in which four isopropylidene-protected glycomonomers (**M2–M5**) were polymerized for 24 h at 130 °C in the presence of **N4** (Entry 19–21, Table 1). At the sole exception of poly**M5**, the resulting polymers had dispersity index  $D < 1.5$ . The protected glycopolymers were thermally stable up to 150 °C and were deprotected by the treatment with TFA/H<sub>2</sub>O (9:1 v/v). Amphiphilic block copolymers were obtained by chain extending poly**M2**·**N4** with styrene followed by deprotection of the carbohydrate residues: Their ability to modify the surface properties of hydrophobic substrates was demonstrated (Entry 23, Table 1) [89].

The synthesis of amphiphilic block copolymers was also the subject of a series of articles by Kakuchi *et al.* Their first study [90] described the polymerization of 4-vinylbenzyl glucoside **M6** and 4-vinylbenzyl maltohexaoside peracetate **M7** in xylene at 120 °C with polystyrene-macroinitiator **N5** ( $M_n = 8100$  Da,  $D = 1.17$ ). The resulting poly**St-block-polyM6** and poly**St-block-polyM7** were fairly uniform ( $D \leq 1.2$ ) and had  $M_n$  of 12,700 Da and 16,200 Da respectively (Entry 24 and 36, Table 1). De-acetylation with sodium methoxide in dry THF provided amphiphilic blocks copolymers that formed micelle-like aggregates in water and reversed micelle-like aggregates in toluene. In an extension to this work, the same group used the bi-functional initiator **N6** to prepare TEMPO-terminated poly**M6**·**N6** ( $M_n = 8500$  Da,  $D = 1.09$ ) that was subsequently chain extended with styrene to afford ABA tri-block copolymers poly**St-block-polyM6-block-polySt** of various chain lengths ( $M_{w,SLS} = 12,500$  Da, 17,900 Da and 29,400 Da;  $D = 1.14–1.17$ ) [91]. Conversion was quite low in all cases though (Entry 25–28, Table 1), and this strategy was later reversed [92] by using a bifunctional poly**St** initiator **N11** for the polymerization of styrenic glycomonomers functionalized with peracetylated glucose or maltohexoe **M10a–b** in chlorobenzene at 120 °C (Entry 29 and 37, Table 1). Higher conversions were achieved in this case ( $p > 70\%$ ), and hydrophilic-hydrophobic-hydrophilic triblock copolymers were obtained after deprotection of the carbohydrate residues.

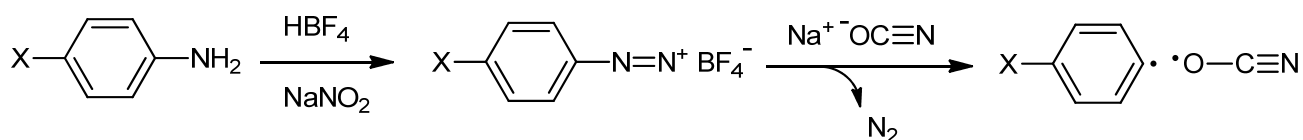
The same group also used a series of peracetylated  $\alpha$ -(1 $\rightarrow$ 4)-glucans-functionalized TEMPO derivatives **N10a-f** for the polymerization of styrene at 120 °C in the presence of dicumyl peroxide (Entry 30, Table 1) [33]. Good control over molar mass was achieved and uniform  $\alpha$ -functionalized polymers with  $M_n$  in the range 4800 Da to 25,000 Da were obtained. After deprotection with sodium methoxide in THF, reverse polymer micelles consisting of a saccharidic core and a polySt shell were observed in chloroform and toluene and their aggregation number was found to depend on the hydrophilic/hydrophobic balance of the polymer.

#### 4.2. SFRP Starting from Unprotected Glycomonomers/Control Agents

##### 4.2.1. Alkene Monomers

Chaikof *et al.* have explored the applicability of cyanoxyl-mediated radical polymerization (CMRP) in the synthesis of well-defined glycopolymers directly from unprotected glycomonomers [76–80,82–85,102,103]. As first noticed by Druliner in the early 1990s and by Gnanou more recently [69–71], a certain degree of control can be achieved when (meth)acrylic monomers are polymerized in the presence of cyanoxyl persistent radicals. In the version used by Chaikof *et al.*, the technique consists in preparing *p*-chlorobenzene-diazonium salts directly into the polymerization flask through the diazotization reaction of *p*-chloroaniline with tetrafluoroborohydride. When a monomer solution containing cyanate anions is added, cyanoxyl persistent radicals and aryl-type initiating radicals are generated by an electron-transfer reaction (Scheme 5) and a pseudo Reversible-Deactivation Radical Polymerization is observed upon heating.

**Scheme 5.** Reaction steps leading to the formation of a cyanoxyl persistent radical and an aryl-type initiating radical as described by Chaikof *et al.* [78].



Unlike nitroxide mediated radical polymerization, CMRP functions under mild reaction conditions (25–70 °C) perfectly adapted to glycopolymer synthesis in water. Control over molar mass is not as good though, and experimental values are systematically much higher than the theoretical ones. This is presumably due to the large proportion of primary aryl radicals being lost by irreversible termination during the initial stages of the process: Values as low as 0.1 were estimated for the initiator efficiency. Also, the molar dispersity index tends to increase significantly with conversion and with decreasing monomer to initiator ratios, and it is generally higher for more reactive monomers such as acrylates [78].

Notwithstanding the above mentioned limitations, this technique enabled the authors to prepare a series of statistical copolymers of alkenyl-derived glycomonomers **M117** and **M119** with acrylamide directly in water (or water-THF mixtures) in a pseudo-controlled fashion (Entry 1–6, Table 1) [76–78]. In all cases, lower molar mass dispersity was achieved at low conversion/short reaction times and when a smaller amount of glycomonomer was added to the initial feed ( $D = 1.1$ – $1.5$ ). By contrast, the length of the spacer did not seem to play a role [76]. After precipitation in MeOH and drying, the

obtained polymers were tested as glycosaminoglycan-mimetic biomaterials for tissue regeneration and wound-healing applications. The effect of sulfated glycopolymers on the binding of fibroblast growth factor-2 (FGF-2) to FGF receptor-1 (FGFR-1) was studied and polymers containing pendant sulfated lactose groups were found to significantly enhance FGF-2 binding to its receptor, even at low polymer concentrations.

#### 4.2.2. (Meth)acrylamide Monomers

CMRP was applied to the homopolymerization of acrylate-derived glycomonomers **M120a/b** and to their statistical co-polymerization with acrylamide directly in water or water-THF mixtures. Compared to alkenyl derives, glycomonomers of the acrylamide type led to somewhat higher molar dispersities ( $\bar{D} = 1.2\text{--}1.6$ ) but had the advantage to homopolymerize, to have faster reaction rates and to achieve higher conversions (up to 80% in 16 h) [79].

The anticoagulant activity of the resulting polymers was studied and was found to be much lower than that of heparin. Nonetheless, lactose heptasulfate-based glycopolymers considerably prolonged the coagulation time and copolymers with acrylamide had a higher anticoagulant activity than the corresponding homopolymers. By contrast, sulfated monosaccharide-based homo- and copolymers obtained from **M118b** showed no activity in this bioassay. These results suggest that anticoagulant activity is dependent upon the presence of sulfated disaccharides and that it can be optimized by modulating the copolymer composition [79].

Copolymers of **M120b** and **M118b** with acrylamide were also tested for their ability to act as molecular chaperone for fibroblast growth factor-2 (FGF-2) and to promote its dimerization and interaction with receptor FGFR-1. It was found that poly(**M120b-stat-M75**) with  $M_n = 9300$  Da,  $\bar{D} = 1.46$  and **M120b/M75** = 1/10 promotes an FGF-2 specific proliferative cell response. This finding suggests its potential applications in areas related to therapeutic angiogenesis [80].

In an extension to this work, a series of biotin-terminated glycopolymers were prepared by copolymerizing lactose-glycomonomer **M120a** and acrylamide with biotin-functionalized initiating system **N13**. The resulting polymers were used to fabricate a series of glycocalyx-mimetic surfaces that showed uniform carbohydrate coating on a membrane-like thin film [84,85] and to functionalize quantum dots and magnetic beads [82].

More recently, Sun *et al.* [81,100] took advantage of the *O*-cyanate  $\omega$ -chain-end of glycopolymers obtained by CMRP to anchor **M120a**/acrylamide copolymers onto amine-functionalized surfaces via isourea bond formation. This way they prepared functionalized silica gel beads suitable for affinity chromatography and glycoarrays designed for probing glycan binding proteins.

#### 4.2.3. (Meth)acrylate Monomers

CMRP was applied to the homopolymerization of acrylate-derived glycomonomers **M118a/b** and to their statistical co-polymerization with acrylamide directly in water or water-THF mixtures. In analogy to what seen for acrylamide derivatives and when compared to the alkenyl-analogies, glycomonomers of the acrylate type led to somewhat higher molar dispersities ( $\bar{D} = 1.2\text{--}1.6$ ) but had the advantage to homopolymerize, to have faster reaction rates and to achieve higher conversions (up to 80% in 16 h) [78].

#### 4.2.4. Styrenic Monomers

Schubert *et al.* [96] described the polymerization of a  $\beta$ -thioglycoside styrenic monomer **M88** in THF/H<sub>2</sub>O 1:1 in the presence of BlocBuilder **N9** (110 °C, 2 h; Entry 38, Table 1). A fairly uniform glycopolymers was obtained that was used for coating superparamagnetic iron oxide nanoparticles: neither the polymer nor the glyconanoparticle were cytotoxic towards 3T3 mouse fibroblasts.

#### 4.3. Glycopolymers from Post-Polymerization Reactions

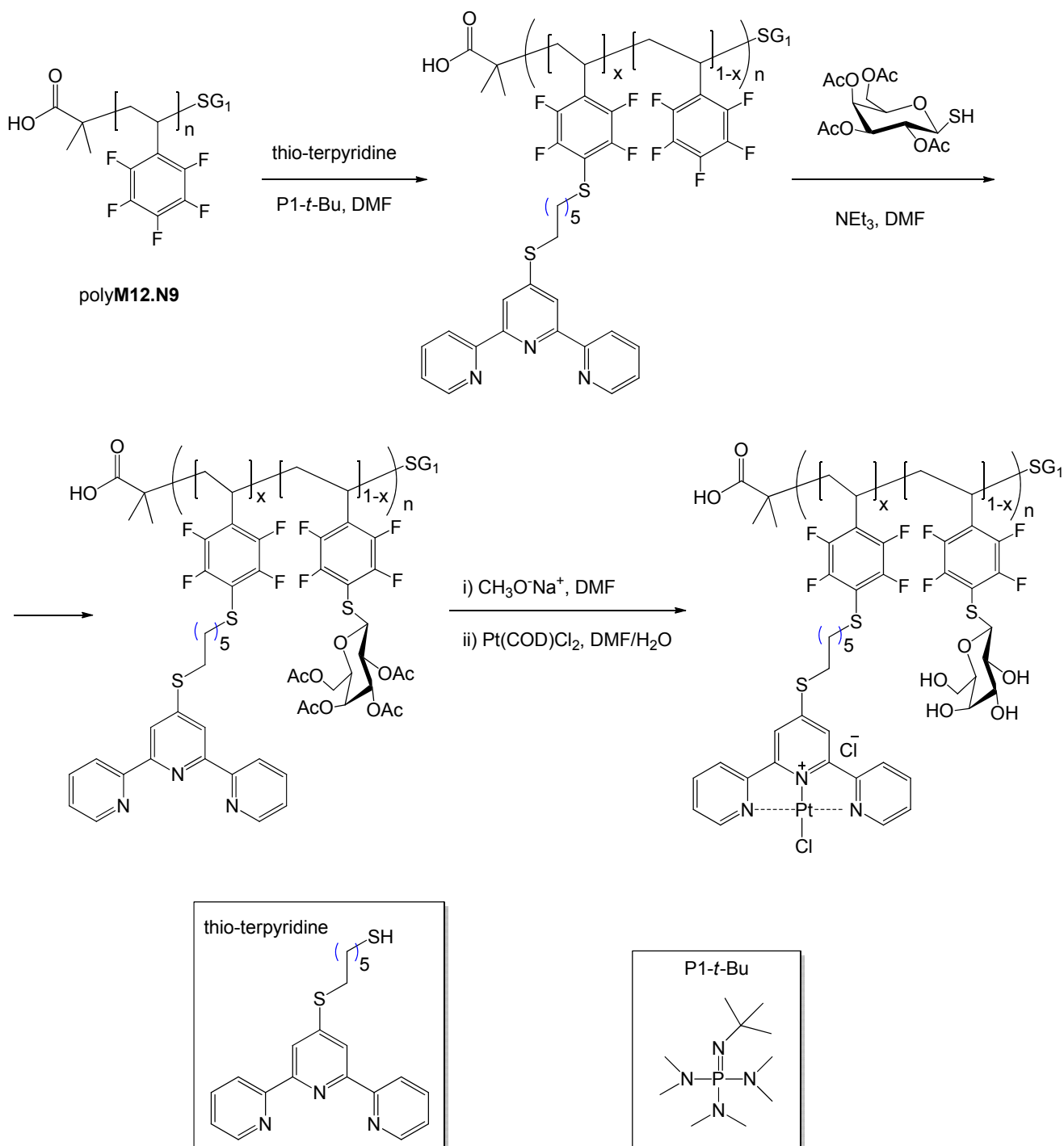
Schubert *et al.* applied a post-polymerization reaction to synthesize  $\beta$ -thioglycoside-functionalized glycopolymers (Entry 39–44, Table 1). In one example, **M12** (pentafluorostyrene) was either homopolymerized or copolymerized with **St** using BlocBuilder **N9** (Scheme 4) as the initiator in THF (110 °C, 5 h) [99]. Nucleophilic attack at the *para* position of the pentafluorostyrene ring with 2,3,4,6-tetra-*O*-acetyl-1-thio- $\beta$ -D-glucopyranose afforded poly**M88** and poly(**M88-stat-St**). SEC analysis indicated that all polymers had narrow molar mass distribution ( $D = 1.03$ – $1.20$ ) and that the copolymers had a molar mass close to the theoretical value. A similar approach was used for the synthesis of poly**M88-block-polySt** and poly**St-block-polyM88**, but in this case more drastic conditions were required to drive the post-polymerization reaction to 90% efficiency (DMF, 50 °C, 6 h). The obtained glycopolymers were then deprotected with sodium methoxide in DMF and purified by precipitation in cold EtOH. The same method was later applied to the synthesis of  $\beta$ -thiogalactoside-functionalized homo and block copolymers [97]. The deprotected block copolymers were used to coat polypropylene microtiter plates and glass slides.

In an extension to this work, Wild *et al.* [98] investigated the synthesis of a Pt<sup>II</sup>-functionalized glycopolymers. To this end, pentafluorostyrene **M12** was polymerized using the **SG1** derivative **N9** (BlocBuilder<sup>®</sup>; 110 °C, 5 h; Entry 41, Table 1). The purified polymer was reacted firstly with a thio-terpyridine (DS = 5%) and secondly with peracetylated 1-thio- $\beta$ -D-galactopyranose (DS  $\cong$  84%). Deprotection with CH<sub>3</sub>ONa in DMF afforded a uniform polymer with  $M_n$  23 KDa and  $D = 1.06$ . Finally, the terpyridine units were complexed with Pt<sup>II</sup> in a DMF/water mixture to yield an anti-leukemic polymer (Scheme 6).

Sun *et al.* [100] enzymatically modified the lactose residues of a poly(**M107a-stat-M75**) copolymer grafted onto glass slides or SPR gold sensor chips to transform them into  $\alpha$ 2,6- and  $\alpha$ 2,3-sialyllactose. To this end, the terminal galactose units of the disaccharide were sialylated with CMPNeu5Ac in the presence of either  $\alpha$ 2,6- or  $\alpha$ 2,3-sialyltransferase. The resulting glycoarrays and SPR sensors were then used for probing glycan binding proteins.



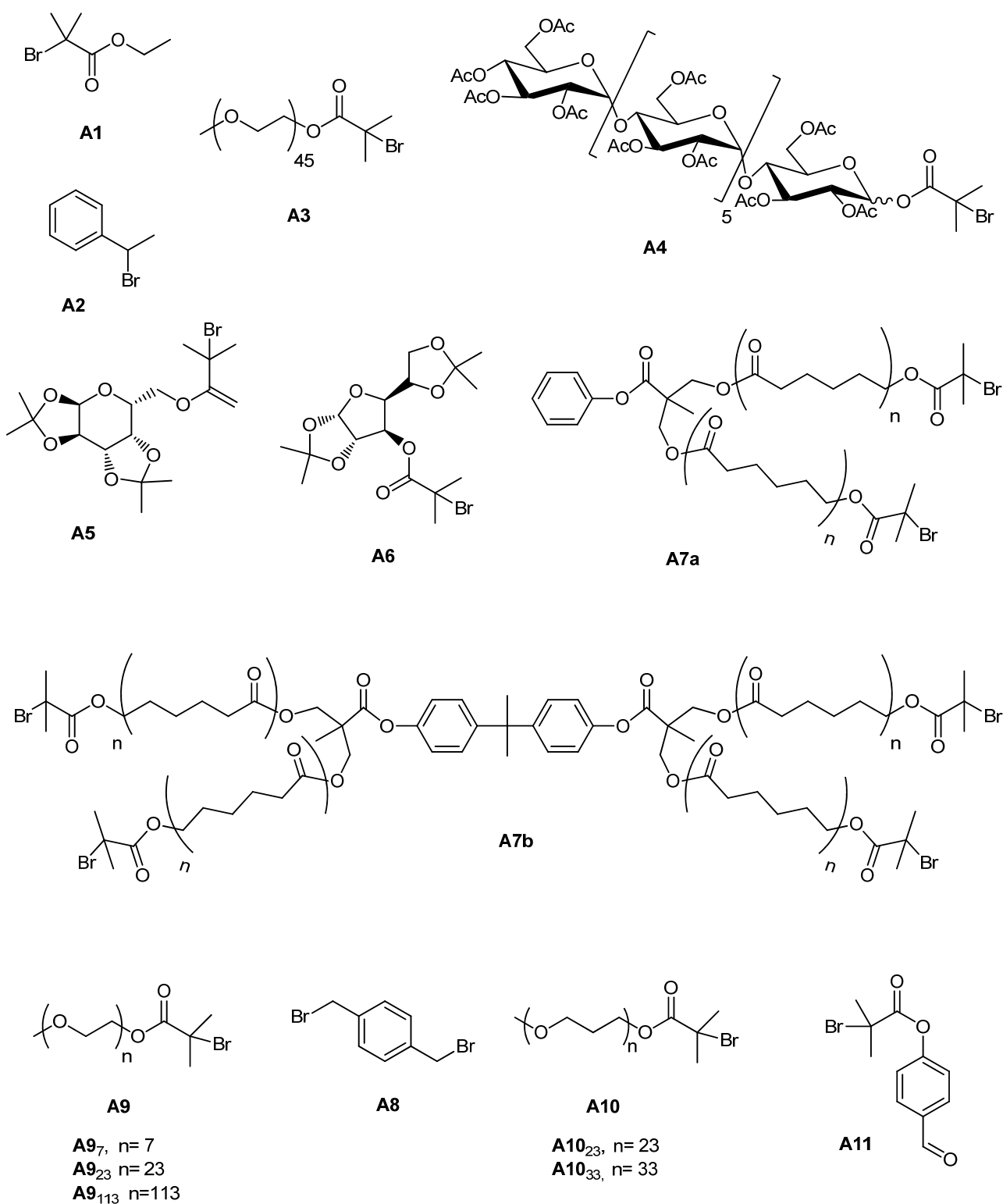
**Scheme 6.** Synthesis of a glycopolymeric platinum carrier as described by Schubert *et al.* [98]. (COD stands for the ligand 1,5-cyclooctadiene.)



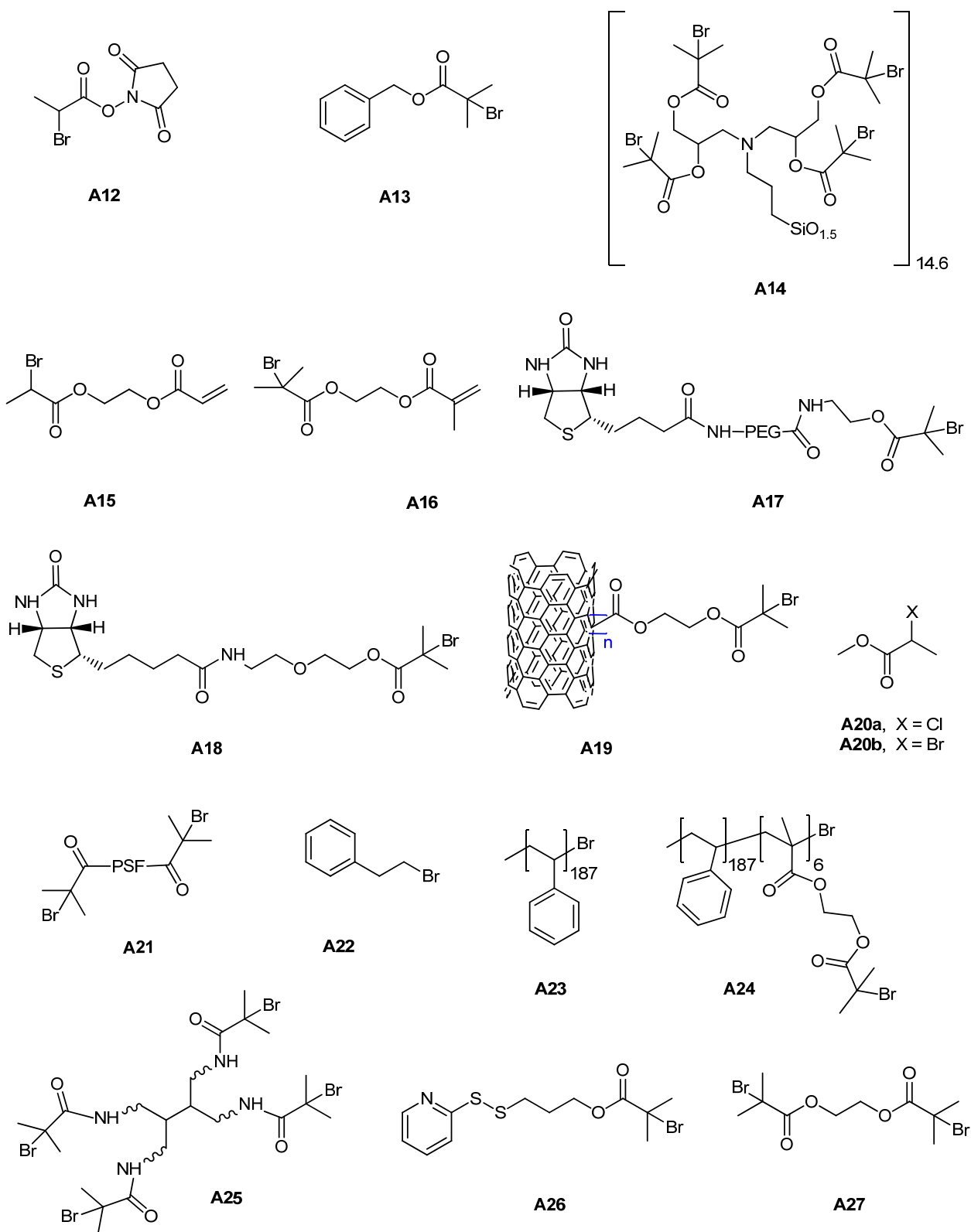
## 5. Synthesis of Glycopolymers by Atom Transfer Radical Polymerization (ATRP)

The structures of the initiators and ligands used in the synthesis of glycopolymers by ATRP are reported in Schemes 7 and 8, respectively.

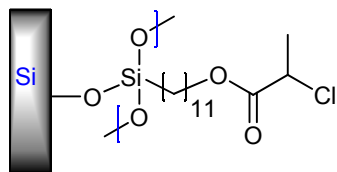
**Scheme 7.** Initiators used in the synthesis of glycopolymers by ATRP.



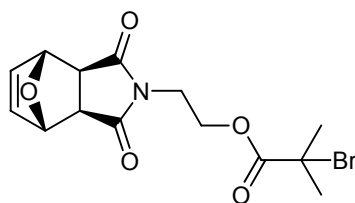
Scheme 7. Cont.



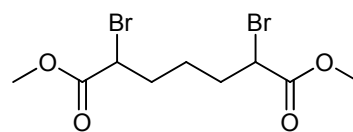
Scheme 7. Cont.



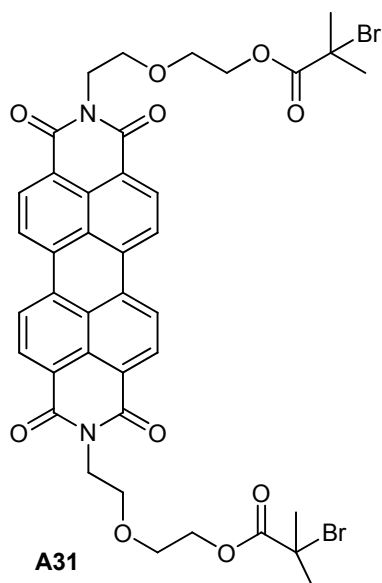
A28



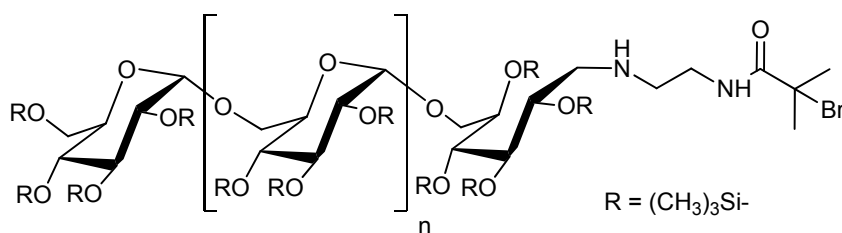
A29



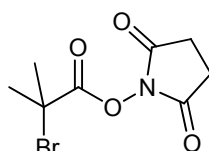
A30



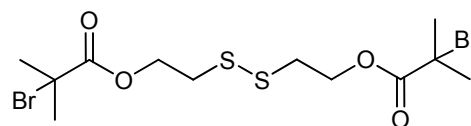
A31



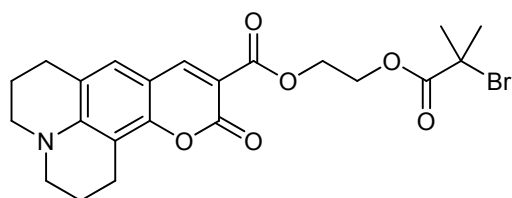
A32



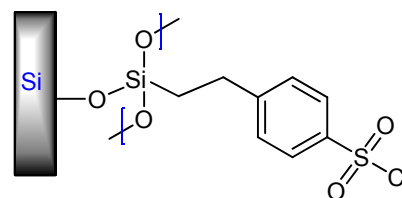
A33



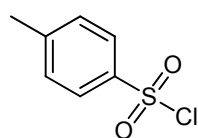
A34



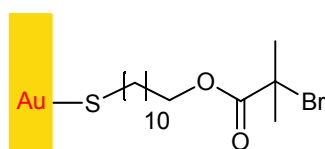
A35



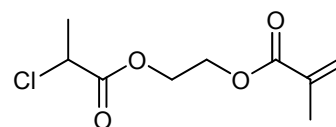
A36



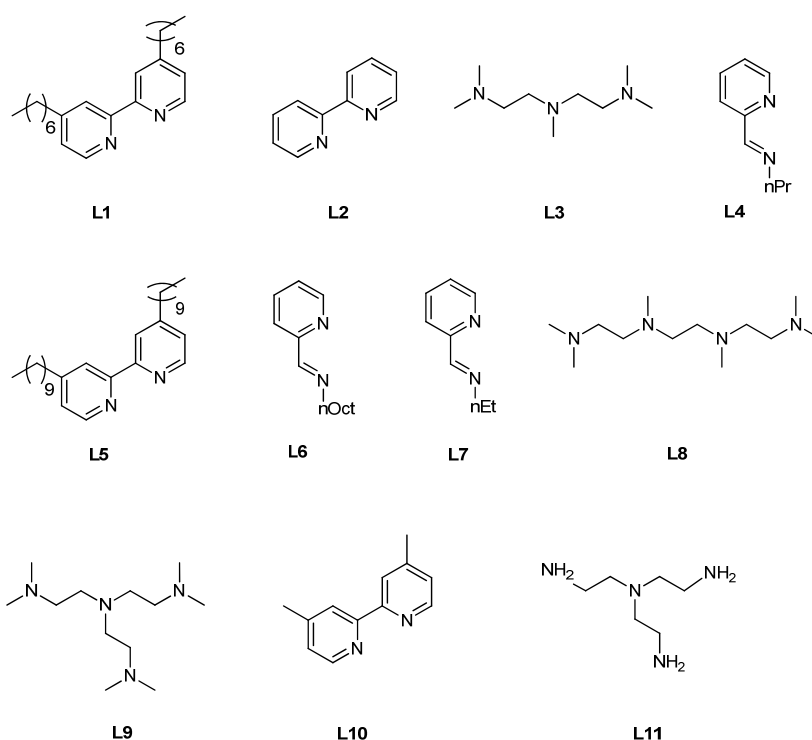
A37



A38



A39

**Scheme 8.** Ligands used in the synthesis of glycopolymers by ATRP.

### 5.1. ATRP Starting from Protected Glycomonomers/Glycoinitiators

#### 5.1.1. (Meth)acrylate Monomers

Table 2 summarizes the results obtained for the synthesis of glycopolymers by ATRP [11,30,34,104–145]. The first glycopolymer obtained by ATRP was reported by Fukuda *et al.* [109] isopropylidene-protected glucose derivative **M13** was polymerized in 1,2-dimethoxybenzene (veratrole; 80 °C, 3.5 h) using ethyl 2-bromoisobutyrate **A1** (Scheme 7) as initiator and CuBr(**L1**) as catalyst (Entry 59, Table 2). By varying the monomer to initiator ratio, polymers with  $M_n$  ranging from  $2.7 \times 10^4$  Da to  $2 \times 10^5$  Da and molar-mass dispersity  $D = 1.27$ – $1.82$  were obtained, with higher monomer to initiator ratios resulting in more uniform polymers. Under similar conditions, the sequential addition of styrene and **M13** afforded the block copolymer polySt-*block*-poly**M13** (Entry 60, Table 2). Deprotection with formic acid gave well-defined water soluble homopolymers and an amphiphilic block copolymer that formed nanostructured films upon solvent casting. The same group provided the first example of grafting-from of a glycopolymer onto a solid substrate [110]. To this end, a monolayer of precursor of the initiator was deposited onto oxidized silicon to give **A36**, the latter was dipped in a solution of **M13**, CuBr(**L1**) and *p*-toluenesulfonyl chloride (**A37**; sacrificial initiator) in 1,2-dimethoxybenzene, and the reaction was carried out at 80 °C for 12 h. The dispersity of the free polymer in solution did not exceed 1.2 and ellipsometric and atomic force microscopy analyses showed the formation of a homogenous graft layer onto the substrate. Moreover, the thickness of the graft layer in the dry state increased monotonically with time and linearly with the  $M_n$  of free polymer in solution. This suggests a controlled growth of the graft chains and a constant graft density, which was estimated at  $0.1 \text{ chain nm}^{-2}$ . Quantitative deprotection of the grafted poly**M13** was effected in formic acid to produce a solid surface densely grafted with a well-defined glucose-carrying polymer.

**Table 2.** Glycopolymers by Atom Transfer Radical Polymerization (ATRP).

Entry	Carbohydrate	Monomer(s)	Initiator	Additive	Conv. %	$M_n (\times 10^{-3})$	$M_n/M_{n,th}^a$	$\bar{D}^b$	Structure	Application sought/tested	Reference
<b>(Meth)acrylamide monomers (unprotected)</b>											
47	mannose ( $\alpha$ -O)	M64	A28/A20b	CuCl(L11), CuCl <sub>2</sub>	–	51.0	–	1.50	brush	lectin recognition	Yu <i>et al.</i> [104]
<b>(Meth)acrylate monomers (protected)</b>											
48	–	M19	I1	Sn(Oct) <sub>2</sub>	–	6.60	1.12	1.14	homo	–	Chen <i>et al.</i> [105]
49	–	M19	I2	Sn(Oct) <sub>2</sub>	–	13.7	1.15	1.12	homo	–	Chen <i>et al.</i> [105]
50	–	M33	A23	CuBr(L3)	45	20.0	0.99	1.14	block AB	–	Ke <i>et al.</i> [106]
51	galactose ( $\alpha/\beta$ , 6-O)	M20	A12	CuBr(L6)	95	7.50	–	1.08	homo	–	Ladmiral <i>et al.</i> [107]
52	galactose ( $\alpha/\beta$ , 6-O)	M20	A12	CuBr(L6)	99	13.4	–	1.10	homo	–	Ladmiral <i>et al.</i> [107]
53	galactose ( $\alpha/\beta$ , 6-O)	M20/M27	A12	CuBr(L6)	87	6.10	–	1.08	A-stat-B	–	Ladmiral <i>et al.</i> [107]
54	galactose ( $\alpha/\beta$ , 6-O)	M20	A7 <sub>2</sub>	CuBr(L5)	65	20.1	–	1.19	block ABA	–	Chen <i>et al.</i> [105]
55	galactose ( $\alpha/\beta$ , 6-O)	M20	A7 <sub>4</sub>	CuBr(L5)	51	35.0	–	1.17	star (4 arm)	–	Chen <i>et al.</i> [105]
56	galactose ( $\beta$ -O)	M98	A8	CuCl(L2)	50	5.5	1.19	1.17	homo	–	Wang <i>et al.</i> [11]
57	galactose ( $\beta$ -O)	M57	A8·polyM98·Br	CuCl(L3)	60	21.6	1.08	1.36	block ABA	insulin release	Wang <i>et al.</i> [11]
58	galactose ( $\alpha/\beta$ , 6-O)	M16, M17	A5	CuBr(L4)	–	10.5	–	1.21	block AB	–	Bes <i>et al.</i> [108]
59	glucose ( $\alpha/\beta$ , 3-O)	M13	A1	CuBr(L1)	83	75.0	0.45	1.82	homo	–	Ohno <i>et al.</i> [109]
60	glucose ( $\alpha/\beta$ , 3-O)	M13	A1·polySt·Br	CuBr(L1)	–	14.4	–	1.34	block AB	nanostructured film	Ohno <i>et al.</i> [109]
61	glucose ( $\alpha/\beta$ , 3-O)	M13	A36	CuBr(L1), A37	–	–	–	–	brush (homo)	–	Ejaz <i>et al.</i> [110]
62	glucose ( $\alpha/\beta$ , 3-O)	M13	A12	CuBr(L6)	90	7.10	–	1.14	homo	–	Ladmiral <i>et al.</i> [107]
63	glucose ( $\alpha/\beta$ , 3-O)	M13	A12	CuBr(L6)	90	14.7	–	1.31	homo	–	Ladmiral <i>et al.</i> [107]
64	glucose ( $\alpha/\beta$ , 3-O)	M13/M27	A12	CuBr(L6)	93	6.10	–	1.18	A-stat-B	–	Ladmiral <i>et al.</i> [107]

Table 2. Cont.

Entry	Carbohydrate	Monomer(s)	Initiator	Additive	Conv. %	$M_n (\times 10^{-3})$	$M_w/M_{n,th}^a$	$\bar{D}^b$	Structure	Application sought/tested	Reference
65	glucose ( $\alpha/\beta$ , 3-O)	M13	A14	CuBr(L8)	8	416	–	1.17	star	–	Muthukrishnan <i>et al.</i> [111]
66	glucose ( $\alpha/\beta$ , 3-O)	M13	A14	CuBr(L8)	6	601	–	1.26	star	–	Muthukrishnan <i>et al.</i> [111]
67	glucose ( $\alpha/\beta$ , 3-O)	M9	A1	CuBr(L3)	88	6.60	1.2	1.13	homo	–	Muthukrishnan <i>et al.</i> [112]
68	glucose ( $\alpha/\beta$ , 3-O)	M9	A1	CuBr(L3)	93	18.5	1.3	1.25	homo	–	Muthukrishnan <i>et al.</i> [112]
69	glucose ( $\alpha/\beta$ , 3-O)	M9	A1	CuBr(L3)	84	31.0	–	1.37	homo	–	Muthukrishnan <i>et al.</i> [112]
70 <sup>c</sup>	glucose ( $\alpha/\beta$ , 3-O)	M9	A15	CuBr(L3)	98	6.60	–	1.92	hyper branched	–	Muthukrishnan <i>et al.</i> [112]
71 <sup>d</sup>	glucose ( $\alpha/\beta$ , 3-O)	M9	A15	CuBr(L3)	96	13.0	–	1.95	hyper branched	–	Muthukrishnan <i>et al.</i> [112]
72 <sup>c</sup>	glucose ( $\alpha/\beta$ , 3-O)	M13	A16	(PPh <sub>3</sub> ) <sub>2</sub> NiBr <sub>2</sub>	> 98	17.6	–	2.12	hyper branched	–	Muthukrishnan <i>et al.</i> [113]
73 <sup>d</sup>	glucose ( $\alpha/\beta$ , 3-O)	M13	A16	(PPh <sub>3</sub> ) <sub>2</sub> NiBr <sub>2</sub>	> 98	23.3	–	1.57	hyper branched	–	Muthukrishnan <i>et al.</i> [113]
74	glucose ( $\alpha/\beta$ , 3-O)	M13	polyA16	CuBr(L8)	10	58.6	–	1.07	brush (cylindrical)	–	Muthukrishnan <i>et al.</i> [114]
75	glucose ( $\alpha/\beta$ , 3-O)	M13	A19	CuBr(L8)	85	37.4	1.16	1.45	homo	bio-nanotechnology	Gao <i>et al.</i> [115]
76	glucose ( $\alpha/\beta$ , 3-O)	M13	A16/A19	(PPh <sub>3</sub> ) <sub>2</sub> NiBr <sub>2</sub>	90	4.37	–	1.81	hyperbranched	bio-nanotechnology	Gao <i>et al.</i> [115]
77	glucose ( $\alpha/\beta$ , 3-O)	M13	A21	CuCl(L10)	51	12.5	–	1.18	block ABA	biomedical	Wang <i>et al.</i> [116]
78	glucose ( $\alpha/\beta$ , 4-O)	M32	A23	CuBr(L3)	62	27.6	0.82	1.32	homo	–	Ke <i>et al.</i> [106]
79	glucose ( $\alpha/\beta$ , 4-O)	St/M32	A22	CuBr(L3)	83	23.7	0.65	1.22	A-stat-B	lectin recognition; film preparation	Ke <i>et al.</i> [106]

Table 2. Cont.

Entry	Carbohydrate	Monomer(s)	Initiator	Additive	Conv. %	$M_n (\times 10^{-3})$	$M_w/M_{n,th}^a$	$\bar{D}^b$	Structure	Application sought/tested	Reference
80	glucose ( $\alpha/\beta$ , 4- <i>O</i> )	M32	A24	CuBr(L3)	53	25.2	0.69	1.43	graft AB	lectin recognition; film preparation	Ke <i>et al.</i> [106]
81	glucose ( $\alpha/\beta$ , 3- <i>O</i> )	M16, M17	A6	CuBr(L4)	–	11.0	–	1.18	block AB	–	Bes <i>et al.</i> [108]
82	glucose ( $\beta$ - <i>O</i> )	M14	A2	CuBr(L2)	55	24.8	1.00	1.34	homo	–	Liang <i>et al.</i> [117]
83	glucose ( $\beta$ - <i>O</i> )	M14	A3	CuBr(L3)	–	–	–	1.12	block AB	lectin interaction	You <i>et al.</i> [118]
84	lactose ( $\beta$ - <i>O</i> )	M21	A8	CuBr(L2)	58	20.6	1.22	1.29	homo	–	Dong <i>et al.</i> [119]
85	lactose ( $\beta$ - <i>O</i> )	M21	A8	CuBr(L2)	96	9.30	1.26	1.24	homo	–	Dong <i>et al.</i> [119]
86	lactose ( $\beta$ - <i>O</i> )	M22	H <sub>2</sub> N·polyM21·NH <sub>2</sub>	–	73	14.3	1.14	1.38	block ABA	–	Dong <i>et al.</i> [119]
87	lactose ( $\beta$ - <i>O</i> )	M62	H <sub>2</sub> N·polyM21·NH <sub>2</sub>	–	–	15.9	1.03	1.33	block ABA	–	Dong <i>et al.</i> [120]
88	maltoheptaose ( $\alpha/\beta$ - <i>O</i> )	M16	A4	CuBr(L4)	80	11.5	0.84	1.15	block AB	–	Haddleton <i>et al.</i> [30]
89	maltoheptaose ( $\alpha/\beta$ - <i>O</i> )	M18	A4	CuBr(L4)	82	–	–	–	block AB	–	Haddleton <i>et al.</i> [30]
90	maltoheptaose ( $\alpha/\beta$ - <i>O</i> )/glucose ( $\alpha/\beta$ , 3- <i>O</i> )	M13	A4	CuBr(L4)	88	16.5	0.65	1.21	block AB	–	Haddleton <i>et al.</i> [30]
91	maltoheptaose ( $\alpha/\beta$ - <i>O</i> )	M15	A4	CuBr(L4)	87	10.1	0.92	1.09	block AB	–	Haddleton <i>et al.</i> [30]
92	<i>N</i> -acetylglucosamine ( $\beta$ - <i>O</i> )	M30	A16	CuCl(L8)	95	11.0	–	1.29	hyperbranched	lectin recognition	Pfaff <i>et al.</i> [121]
93	<i>N</i> -acetylglucosamine ( $\beta$ - <i>O</i> )	M30	polySt·Br (latex)/A1	CuCl(L8)	95	96.7	0.45	1.12	brush	–	Pfaff <i>et al.</i> [122]



Table 2. Cont.

Entry	Carbohydrate	Monomer(s)	Initiator	Additive	Conv. %	$M_n (\times 10^{-3})$	$M_w/M_n$ <sup>a</sup>	$\bar{D}$ <sup>b</sup>	Structure	Application sought/tested	Reference
<b>(Meth)acrylate monomers (unprotected)</b>											
94 <sup>e</sup>	gluconic acid (amide)	M23	A9 <sub>23</sub>	CuBr(L2)	> 97	11.4	–	1.23	block AB	–	Narain <i>et al.</i> [123,124]
95 <sup>f</sup>	gluconic acid (amide)	M23	A9 <sub>23</sub>	CuBr(L2)	> 97	12.6	–	1.48	block AB	–	Narain <i>et al.</i> [123,124]
96 <sup>g</sup>	gluconic acid (amide)	M23	A9 <sub>23</sub>	CuBr(L2)	> 97	13.4	–	1.82	block AB	–	Narain <i>et al.</i> [123,124]
97	gluconic acid (amide)	M23	A25	CuBr(L2)	64.5 <sup>i</sup>	84.6	–	1.26	star (4-arms)	lectin recognition and drug delivery	Qiu <i>et al.</i> [125]
98 <sup>h</sup>	gluconic acid (amide)/ lactobionic acid (amide)	M23	A10-polyM25·Br	CuBr(L2)	68 <sup>i</sup>	21.2	–	1.28	block ABA	–	Narain <i>et al.</i> [126]
99	gluconic acid (amide)	M23	Au-modified surface	CuBr(L2)	–	19.7	–	1.6	brush	lectin recognition, SPR	Mateescu <i>et al.</i> [127]
100	glucose ( $\alpha/\beta$ -O)	M34a	A34	CuBr(L2)	–	8.6	–	1.44	homo	amyloid $\beta$ -peptide adsorption	Kitano <i>et al.</i> [128]
101	glucose ( $\alpha$ -methyl, 6-O)	M36	polyA16	CuBr(L4)	49	532	–	1.48	brush (cylindrical)	–	Fleet <i>et al.</i> [129]
102	glucose ( $\alpha$ -methyl, 6-O)	M36	poly(A16- <i>stat</i> -M15)	CuBr(L4)	30	196	–	1.49	brush (cylindrical)	–	Fleet <i>et al.</i> [129]
103	glucose ( $\alpha$ -methyl, 6-O)	M36	poly(A16- <i>block</i> -M15)	CuBr(L4)	41	320	–	1.52	brush (cylindrical)	–	Fleet <i>et al.</i> [129]
104	glucose ( $\alpha$ -methyl, 6-O)	M36	poly(M58- <i>alt</i> -MANh)	CuBr(L4)	45	565	–	1.21	brush (cylindrical)	–	Fleet <i>et al.</i> [129]
105 <sup>h</sup>	lactobionic acid (amide)	M25	A10 <sub>23</sub>	CuBr(L2)	–	22.5	–	1.24	block AB	–	Narain <i>et al.</i> [123]

Table 2. Cont.

Entry	Carbohydrate	Monomer(s)	Initiator	Additive	Conv. %	$M_n (\times 10^{-3})$	$M_n/M_{n,th}^a$	$\bar{D}^b$	Structure	Application sought/tested	Reference
106 <sup>f</sup>	lactobionic acid (amide)	M25	A10 <sub>23</sub>	CuBr(L2)	> 95	23.4	–	1.10	block AB	–	Narain <i>et al.</i> [123]
107 <sup>g</sup>	lactobionic acid (amide)	M25	A10 <sub>23</sub>	CuBr(L2)	> 95	34.8	–	1.60	block AB	–	Narain <i>et al.</i> [123]
108 <sup>f</sup>	lactobionic acid (amide)	M24	A10-polyM25·Br	CuBr(L2)	–	17.9	–	1.34	block ABC	–	Narain <i>et al.</i> [126]
109 <sup>h</sup>	lactobionic acid (amide)	M26	A10-polyM25·Br	CuBr(L2)	72 <sup>i</sup>	18.1	–	1.29	block ABC	–	Narain <i>et al.</i> [126]
110	lactobionic acid (amide)	M25	A17	CuBr(L2)	80 <sup>i</sup>	24.0	1.02	1.32	block AB	streptavidin binding	Narain <i>et al.</i> [130]
111	lactobionic acid (amide)	M25	A38, A1 or A38	CuBr(L2), CuBr <sub>2</sub>	–	68.0	1.8	–	brush	lectin recognition, SPR	Mateescu <i>et al.</i> [127]
112	lactobionic acid (amide)	M25	A39	CuBr(L2), CuBr <sub>2</sub>	–	–	–	–	brush (linear)	lectin binding	Yang <i>et al.</i> [131]
113	lactobionic acid (amide)	M25	A39	CuBr(L2), CuBr <sub>2</sub>	–	–	–	–	brush (comb)	lectin binding	Yang <i>et al.</i> [131]
114	mannose ( $\alpha$ -O)	M67	A35	CuBr(L7)	80	28.8	–	1.25	homo	–	O'Connell <i>et al.</i> [132]
115	mannose ( $\alpha$ -O)	M89, 2-propynyl- $\alpha$ -Man	A31	CuBr(L3)	–	49.9	–	1.33	homo	cell imaging	Xu <i>et al.</i> [133]
116	mannose ( $\alpha/\beta$ -O)	M34b	A34	CuBr(L2)	–	7.8	–	1.20	homo	lectin binding	Kitano <i>et al.</i> [134]
117	mannose ( $\alpha$ -O)	M67	A29	CuBr(L7)	–	26.1	–	1.20	homo	lectin recognition	Geng <i>et al.</i> [135]
118	<i>N</i> -acetylglucosamine ( $\beta$ -O)	M30	A18	CuBr(L9)	94	40.7	1.88	1.17	homo	biotin-protein binding	Vazquez-Dorbatt <i>et al.</i> [136]
119	<i>N</i> -acetylglucosamine ( $\beta$ -O)	M31	A18	CuBr(L9)	86	43.1	3.01	1.07	homo	biotin-protein binding	Vazquez-Dorbatt <i>et al.</i> [136]
120	<i>N</i> -acetylglucosamine ( $\beta$ -O)	M31	A26	CuBr(L2), CuBr <sub>2</sub>	80	10.2	–	1.12	homo	siRNA conjugation	Vazquez-Dorbatt <i>et al.</i> [137]
121	<i>N</i> -acetylglucosamine ( $\alpha/\beta$ , <i>N</i> )	M63	A1	CuBr(L3)	90	70	–	1.20	homo	lectin recognition	Leon <i>et al.</i> [138]
122	<i>N</i> -acetylglucosamine ( $\alpha/\beta$ , <i>N</i> )	M63	A27	CuBr(L3)	75	27.0	–	1.15	homo	lectin recognition	Leon <i>et al.</i> [138]

Table 2. Cont.

Entry	Carbohydrate	Monomer(s)	Initiator	Additive	Conv. %	$M_n (\times 10^{-3})$	$M_w/M_{n,th}^a$	$\mathcal{D}^b$	Structure	Application sought/tested	Reference
123	<i>N</i> -acetylglucosamine ( $\alpha/\beta$ , <i>N</i> )	M47	A1·polyM63·Br	CuCl(L3)	90	15.0	0.87	1.31	block AB	lectin recognition	Leon <i>et al.</i> [138]
124	<i>N</i> -acetylglucosamine ( $\alpha/\beta$ , <i>N</i> )	M47	A27·polyM63·Bt	CuCl(L3)	93	17.6	0.98	1.38	block ABA	lectin recognition	Leon <i>et al.</i> [138]
125	<i>N</i> -acetylglucosamine ( $\alpha/\beta$ , <i>N</i> )	M63	A20a·polyM47·Br	CuCl(L3)	73	33.9	1.48	1.37	block AB	lectin recognition	Leon <i>et al.</i> [139]
126	<i>N</i> -acetylglucosamine ( $\alpha/\beta$ , <i>N</i> )	M63	A30·polyM47·Br	CuCl(L3)	93	38.5	1.23	1.32	block ABA	lectin recognition	Leon <i>et al.</i> [139]
127	<i>N</i> -acetylglucosamine ( $\alpha/\beta$ , <i>N</i> )	M46	A1·polyM63·Br	CuCl(L3)	45	32.7	1.20	1.30	block AB	polymeric surfactant, lectin recognition	Munoz-Bonilla <i>et al.</i> [140]
128	<i>N</i> -acetylglucosamine ( $\alpha/\beta$ , <i>N</i> )	M63	A1·polyM15·Br	CuCl(L3)	15	16.5	0.93	1.12	block AB	lectin recognition; film preparation	de León <i>et al.</i> [141]
<b>Styrenic monomers (protected)</b>											
129	dextran (1-deoxy-1-amide)	St	A32	CuBr(L3)	–	82.2	–	1.70	block AB	carrier	Houga <i>et al.</i> [34]
130	glucose ( $\alpha/\beta$ , 3- <i>O</i> )	M109	A1	CuCl(L3)	68 <sup>i</sup>	12.3	–	1.19	homo	–	[142]
131	glucose ( $\alpha/\beta$ , 3- <i>O</i> )	M110	polyM109	CuCl(L3)	55 <sup>i</sup>	21.2	–	1.46	block AB	biomedical	Menon <i>et al.</i> [142]
132	maltoheptaose ( $\alpha/\beta$ - <i>O</i> )	St	A4	CuBr(L4)	91	10.7	1.20	1.48	block AB	–	Haddleton <i>et al.</i> [30]
<b>Glycopolymers from post-polymerization reaction</b>											
133	–	M28/M15	A13	CuBr(L7)	>80	8.90	1.56	1.09	<i>A-stat-B</i>	–	Ladmiral <i>et al.</i> [143]
134	–	M28/M29	A13	CuBr(L7)	>80	11.9	1.52	1.12	<i>A-stat-B</i>	–	Ladmiral <i>et al.</i> [143]
135	galactose ( $\beta$ - <i>N</i> )	M112	A1	CuBr(L3)	70	11.4	0.64	1.16	homo, <i>A-stat-B</i>	lectin recognition <sup>j</sup>	Richards <i>et al.</i> [144]
136	galactose ( $\alpha$ - <i>O</i> ), mannose ( $\alpha$ - <i>O</i> )	M28	A13	CuBr(L7)	>80	17.6	2.31	1.17	homo	lectin recognition <sup>j</sup>	Ladmiral <i>et al.</i> [143]
137	mannose ( $\alpha$ - <i>O</i> )	M28/M93	A29	CuBr(L7)	–	16.4	–	1.28	homo	lectin recognition <sup>j</sup>	Geng <i>et al.</i> [135]
138	mannose ( $\alpha$ - <i>O</i> )	M28	A34	CuBr(L7)	–	7.5	–	1.32	homo	–	Gou <i>et al.</i> [145]

<sup>a</sup> Degree of control,  $M_{n,th}$  is the number average theoretical molar mass; <sup>b</sup>  $\mathcal{D} = M_w/M_n$ , dispersity index; <sup>c</sup>  $[Mi]_0/[Ai]_0 = 1.5$ ; <sup>d</sup>  $[Mi]_0/[Ai]_0 = 10$ ; <sup>e</sup> in methanol, <sup>f</sup> in methanol/water 3:2 v/v; <sup>g</sup> in water; <sup>h</sup> in *N*-methyl-2-pyrrolidone; <sup>i</sup> isolated yield; <sup>j</sup> after post-polymerization modification.

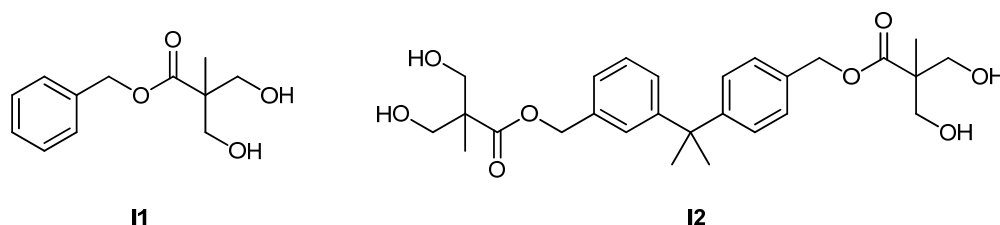
$\beta$ -Glucoside derivative **M14** was polymerized by Li *et al.* [117] in the presence of (1-bromoethyl)benzene **A2** as initiator and CuBr(**L2**) as catalyst (chlorobenzene, 80 °C). Pseudo-first order kinetics were observed and molar mass increased linearly with conversion. Molar mass distribution remained narrow up to 70% conversion and, by varying the monomer to initiator ratio, polymers with  $M_n$  in the range 5–25 KDa and  $D = 1.26$ – $1.34$  were obtained (Entry 82, Table 2). The resulting polymers were quantitatively deprotected by modified Zemplén deacetylation (MeONa in  $\text{CHCl}_3/\text{MeOH}$ , RT). The same polymerization conditions were used to chain extend PEO macro-initiator **A3** with **M14** in the presence of CuBr(**L3**) (Entry 83, Table 2) [118]. The resulting PEO<sub>45</sub>-*block*-poly**M14**<sub>27</sub> glycopolymer was deprotected and its interaction with ConA was compared to that of poly**M14**<sub>10</sub>. While both polymers formed aggregates with the lectin, only those from PEO-*block*-poly(deprotected **M14**) were stable in water, presumably due to the hydrophilic PEO segments.

Haddleton *et al.* studied the synthesis of a series of carbohydrate-functionalized ATRP initiators and their use for the polymerization of a number of monomers (Entry 58, 81, 88–91, 132, Table 2) [30]. Hence peracylated maltoheptaoside **A4** was obtained from the ring opening of  $\beta$ -cyclodextrin and was used as glycoinitiator for the polymerization of **M13**, **M15**–**M18** and **St** using CuBr(**L4**) as the catalyst (xylene or toluene, 90 °C, 110 °C for styrene; Entry 88–91 and 132 in Table 2). The polymerization of methacrylate monomers proceeded with good control over the molecular mass and led to uniform polymers ( $D \leq 1.21$ ) while the polymerization of styrene resulted in the broadening of the molar mass distribution ( $D = 1.48$ ), a phenomenon already observed with other types of  $\alpha$ -bromoester initiators [34]. The resulting polymers were quantitatively deprotected by modified Zemplén deacetylation (MeONa in  $\text{CHCl}_3/\text{MeOH}$  at room temperature). Amphiphilic block copolymers poly**M16**-*block*-poly**M17** containing a carbohydrate residue at their  $\alpha$ -end were synthesized in a similar way using galactose- and glucose-derived initiators **A5** and **A6**, respectively [108]. In all experiments, the first block (**M16**) was polymerized at 60 °C since reaction at higher temperatures reduced the proportion bromine groups at the  $\omega$ -end, whereas chain extension with **M17** (benzyl methacrylate) was carried out at 90 °C (toluene, CuBr(**L4**) as the catalyst; (Entry 58, 81 in Table 2). Both polymerizations proceeded with pseudo-first order kinetics and led to uniform copolymers with predetermined molar mass. Only low degrees of polymerization were targeted for each block, though ( $DP_n = 5$ – $28$ ). After deprotection of the carbohydrate residue (50% TFA, room temperature), carbohydrate-decorated micelles were prepared by dialysis solvent exchange with water: DLS indicated a unimodal size distribution with hydrodynamic diameters in the range 35 nm–41 nm.

Ladmiral *et al.* [107] described the synthesis of a series of *N*-hydroxysuccinimidyl ester-terminated glycopolymers. To this aim, glucose (**M13**) and galactose (**M20**) monomers were polymerized in toluene at 70 °C in the presence of the activated  $\alpha$ -bromoester **A12**. Polymerizations proceeded with pseudo-first order kinetics and a linear increase of molar mass with conversion but the efficiency of the initiator was low (37%–53%). Glycopolymers with  $M_n$  in the range 7000–15,000 Da and  $D = 1.10$ – $1.31$  were obtained at high conversions (Entry 51–53, 62–64, Table 2). Deprotection of the sugar moieties was carried out with formic acid at room temperature. Under the same conditions, fluorescent statistical copolymers were synthesized by copolymerizing glycomonomers **M13** and **M20** with fluorescent comonomer **M27** ( $p = 90\%$ ,  $D < 1.19$ ).

Chen *et al.* [105] combined ring opening and atom transfer radical polymerizations for the synthesis of amphiphilic linear and star block copolymers (Entry 54–55, Table 2). Hence, bi- and tetrafunctional initiators **I1** and **I2** (Scheme 9) were used in the ring opening polymerization of  $\epsilon$ -caprolactone **M19** (110 °C, 24 h) to obtain hydroxyl-terminated uniform polyesters ( $D < 1.16$ ; Entry 48–49, Table 2). The latter were then reacted with 2-bromo-2-methylpropionyl bromide to give ATRP macro-initiators **A7<sub>a</sub>** and **A7<sub>b</sub>**. Chain extension, with galactose-derived methacrylate **M20** (90 °C, anisole) yielded ABA and 4-arm star block glycopolymers. Maximum conversion in ATRP experiments was achieved after 30 min ( $p = 65\%$  and  $51\%$  for linear and star polymers, respectively) with no further monomer was consumption later-on. The lack of high molar mass peaks in SEC traces suggests that no star-star coupling took place. Finally, the carbohydrate residues in the copolymer were deprotected with 80% formic acid at room temperature.

**Scheme 9.** Initiators used by Chen *et al.* [105] for the ring-opening polymerization of  $\epsilon$ -caprolactone **M19**.

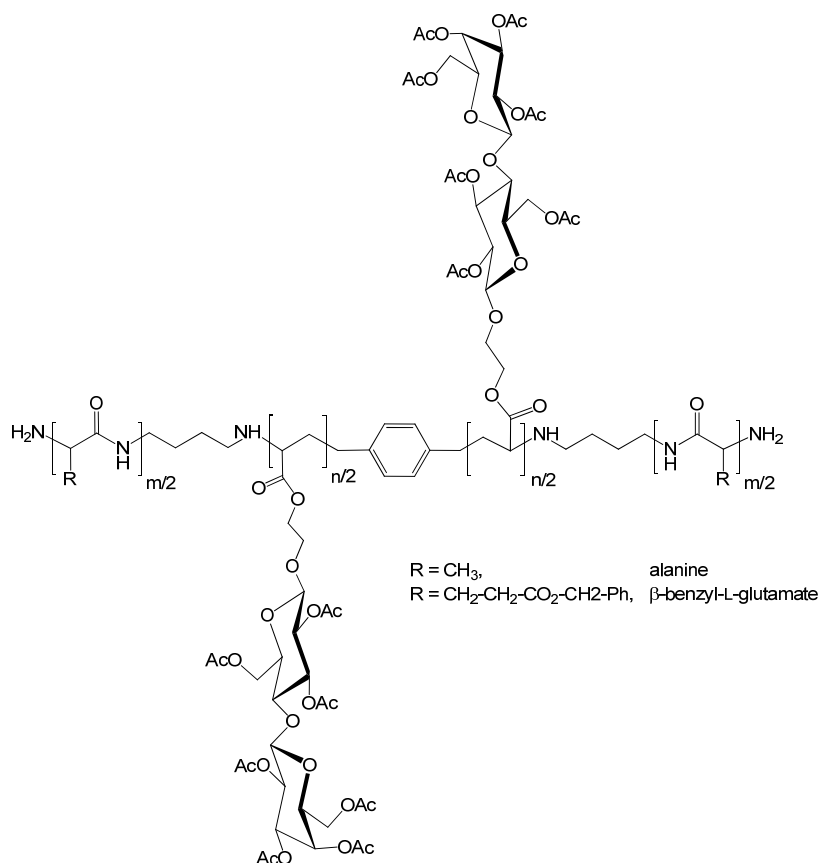


Chaikof *et al.* [119,120] prepared well-defined glycopolymer-polypeptide triblock copolymers of structure poly(L-alanine)-*block*-poly**M21**-*block*-poly(L-alanine) and poly(L-glutamate)-*block*-poly**M21**-*block*-poly(L-glutamate) by combining ATRP with the ROP of *N*-carboxyanhydrides (Entry 84–87, Table 2). First,  $\beta$ -lactoside **M21** was polymerized using **A8** as bifunctional initiator and CuBr(**L2**) as the catalyst (100 °C, chlorobenzene). Second, the obtained glycopolymers were converted into ROP macroinitiators by introducing a primary amine at their chain ends. Third, chain extension with L-alanine *N*-carboxyanhydride **M22** or  $\beta$ -benzyl-L-glutamate *N*-carboxyanhydride **M62** (DMF, R.T., 48–64 h) afforded the target block copolymers poly**M22**-*block*-poly**M21**-*block*-poly**M22** and poly**M62**-*block*-poly**M21**-*block*-poly**M62** (Scheme 10). Benzyl groups were then removed by hydrogenation (Pd/C, H<sub>2</sub>, RT) and carbohydrate residues were deprotected with hydrazine (DMSO, 0 °C). The resulting amphiphilic triblock glycopolymers self-assembled in aqueous solution to form nearly spherical aggregates 100–600 nm in diameter that specifically interacted with RCA<sub>120</sub> lectins.

Muller *et al.* [111] employed silsesquioxane-derived macroinitiators for the synthesis of glycopolymer-inorganic hybrid stars. To this end, silsesquioxane nanoparticles were reacted with 2-Bromo-2-methylpropionyl bromide in Py/CHCl<sub>3</sub> to yield initiator **A14** ( $M_n = 10,500$  Da,  $D = 1.25$ ). The latter was used for the polymerization of glucofuranose methacrylate **M13** (ethyl acetate, 60 °C, 25 min) in the presence of CuBr(**L8**) to obtain glycostars with molar masses up to 600,000 Da and  $D \leq 1.26$  (Entry 65–66, Table 2). The reaction worked best when stopped at low conversion and when high monomer to initiator ratios were used. The efficiency of the initiating sites (43%–44%) was estimated by comparing the experimental and theoretical  $DP_n$  of the cleaved arms; the same estimation indicated  $\sim 25$  arms per star. Both protected and deprotected (80% formic acid) glycostars adopted a

spherical structure in THF and water solution, respectively, of comparable size (30–40 nm). However, deprotected glycostars in water partially aggregated via hydrogen-bonding interactions.

**Scheme 10.** Structure of the ABA triblock glycopolymers prepared by Chaikof *et al.* (Entry 84–87, Table 2) [119,120].

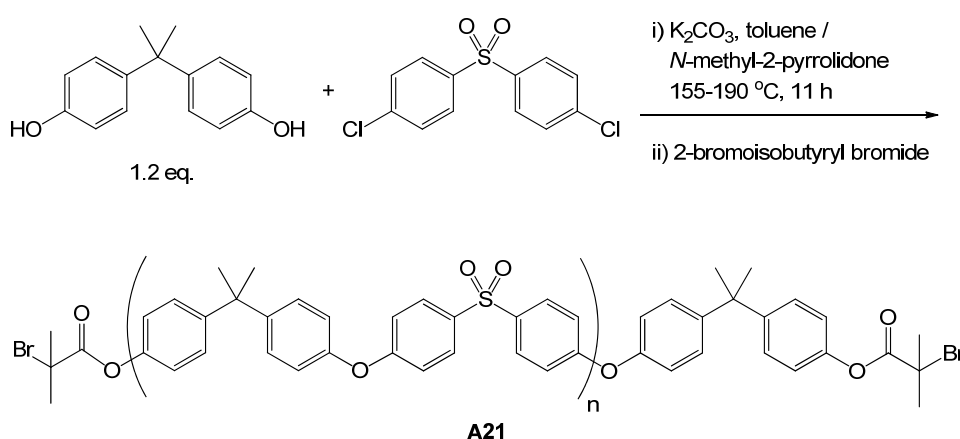


The same group [112] synthesized hyper-branched glycopolymers by self-condensing vinyl copolymerization (SCVCP) of an acrylic inimer **A15** with a protected glucofuranoside **M9**. In a preliminary study, the polymerization of **M9** using **A1** as the initiator and CuBr(**L3**) as the catalyst was investigated (ethyl acetate, 60 °C; Entry 67–69, Table 2). By varying the monomer to the initiator ratio, polymers with molar mass up to 30,000 Da were obtained in a controlled fashion ( $M_n/M_{n,th} \leq 1.3$ ), but molar mass dispersity increased monotonically with increasing molar mass ( $M_n = 7000$  Da,  $D = 1.13$ ;  $M_n = 30,000$  Da,  $D = 1.37$ ). The same conditions were then applied to the SCVCP of **A15** and **M9** (Entry 70–71, Table 2). As expected, the MHS exponent for the branched polymers in THF was found to be significantly lower than that for linear poly**M9** for  $M > 10^4$  Da, indicating more compact polymers. By increasing the monomer to inimer ratio higher molar mass copolymers could be obtained, but when ratios higher than 5 were tested multimodal mass distributions were observed in SEC. Finally, water soluble branched glycopolymers were obtained by deprotection with 80% formic acid at room temperature. This study was extended to the SCVCP of methacrylate inimer **A16** with glucofuranoside methacrylate **M13** using  $(\text{PPh}_3)_2\text{NiBr}_2$  as the catalyst (ethyl acetate, 100 °C) [113]. Higher polymerization rates were observed in this case (total conversion after 2–5 h) when compared to the analogous study with acrylate species and polymers with  $M_n$  up to 20,000 Da and  $D \leq 2.12$  were obtained (Entry 72–73, Table 2).

In an extension to this study, Muthukrishnan *et al.*, (Entry 74, Table 2) [114], synthesized well-defined cylindrical brushes by using a macromolecular initiator (poly**A16**) for the polymerization of glucofuranoside methacrylate **M13** in the presence of CuBr(**L8**) (ethyl acetate, 60 °C, 10–40 min). Reactions were stopped at low conversion ( $p < 11\%$ ) and analysis of the side chains detached by basic solvolysis indicated a grafting efficiency  $f \cong 0.20\text{--}0.40$ . After deprotection of the carbohydrate residues, stretched wormlike structures were observed. In a similar way [115], poly**M13** was grafted from the surface of multiwalled carbon nanotubes (MWNTs) functionalized with 2-bromo-2-methylpropionyl moieties (**A19**). In some cases **A1** was also added as sacrificial initiator (Entry 75, Table 2). Kinetic investigations revealed that the content of polymer grafted on MWNTs increased with monomer conversion, that grafted chains of up to 37,000 Da were obtained and that molar mass dispersity increased with conversion ( $\bar{D} = 1.27$  for  $p = 0.18$ ;  $\bar{D} = 1.45$  for  $p = 0.85$ ). Hyperbranched glycopolymers were also grafted from MWNTs by self-condensing vinyl copolymerization (SCVCP) of **M13** and inimer **A16** in the presence of  $(\text{PPh}_3)_2\text{NiBr}_2$  (EtOAc, 100 °C; Entry 76, Table 2). After deprotection with 80% formic acid, MWNTs with high grafting density of hydroxyl groups and a core-shell structure were obtained that could be redispersed in water, methanol, DMSO and DMF.

Wang *et al.* [116] reported the synthesis of an amphiphilic ABA triblock glycopolymer starting from a bromo-terminated difunctional polysulfone macroinitiator (Entry 77, Table 2). First, bifunctional polysulfone (PSF) macroinitiator **A21** was obtained from the reaction of bisphenol A and 4,4-dichlorophenyl sulfone in basic conditions (Scheme 11) followed by esterification with 2-bromoisobutyryl bromide. Chain extension with a protected glucofuranoside derivative **M13** (anisole, 90 °C, 24 h) catalyzed by CuCl(**L10**) afforded a triblock copolymer with  $M_n = 12,500$  Da and  $\bar{D} = 1.18$ . Deprotection with formic acid yielded an amphiphilic triblock glycopolymer that self-assembled into spherical aggregates in aqueous solution.

**Scheme 11.** Synthesis of bifunctional polysulfone macroinitiator **A21** from Bisphenol A and 4,4-dichlorophenyl sulfone according to Wang *et al.* [116].



Linear and comb-like glycopolymers were synthesized by Ke *et al.*, (Entry 78–80, Table 2) [106]. Polymerization conditions were similar in all cases and only the graft-copolymer synthesis will be described in here. Poly**St-block-polyHEMA** macroinitiator (**A24**) was synthesized by the chain extension of poly**St-Br** with HEMA (**M33**, 2-hydroxyethyl methacrylate) using CuBr(**L3**) as the catalyst (chlorobenzene, 80 °C) followed by esterification of the polyHEMA block with 2-bromoisobutyryl

bromide. The resulting macroinitiator was then used in the polymerization of **M32** under similar conditions to obtain poly**St-block-(polyHEMA-graft-polyM32)** with  $M_n = 25,000$  Da and  $D = 1.43$ . All glycopolymer samples were then used for the preparation of honeycomb-patterned films by the breath figure method. Preliminary studies demonstrated that the glucose-decorated films had “specific” interactions with ConA.

Pfaff *et al.* [121] grafted linear and branched glycopolymers onto poly(divinylbenzene) (PDVB) microspheres ( $d = 1.5$   $\mu\text{m}$ ) through standard and self-condensing vinyl copolymerization (SCVCP) ATRP, respectively. To this aim, a kinetic study of the SCVCP of acetylglucosamine-derived monomer **M30** and **A16** in different ratios was first investigated (DMSO, RT; Entry 92, Table 2). The study was then extended to the use of PDVB microspheres and after deprotection with MeONa, *N*-acetyl- $\beta$ -D-glucosamine-displaying microspheres were obtained that could be easily dispersed in water and bind wheat germ agglutinin (WGA). In an extension to this work [122], poly(**M30**) chains were grafted from polystyrene latex nanospheres ( $d = 100$  nm) pre-functionalized with 2-bromoisobutyryloxy groups (Entry 93; Table 2). Analysis of the free chains indicated a uniform glycopolymer ( $D = 1.12$ ) of  $M_n = 96,700$  Da, which corresponds to an initiator efficiency of  $\sim 0.45$ . SEM showed that the diameter of the nanospheres had doubled following the grafting process and a grafting density of 0.54 chains per  $\text{nm}^2$  of surface area was calculated. Following Zemplén deacetylation, the latex particles were used as carriers for catalytically active gold nanoparticles ( $d = 6.3$  nm; synthesized *in situ* by the reaction of  $\text{HAuCl}_4$  and  $\text{NaBH}_4$ ) and for binding WGA.

Wang *et al.* [11] reported the synthesis of an ABA triblock copolymer based on acrylic acid **M97**, 3-acrylamidophenylboronic acid **M95**, and  $\beta$ -galactoside acrylate **M98** for insulin release (Entry 56–57, Table 2). First, **M98** was homopolymerized in the presence of bifunctional initiator **A8** and  $\text{CuBr(L2)}$  (chlorobenzene, 80 °C) to afford a fairly uniform polymer ( $D = 1.17$ ) with  $M_n = 5500$  Da. Second, *t*-butyl acrylate **M57** was polymerized in the presence of the macroinitiator poly**M98-Br** and (butanone/2-propanol 7:3; 90 °C,  $\text{CuBr(L3)}$ ) to yield the triblock copolymer poly**M57-block-polyM98-block-polyM57** ( $M_n = 21.6$ ,  $D = 1.36$ ). *t*-Butyl groups were then removed with trifluoroacetic acid and 3-aminophenylboronic acid was coupled to the acrylic acid units (EDC/HOBT, DMF) to afford poly(**M97-stat-M95**)-block-poly**M98-block-poly(M97-stat-M95)**. After deprotection of the galactose moieties, insulin-loaded nanoparticles were prepared by nanoprecipitation in water. As expected, the release of insulin in solution was enhanced by acidic pH ( $\sim 95\%$  of the insulin released after 8 h at pH 1–3) and by and increasing concentration of glucose at physiological pH (thanks the boronic acid groups).

### 5.1.2. Styrenic Monomers

Menon *et al.* [142] described the synthesis of a photoresponsive amphiphilic glycopolymer and examined its self-assembly in aqueous solution (Entry 130–131, Table 2). To this end, styrenic glucufuranoside **M109** was polymerized in the presence of **A1** as the initiator and  $\text{CuBr(L3)}$  as the catalyst (THF, 60 °C). The resulting poly**M109-Br** ( $M_n = 12,300$  Da,  $D = 1.19$ ) was then used as macroinitiator for the polymerization of pyrenylmethyl methacrylate **M110** under the same conditions to give poly**M109-block-polyM110** ( $M_n = 21,200$  Da,  $D = 1.46$ ). After deprotection under acidic conditions (80%  $\text{HCOOH}$ ), an amphiphilic glycopolymer was obtained that self-assembled in aqueous



solution into spherical aggregates. The latter could be disrupted by cleaving the pyrenylmethyl ester bonds under UV irradiation.

Houga *et al.* [34,146] described the synthesis and self-assembly of a dextran/polySt diblock copolymer (Entry 129, Table 2). To this end, a 2-bromo-2-methylpropionamide group was introduced at the reducing end of dextran ( $M_n = 6600$  Da,  $D = 1.4$ ) by reductive amination to afford, after silylation the hydroxyl groups, macroinitiator **A32**. The latter was used for the polymerization of styrene catalyzed by CuBr(**L3**) (toluene, 90–100 °C, 20–90 min) to afford non-uniform polymers ( $1.4 \leq D \leq 1.9$ ) with  $M_n$  in the range of 17,000–160,000 Da. After deprotection with HCl the amphiphilic glycopolymers self-assembled in water/DMSO (THF) to give micelle-like aggregates and polymersomes, depending on the exact system composition.

## 5.2. ATRP Starting from Unprotected Glycomonomers/Glycoinitiators

### 5.2.1. (Meth)acrylamide Monomers

Yu *et al.* [104] prepared three novel glycomonomers containing  $\alpha$ -mannoside (**M64**),  $\alpha$ -galactoside (**M65**), and  $\alpha$ -glucoside (**M66**) residues and studied their grafting from silica wafers by surface initiated ATRP (Entry 47, Table 2), the wider aim being to prepare artificial glycocalyx. To this end, silicon wafers were functionalized with 2-chloropropionate groups (**A28**) and used as substrate for ATRP polymerizations. Methyl 2-chloropropionate was used as sacrificial initiator and the best results were obtained by conducting the polymerization in water (RT, 24 h) with CuCl(**L11**) as the catalyst ( $M_n = 51,000$  Da,  $D = 1.5$ ). The glycopolymer brushes showed ultralow adsorption of bovine serum albumin (BSA) and fibrinogen (Fb) and retained specific lectin recognition capacity. In a later study [147], their interaction with blood was also examined and it was found that the nature of the sugar residue (Glc, Man, or Gal) has an effect on the amount and type of plasma proteins being adsorbed, with glucose-functionalized brushes leading to the lowest adsorption.

### 5.2.2. (Meth)acrylate Monomers

The first examples in this class were reported by Armes and coworkers: [123,124,126] 2-gluconamidoethyl methacrylate **M23** and 2-lactobionamidoethyl methacrylate **M25** were polymerized at 20 °C using three different ATRP initiators (**A9<sub>n</sub>**, **A10<sub>n</sub>** and **A11**) and CuBr(**L2**) in methanol, methanol/water, water, and *N*-methyl-2-pyrrolidone. For **M23** a higher proportion of water in the system resulted in a faster polymerization rate and a higher molar mass dispersity (Entry 94–96, Table 2). Chain extension of poly**M23**·Br with 2-(diethylamino) ethyl methacrylate (**M24**) in methanol afforded a pH-responsive diblock glycopolymer ( $M_n = 17,300$  Da,  $D = 1.30$ ). Similar results were obtained for the homopolymerization of **M25** (using **A10<sub>n</sub>** or **A11**), but in this case methanol was not tested due to solubility problems (Entry 105–107, Table 2). The blocking efficiency of poly**M25**·Br was investigated by sequential addition of other methacrylates, namely glycerol monomethacrylate **M26**, 2-(diethylamino) ethyl methacrylate **M24** and **M23** (Entry 98, 108–109, Table 2). Finally, the pH- and temperature-dependent self-assembly of the block copolymers in water was demonstrated [126].

Building on these results, Narain [130] devised a versatile new approach for the preparation of well-defined streptavidin-glycopolymer bioconjugates. To this end **M25** was polymerized using

biotin-PEG macroinitiator **A17** ( $M_n = 5100$  Da,  $D = 1.07$ ) and CuBr(**L2**) as the catalyst (*N*-methyl-2-pyrrolidinone, 20 °C; Entry 110, Table 2). Fairly uniform polymers ( $D \leq 1.32$ ) with  $M_n$  up to 24,000 Da whose rate of binding to streptavidin (tetrameric lectin) decreased with increasing molar mass.

The synthesis of well-defined glycopolymers biotinylated at their  $\alpha$ -end was also the subject of a study by Maynard *et al.* (Entry 118–119; Table 2) [136]. Methacrylates with pendent *N*-acetyl- $\beta$ -D-glucosamine **M30** (peracetylated) and **M31** were polymerized in DMSO (23 °C) and MeOH (30 °C), respectively, using CuBr(**L9**) or CuBr(**L2**) as the catalysts and biotin derivative **A18** as the initiator. Polymerization in DMSO with CuBr(**L9**) was much faster than that in MeOH with CuBr(**L2**) (15 min vs. 90 min) but fairly uniform polymers were obtained in all cases ( $D \leq 1.23$ ) and molar mass increased linearly with conversion. Nevertheless, the latter was systematically much higher than the theoretical one. Following modified Zemplén deacetylation (when applicable). The ability of the biotinylated glycopolymers to interact with streptavidin was confirmed by SPR and  $^1\text{H-NMR}$ .

The same group devised a different strategy for the bioconjugation of glycopolymers [137]: *N*-Acetyl- $\beta$ -D-glucosamine derivative **M31** was polymerized in the presence of an initiator carrying a pyridyl disulfide group (**A26**, MeOH/H<sub>2</sub>O 3:1, 30 °C, 90 min) to yield a uniform polymer ( $D = 1.12$ ) with  $M_n = 10,000$  Da (Entry 120, Table 2). After purification the glycopolymer was conjugated to a 5'-thiol modified short interfering RNA (siRNA) double strand via disulfide bond exchange and used for surface micro-patterning through micro-contact printing.

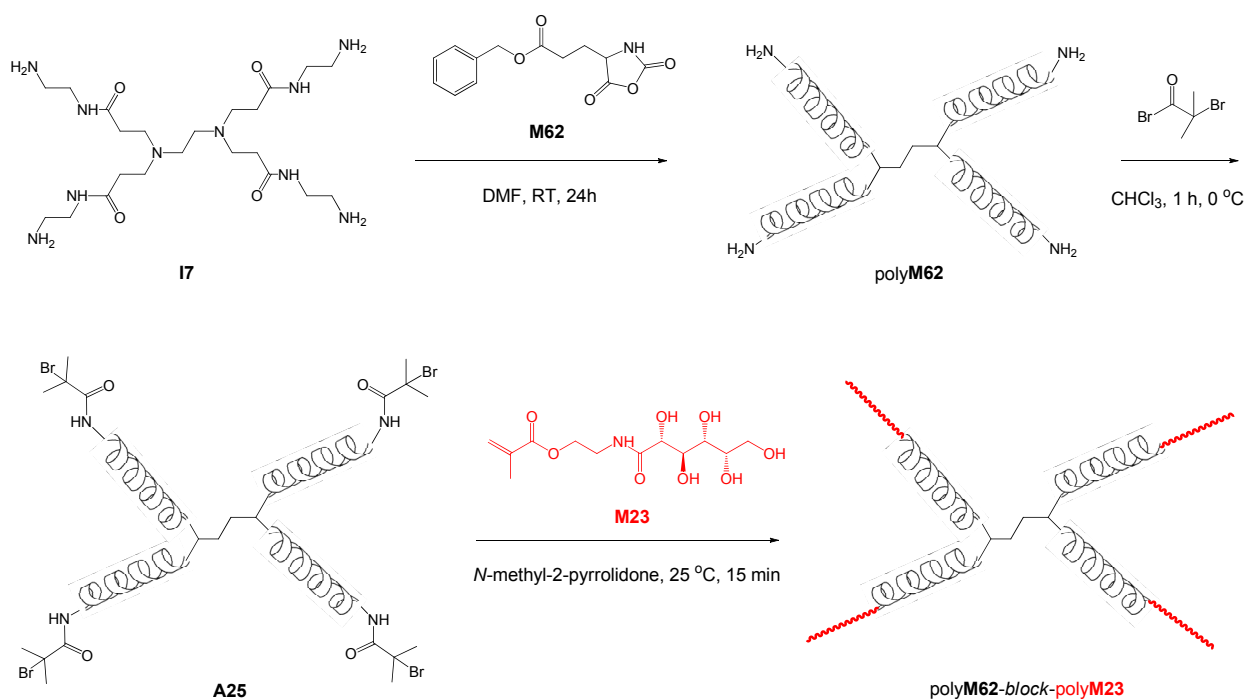
Mateescu *et al.* [127] immobilized a self-assembled monolayer of  $\omega$ -mercaptoundecyl bromoisobutyrate onto a gold surface and used it to grow glycopolymer brushes based on D-gluconamidoethyl methacrylate **M23** and 2-lactobionamidoethyl methacrylate **M25** (CuBr(**L2**), water or water/methanol). The resulting surface roughness was below 1 nm (as measured by AFM) suggesting the preparation of very smooth glycopolymer films. Finally, the latter exhibited strong binding interactions with specific lectins (ConA and RCA<sub>120</sub>).

Qiu *et al.* [125] synthesized star-shaped polypeptide/glycopolymer block copolymers (Scheme 12). To this aim, poly( $\beta$ -benzyl-L-glutamate) was synthesized by the ring opening polymerization of **M62** initiated by a tetra-functional polyamidoamine **I7**. The resulting polymer was transformed into macroinitiator **A25** and used in the polymerization of D-gluconamidoethyl methacrylate **M23** to afford a 4-arm star with a  $M_n = 64,500$ – $87,400$  Da and  $D = 1.18$ – $1.45$  (Entry 97, Table 2). In aqueous solution these biohybrid polymers self-assembled into large spherical aggregates with a helical polypeptide core surrounded by a multivalent glycopolymer shell. Following deprotection of the polypeptide block, the same polymers showed a pH-sensitive self-assembly behavior. Finally, these nanoparticles showed a higher doxorubicin loading efficiency and a longer drug-release time than those obtained with the analogous linear polymers.

Leon *et al.* [138,139] reported the synthesis of amphiphilic block glycopolymers derived from D-glucosamide methacrylate **M63**. According to one strategy (Entry 121–124, Table 2), **M63** was homopolymerized using a monofunctional (**A1**) or a bifunctional initiator (**A27**) at 40 and 50 °C respectively (DMF, CuBr(**L3**)). The resulting mono- and bi-functional macroinitiators were used to synthesize amphiphilic diblock and triblock glycopolymers with *n*-butyl acrylate **M47** (DMF, 90 °C). Fairly uniform copolymers were thus obtained ( $D \leq 1.38$ ) with good to excellent control over the molar mass ( $0.87 \leq M_n/M_{n,th} \leq 0.98$ ). The self-assembly of these glycopolymers in NaCl 0.1 mol L<sup>-1</sup>

led to aggregates with  $d = 38\text{--}44$  nm. Also, their interaction with ConA was found to depend on molar mass and copolymer composition. According to an alternative strategy (Entry 125–126, Table 2), *n*-butyl acrylate was polymerized in bulk using a monofunctional (**A20a**) or a bifunctional initiator (**A30**) at 100 °C and 70 °C, respectively. The resulting macroinitiators were then chain extended with **M63** (DMF, 90 °C) to afford amphiphilic di- and tri-block glycopolymers that self-assembled in aqueous solution to give spherical micelles polymersomes.

**Scheme 12.** Synthetic strategy used by Qui *et al.* [125] for the synthesis of four-arm star biohybrids.



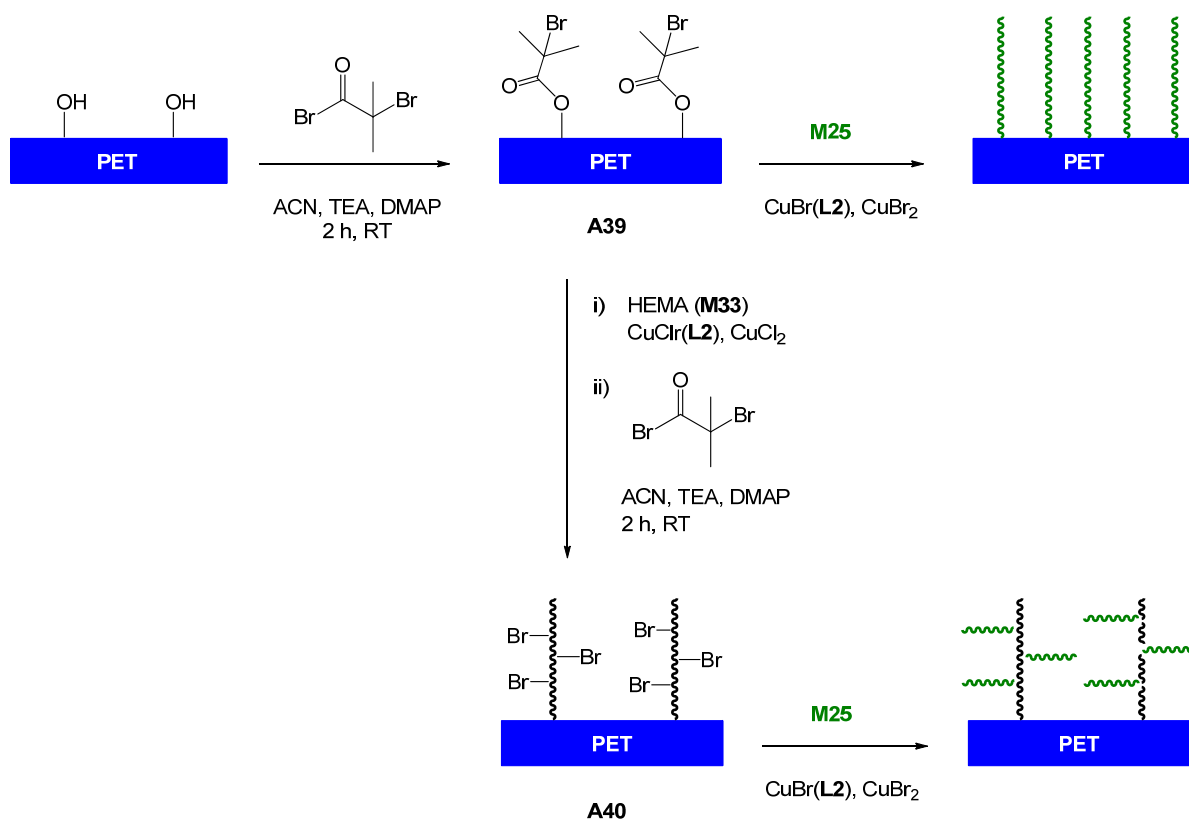
The same group [140] demonstrated the use of these amphiphilic block glycopolymers as polymeric surfactants for the emulsion polymerization of butyl methacrylate and the preparation of glycosylated latex particles. To this aim, poly**M63**-*block*-poly**M46** was prepared as described above ( $M_n$  32,700 Da, 20% butyl methacrylate w/w; Entry 127, Table 2) and the monomer content in emulsion experiments was adjusted to 5% w/w. An increasing amount of glycopolymer surfactant (2% to 8% w/w of butyl methacrylate) was found to increase the rate of polymerization and to reduce the z-average particle diameter of the final latex. By contrast, the polydispersity index of all latex samples was lower than 0.1, implying narrow particle size distribution. Polymer films were prepared from these glycosylated latexes which specifically interacted with ConA.

The same group [141] extended the study of amphiphilic glycopolymers based on poly**M63** to their use for the preparation of porous films and microspheres using the breath figures technique. To this aim poly**M15**-**A1** (PMMA) was chain extended with glucosamine-derived methacrylate **M63** using CuCl(**L3**) as the catalyst (DMF, 40 °C) to afford a uniform block copolymer with  $M_n = 16,500$  Da and  $D = 1.12$  (Entry 128, Table 2). Polymer blend solutions of PMMA and glycopolymer (poly**M15**-*block*-poly**M63** or poly**M15**-*stat*-poly**M63**) were prepared in THF/H<sub>2</sub>O and were cast onto glass wafers inside a closed chamber under controlled humidity. Depending on the morphology of the

copolymer (statistical or block), humidity of the atmosphere and the amount of water in THF, the authors were capable of tuning the final pattern structures from microporous films to microparticles. The availability of carbohydrate moieties on the surface of these structures was confirmed by their interaction with ConA lectin.

Yang *et al.* [131] grafted linear and comb-like glycopolymer chains onto poly(ethylene terephthalate) (PET) track etched membranes by surface-initiated ATRP (Entry 112–113; Table 2). To this end, 2-bromo-2-methylpropionate was immobilized onto the membrane surface (Scheme 13) and the resulting substrate **A39** was used for the polymerization of lactobionic acid derivative **M25** (water or *N*-methyl-2-pyrrolidone, RT) to yield linear glycopolymer brushes. Alternatively, poly(HEMA) was grafted from the surface of **A39** and transformed into poly(**A16**) by reaction with 2-bromo-2-methylpropionyl bromide. The resulting substrate **A40** was then used for the polymerization of **M25** as described above to yield comb-like polymer brushes. Polymerizations worked best in *N*-methyl-2-pyrrolidinone, whereas the use of water led to high radical concentration and loss of control. A relatively low grafting density of poly(**M25**) and, most likely, poly(HEMA) led to a “mushroom” conformation of the linear chains. Accordingly, the transformation of poly(**A16**) into poly(HEMA)-*graft*-poly(**M25**) resulted in a large increase in dry layer thickness of grafted polymer. Both linear and the comb-like grafted layers showed very high binding capacities for PNA lectin under static and dynamic conditions but negligible nonspecific protein binding.

**Scheme 13.** Strategy for the grafting of linear and comblike poly**M25** on track etched poly(ethylene terephthalate) membranes described by Yang *et al.* [131].

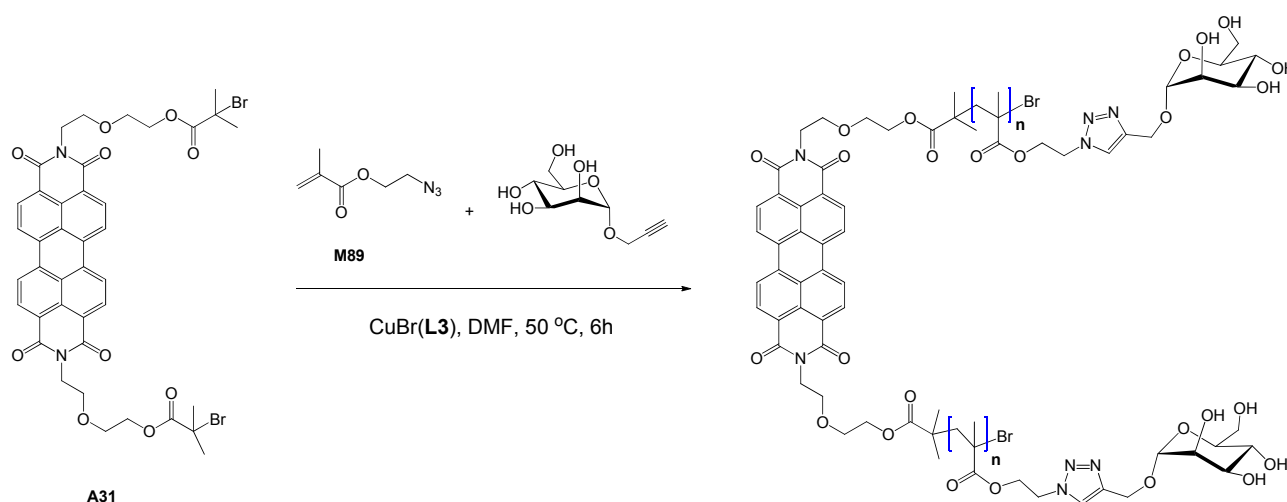


Klumperman *et al.* [129,148,149] described the synthesis of a series of cylindrical brushes carrying  $\alpha$ -methylglucoside-functionalized graft chains and investigated their thermal and mechanical

properties (Entry 101–104, Table 2). To this end, four macroinitiators based on HEMA (**M33**), MMA (**M15**), 4-vinylbenzyl chloride (**M58**), and maleic anhydride (**MANh**) were synthesized by ATRP or RAFT copolymerization, followed by chemical modification with 2-bromo-2-methylpropionyl bromide as needed. The macroinitiators were then used in the ATRP polymerization **M36** using CuBr(**L4**) as the catalyst (DMF, 60 °C, 1–1.5 h) to afford cylindrical glycopolymer brushes with different grafting densities. All glycopolymers showed similar thermal degradation profiles irrespective of the number of graft chains. The storage modulus in bulk at room temperature was found to be high for all glycopolymer brushes due to the great number of hydrogen bonding interactions that confer sufficient rigidity to the material in spite of its amorphous nature. Just above  $T_g$  both the storage modulus  $G'$  and the loss modulus  $G''$  increased rapidly with increasing frequency, with  $G'$  being dominant at low frequencies. Solutions of glycopolymer brushes in DMF showed non-Newtonian shear-thinning behaviour, in which the viscosities linearly decreased with increasing frequency up to about  $10 \text{ rad s}^{-1}$ ; afterwards the complex viscosity tended to increase and exhibited shear-thickening behavior. The same macromolecular architectures were also synthesized starting from macroinitiators prepared by RAFT polymerization mediated by cyanoisopropyl dithiobenzoate **R10** (AIBN **I4**, at 60 °C) [149].

The synthesis of a fluorescent glycopolymer in a “one pot” reaction by the combination of click chemistry and ATRP was described by Xu *et al.* [133] Hence 2-Azidoethyl methacrylate **M89** was polymerized using a fluorescent bifunctional initiator **A31** and in the presence of 2-propynyl- $\alpha$ -D-mannopyranoside (Scheme 14): the same copper complex catalyzed the ATRP process and the Huisgen 1,3-dipolar cycloaddition. Fairly uniform water soluble glycopolymers with  $M_n$  ranging from 20,000 Da to 50,000 Da and  $D = 1.21$ – $1.33$  were thus obtained that exhibited strong affinity to *E. coli* and low toxicity for 3T3 fibroblasts, macrophages and KB cells. This type of glycopolymer could be used for targeted cell imaging.

**Scheme 14.** One pot synthesis of a fluorescent glycopolymer as described by Xu *et al.* [133].



Yuan *et al.* [150] described the surface glycosylation of a poly(vinylidene difluoride) (PVDF) microporous membrane using Activators Generated by Electron Transfer Atom Transfer Radical Polymerization (AGET ATRP). To this aim, the surface methylene fluoride groups of PVDF were used as initiators for the polymerization of D-gluconamidoethyl methacrylate **M23** in the presence of

CuCl<sub>2</sub>(**L3**) and of ascorbic acid as the reducing agent (water of water/MeOH, 30 °C). The highest grafting density (2.40 μmol of **M23**/cm<sup>2</sup>) was obtained in H<sub>2</sub>O after 40 h of reaction and with ascorbic acid/CuCl<sub>2</sub> ratio of 13/29. It is worth noting that in H<sub>2</sub>O the polymerization rate slowed down with time due irreversible termination of propagating radicals. The hydrophilic character of the glycosylated membrane was confirmed by a reduction of water contact angle from 110° to 30°, which enhanced the anti-fouling properties and biocompatibility of the membrane.

The same group [151] also investigated the glycosylation of chloromethylated polysulfone (CMPSF) microporous membrane using surface-initiated ATRP. To this end, poly**M23** was grafted from the surface of CMPSF using CuCl(**L3**) as the catalyst (water, 30 °C). The grafting yield increased linearly during the first four hours but reached a plateau of 6 mg/cm<sup>2</sup> after 16 h. The capacity of such membrane to complex boric acid in aqueous solution increased when pH increased from 6 to 9 and with increasing ionic strengths (up to 100 mM NaCl). Interestingly, the membrane could be regenerated upon acid treatment (“acid leaching method”) without any degradation.

Kitano *et al.* [128,134] reported the synthesis of thiol-terminated glycopolymers (Entry 100 and 116; Table 2) and their grafting on a colloidal gold-immobilized glass substrate for the study of binding and adsorption processes by UV–Vis spectrophotometer with the help of a localized surface plasmon resonance. To this end, 2-(2-bromoisobutyroxy)ethyl disulfide **A34** was used to initiate the polymerization of glucoside methacrylate **M34a** and mannoside methacrylate derivatives **M34b** catalyzed by CuBr(**L2**) in MeOH, MeOH/H<sub>2</sub>O, *N*-methyl-2-pyrrolidinone or *N*-methyl-2-pyrrolidinone/H<sub>2</sub>O mixtures (RT, 5–24 h). Fairly uniform polymers were obtained from **M34b** ( $\bar{D} = 1.20–1.37$ ) having  $M_n$  in the range 7800–15,000 Da, whereas the results from **M34a** were mediocre ( $\bar{D} = 1.44–1.64$  with  $M_n = 1800–8600$  Da). Subsequently, the hydroxyl groups of poly**M34a** were sulfated with SO<sub>3</sub>/pyridine complex (DMF, RT,  $0.7 < DS < 3.9$ ) and both polymers were grafted to gold colloid-glass chip via their disulfide bond. The binding of ConA lectin to *D*-mannopyranoside-carrying poly**M34b** brushes was then studied, whereas it was demonstrated that sulfated poly**M34a** brushes adsorbed amyloid β-peptide molecules. The latter are suspected to cause the neurodegeneration in Alzheimer’s disease following their deposition in plaques in brain tissue [152].

O’Connell *et al.* [132] examined the adsorption kinetics and behavior of an α-D-mannoside-derived glycopolymer on planar surfaces of silica and cellulose- or poly(L-glutamic acid)-covered silica using Evanescent Wave Cavity Ring-Down Spectroscopy (EW-CRDS). To this end, poly**M67** was synthesized in a one-pot two-step reaction catalyzed by CuBr(**L7**): First 2-azidoethyl-*O*-α-D-mannopyranoside was coupled with propargyl methacrylate to yield **M67**, second its polymerization was initiated by the introduction of coumarin-derived initiator **A35** (DMSO, 60 °C, 30 min). A fairly uniform polymer was thus obtained having  $M_n = 28,800$  Da and  $\bar{D} = 1.25$  (Entry 114, Table 2) and carrying a coumarin tag at its α-end. Its adsorption kinetics were seen to be highly surface dependent with highest rates on cellulose-modified surfaces and on basic silica surfaces.

### 5.2.3. Styrenic Monomers

The synthesis of polystyrene particles decorated with pendant thio-glucoside and thio-lactoside residues was reported by Kohri *et al.* [153] Initially, polystyrene particles bearing ATRP initiating sites were prepared by emulsifier-free emulsion polymerization of **St** and 2-chloropropoxyethyl

methacrylate **A39**. The resulting latex was then used in the polymerizations of *S*-glucoside- derived (**M90**) or *S*-lactoside- derived (**M91**) monomers in water or methanol/water (1:4) mixtures catalyzed by CuCl(**L9**) (30 °C, 24 h). Glycopolymer-decorated particles were thus obtained having a hydrated graft layer of 15–65 nm and a core ~400 nm in diameter; these particles showed a highly specific response toward lectins ConA and PNA.

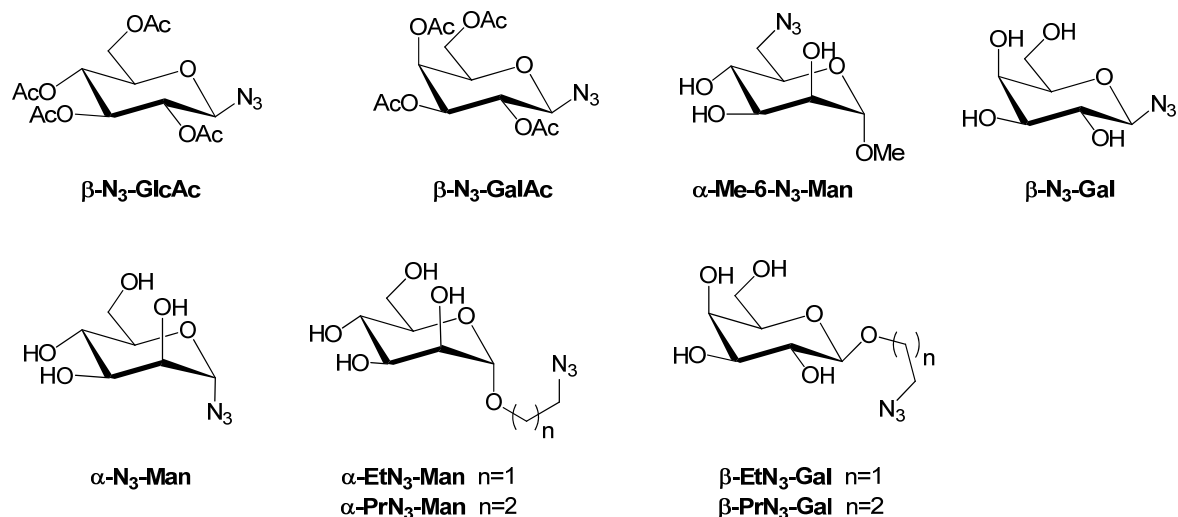
### 5.3. Glycopolymers from Post-Polymerization Reactions

Haddleton *et al.* [143] synthesized a series of glycopolymers by combining copper-catalyzed Huisgen 1,3-dipolar cycloaddition (“click” chemistry) and ATRP. To this end, alkyne side chain polymers were prepared either by the homopolymerization of (trimethylsilyl)ethynyl methacrylate **M28** or by its copolymerization with MMA **M15** or PEG methacrylate **M29** in presence of CuBr(**L7**) as the catalyst (initiator **A13**, toluene, 70 °C; Entry 133, 134, and 136, Table 2). A kinetic study showed first order plots for monomer consumption combined with a non-linear increase of the molar mass with conversion. Uniform polymers ( $D < 1.16$ ) with molar mass up to 17,600 Da were obtained but the control over the latter was rather poor ( $M_n/M_{n,th} > 1.5$ ). Following deprotection of the trimethylsilyl groups (AcOH, TBAF, THF), azido-functionalized monosaccharides (Scheme 15) were coupled to the ethynyl groups of the polymers via a Cu(I)-catalyzed “click” reaction. In particular, the same precursor polymer was functionalized with  $\alpha$ -mannoside and (or)  $\alpha$ -galactoside residues to afford a number of ligands differing only in the density of lectin epitopes. The interaction of these glycoligands with ConA ( $\alpha$ -mannoside selective) and RCA I ( $\alpha$ -galactoside selective) was tested: The rate of formation and stability of the ligand-ConA conjugates was directly proportional to the mannoside density in the polymer and the average number of ConA tetramers bound by each polymer chain reached a plateau for 75% mannoside content. In a later study, [154] the same glycoligands were tested for their ability to inhibit the interaction between human DC-SIGN (a C-type lectin receptor present on both macrophages and dendritic cells) and the HIV envelope glycoprotein gp120: The fully mannosylated polymer was found to have an  $IC_{50}$  of 37 nM, although it is not clear if this value refers to the concentration of carbohydrate residues.

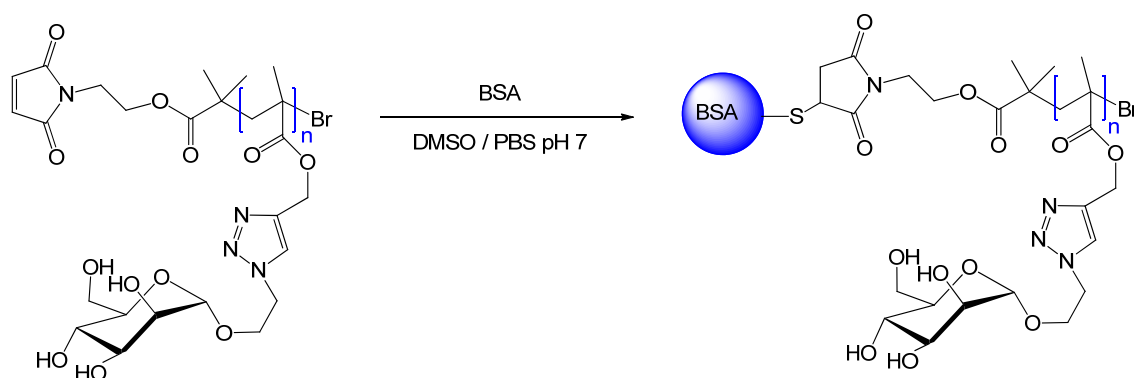
The same group [135] studied the synthesis of well-defined protein-glycopolymer biohybrid materials and their ability of binding mammalian lectins and inducing immunological reactions. Starting from the azidosugar  $\alpha$ -PrN<sub>3</sub>-Man (Scheme 15), two synthetic pathways were followed for the synthesis of mannoside-functionalized glycopolymers: Glycomonomer **M67** was obtained from the coupling of  $\alpha$ -PrN<sub>3</sub>-Man with (trimethylsilyl)ethynyl methacrylate and copolymerized with rodamine methacrylate **M93** (1 mole %) using protected maleimide initiator **A29** (MeOH/H<sub>2</sub>O 5:2, RT). A fairly uniform polymer ( $D = 1.20$ ) was thus obtained having a molar mass of 26,100 Da (Entry 117, Table 2). Alternatively, (trimethylsilyl)ethynyl methacrylate **M28** and rodamine methacrylate **M93** (1 mol %) were copolymerized first (toluene, 30 °C) and  $\alpha$ -PrN<sub>3</sub>-Man was clicked to the polymeric backbone after the removal of the silyl group ( $M_n = 16,400$  Da,  $D = 1.28$ ). Finally, the maleimide group at the  $\alpha$ -end of the glycopolymer was deprotected by simple heating and used for conjugation to BSA through its single cysteine residue (Scheme 16). Surface plasmon resonance tests carried out in the presence of a model mammalian lectin revealed a significant and dose-dependent binding of the latter

to the BSA-glycopolymer conjugates. ELISA tests also revealed that the latter were able to activate the complement system via the lectin pathway.

**Scheme 15.** Azidosugars used by Haddleton *et al.* for the functionalization of poly(alkyne methacrylate)s [135,143].



**Scheme 16.** Conjugation of a glycopolymer with bovine serum albumin (BSA) as described by Haddleton *et al.* [135].

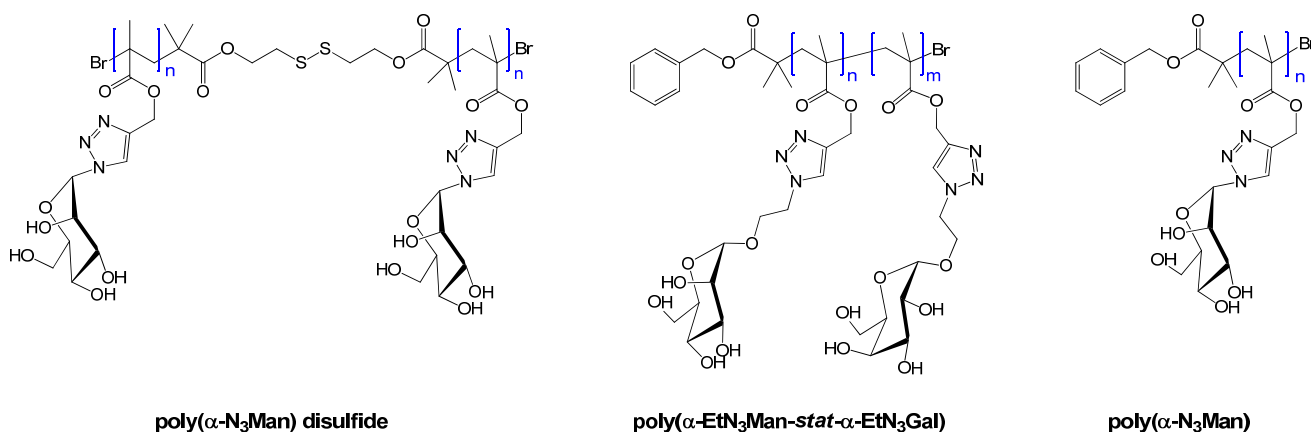


Gou *et al.* [145] studied the layer-by-layer assembly of glycopolymers and lectins by quartz crystal microbalance with dissipation monitoring (QCM-D). To this end, (trimethylsilyl)ethynyl methacrylate **M28** was polymerized using bifunctional disulfide initiator **A34** ( $\text{CuBr(L7)}$ , toluene,  $90^\circ\text{C}$ ) and the resulting polymer was deprotected as described above (Entry 138, Table 2). Azido-mannoside  $\alpha\text{-N}_3\text{-Man}$  (Scheme 15) was then clicked to the polymer backbone to afford the desired glycopolymer **poly( $\alpha\text{-N}_3\text{-Man}$ ) disulfide** ( $M_n = 35,700$  Da,  $D = 1.84$ ). **Poly( $\alpha\text{-N}_3\text{-Man}$ )** and **poly( $\alpha\text{-EtN}_3\text{-Man-stat-}\alpha\text{-EtN}_3\text{-Gal}$ )** were synthesized in a similar way (Scheme 17) [135]. Two approaches were then followed for preparing the LBL assemblies: either **poly( $\alpha\text{-N}_3\text{-Man}$ ) disulfide** was deposited first on the QCM-D gold chips, or the latter were chemically modified with the NHS ester of 11-mercaptoundecanoic acid and a first layer of ConA was immobilized on it. In both cases, what followed was the deposition of alternate layers of ConA (an  $\alpha\text{-Man}$  selective lectin), **poly( $\alpha\text{-EtN}_3\text{-Man-stat-}\alpha\text{-EtN}_3\text{-Gal}$ )** ( $M_n = 22,000$  Da,  $D = 1.29\text{--}1.34$ ), and PNA (an  $\alpha\text{-Gal}$  selective lectin). By varying the concentration of the polymer and lectins the mass and thickness of layers could



be tuned and the composition of the copolymer influenced the interaction with the lectins (e.g., the adsorption of PNA was maximum for a 50:50 Man/Gal copolymer). A study of the link between surface binding and solution inhibition was also conducted with the same set-up, but the preliminary results are inconclusive [155].

**Scheme 17.** Polymers synthesized by Gou *et al.* [145,155] in their study.



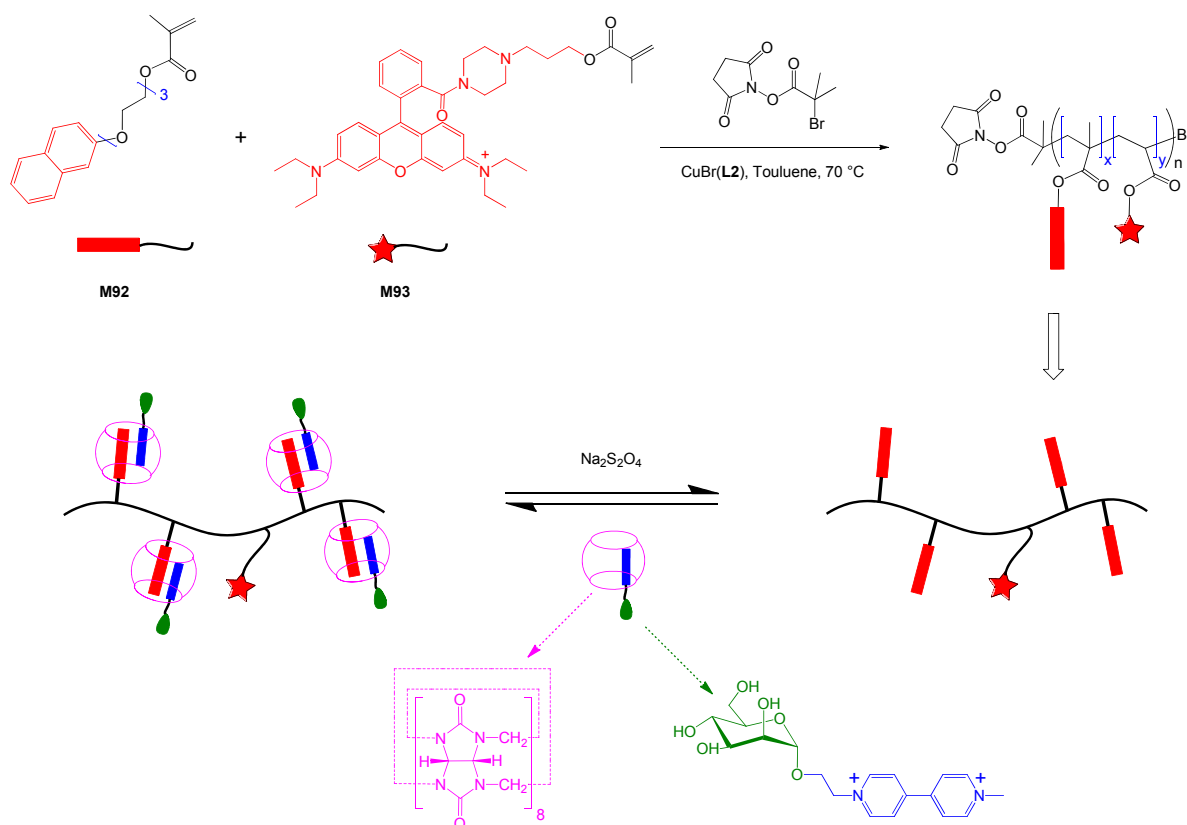
Scherman *et al.* [156] described a sophisticated strategy for the synthesis of a flexible and reversible supramolecular glycopolymer based on cucurbit(8)uril (supramolecular “handcuff”) and viologen  $\alpha$ -mannoside (Scheme 18). First, 2-naphthol methacrylate **M92** was either homopolymerized or copolymerized with fluorescent rhodamine methacrylate **M93** in the presence of **A33** and CuBr(**L2**) (toluene, 70 °C) to afford a uniform polymer scaffold with  $M_n = 4200$ –14,100 Da and  $D = 1.04$ –1.11. Second, the latter polymer was added to an aqueous solution of cucurbit(8)uril/viologen  $\alpha$ -mannoside complex to afford a multivalent glycopolymer complexes. Then, the binding of such glycopolymers with ConA was demonstrated.

Muñoz-Bonilla *et al.* [157] described the synthesis of diblock and triblock amphiphilic glycopolymers with pendant D-glucosamine or *N*-(4-aminobutyl)-D-gluconamide residues. To this end, 2-hydroxyethyl methacrylate **M33** polymerized using two poly(butyl acrylate) macroinitiators (poly**M47**-Br,  $M_n = 8200$  Da,  $D = 1.16$ ; or Br-poly**M47**-Br,  $M_n = 11,600$  Da,  $D = 1.16$ ) in the presence of CuCl(**L2**) in DMF at 80 °C. Both polymerizations proceeded with first order kinetics and a linear increase of molar mass with conversion to afford reasonably uniform polymers ( $D = 1.2$ –1.5). The hydroxyl groups of the polymer backbone were part activated with *p*-nitrophenyl chloroformate and amino-sugars were introduced by nucleophilic attack. The self-assembly of some of these glycopolymers in water was then studied by DLS: These copolymers engage in strong hydrogen bond interactions that could be disrupted by the addition of salt (NaCl 0.1 mol L<sup>-1</sup>). Interestingly, glycopolymers bearing *N*-glucosamine residues bound to ConA, although the exact extent and selectivity of such interaction was not quantified.

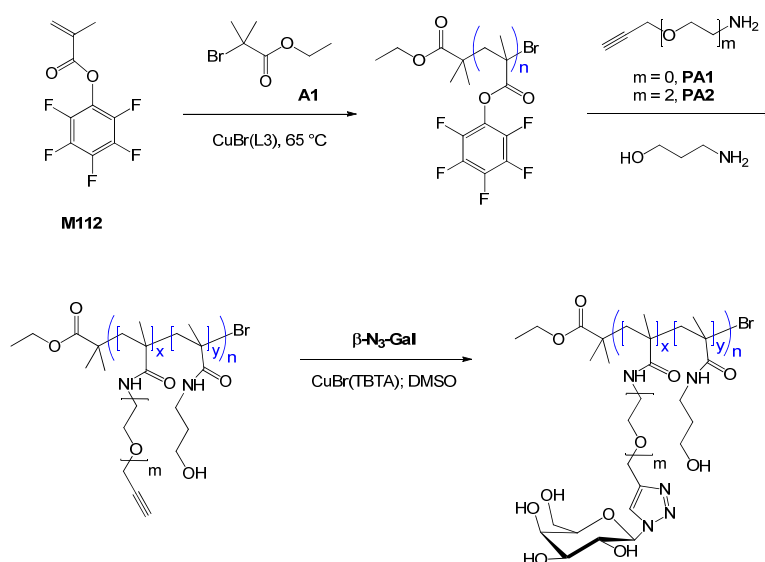
Richards *et al.* [144] studied the influence of carbohydrate density and linker length on the binding of a glycopolymer to toxin Ctx secreted by *Vibrio cholerae*. To this end, pentafluorophenyl methacrylate **M112** was polymerized in the presence of **A1** as the initiator and of CuBr(**L3**) as the catalyst (toluene, 65 °C). Fairly uniform polymers ( $D \leq 1.20$ ) with  $M_n$  in the range 7800–11,400 Da were obtained (Entry 135, Table 2) that were modified with a propargyl amine derivative (**PA1** or

**PA2**) and 3-aminopropanol (Scheme 19). The propargyl groups were then coupled with  $\beta$ -N<sub>3</sub>-Gal to afford glycopolymers with various linker lengths and sugar densities ( $M_n = 5000$ – $12,000$  Da,  $D \leq 1.32$ ). Increasing inhibition of the B subunit of Ctx was observed when glycopolymers with longer linkers were used. Also, the highest and lowest density polymers tested (100% and 10%) were most active on a per-sugar basis.

**Scheme 18.** Synthesis of a supramolecular glycopolymer as described by Scherman *et al.* [156].



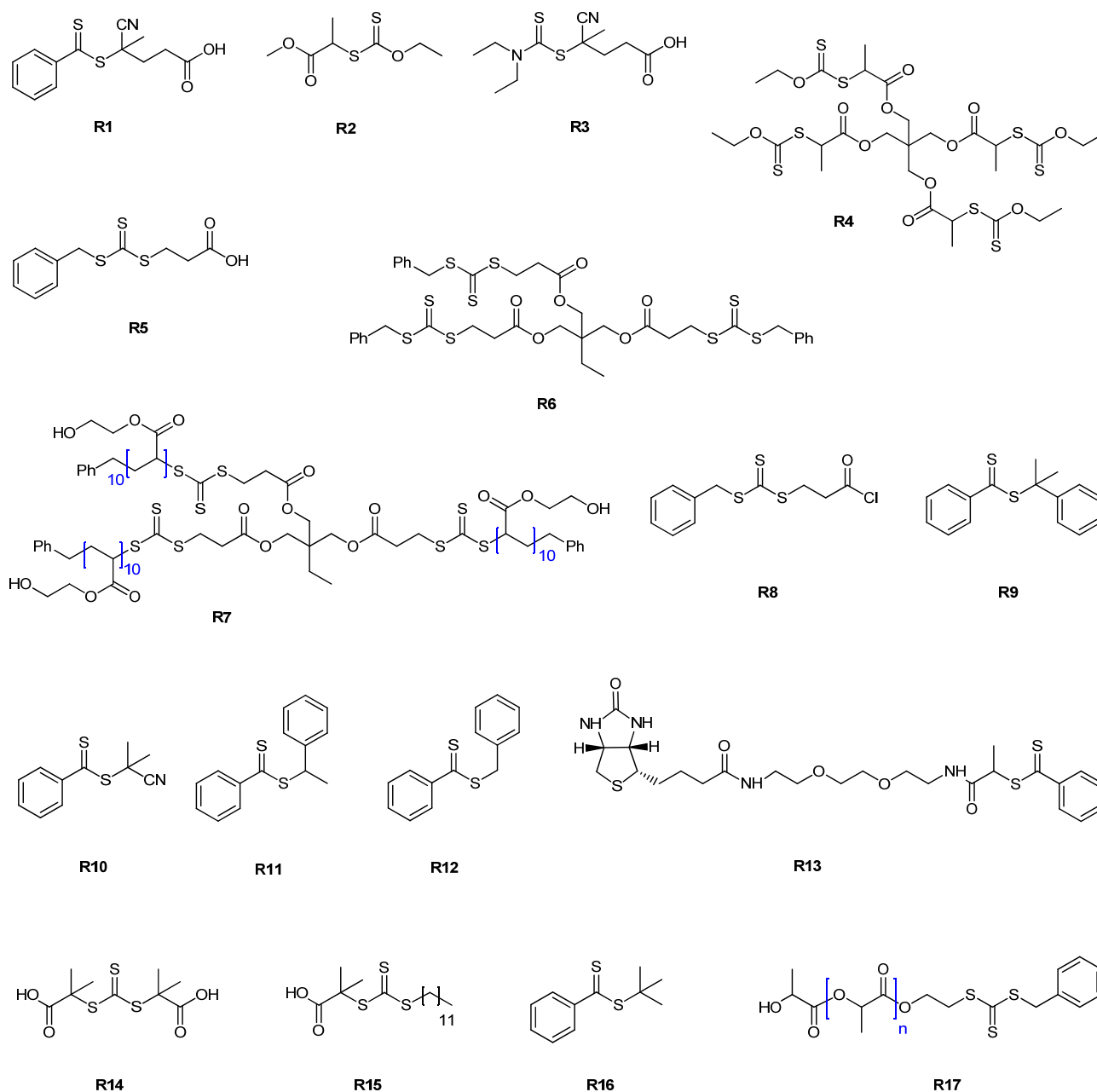
**Scheme 19.** Post-modification route described by Richards *et al.* [144] for the synthesis of glycopolymers.



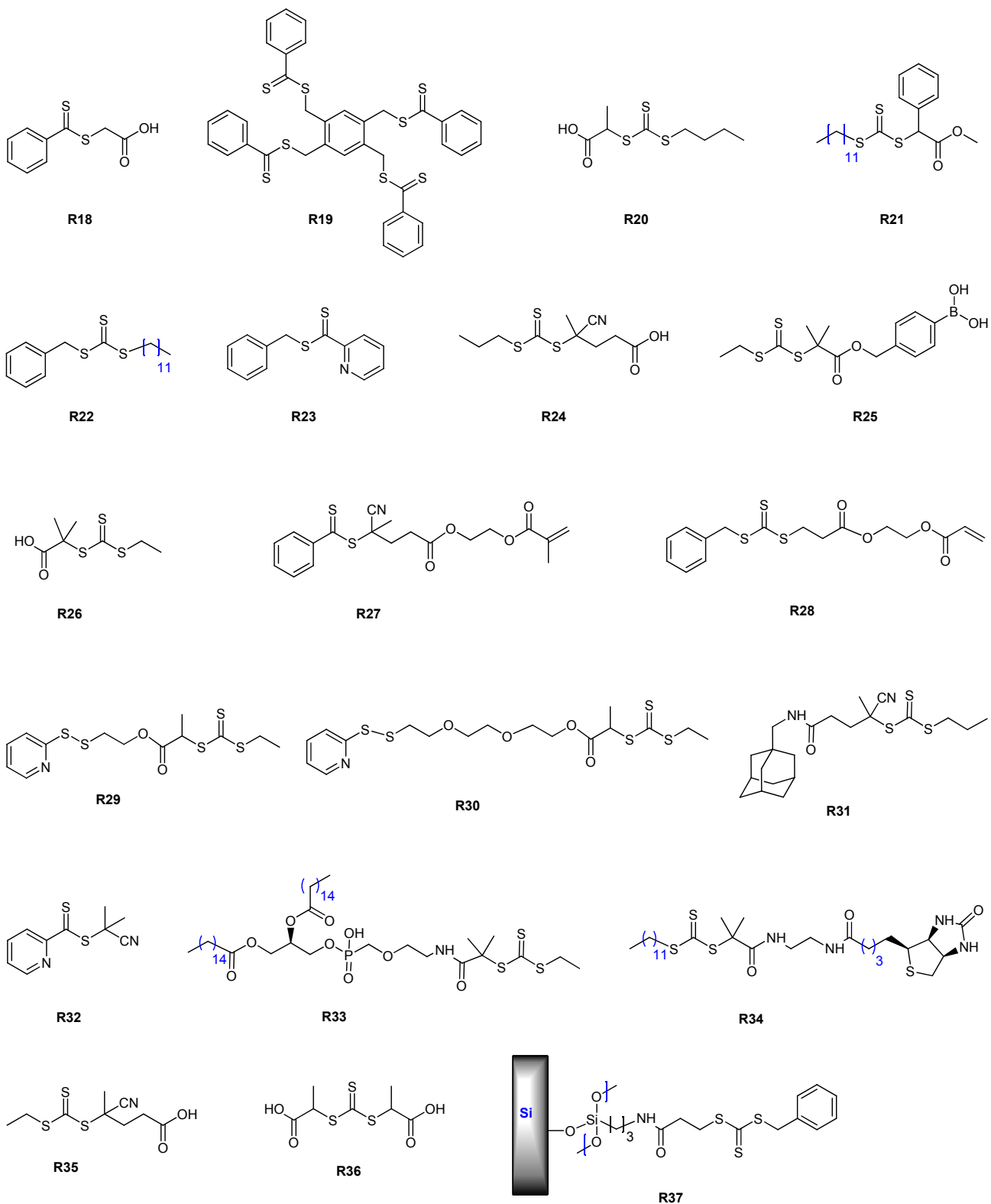
## 6. Reversible Addition-fragmentation Chain Transfer (RAFT) Polymerization

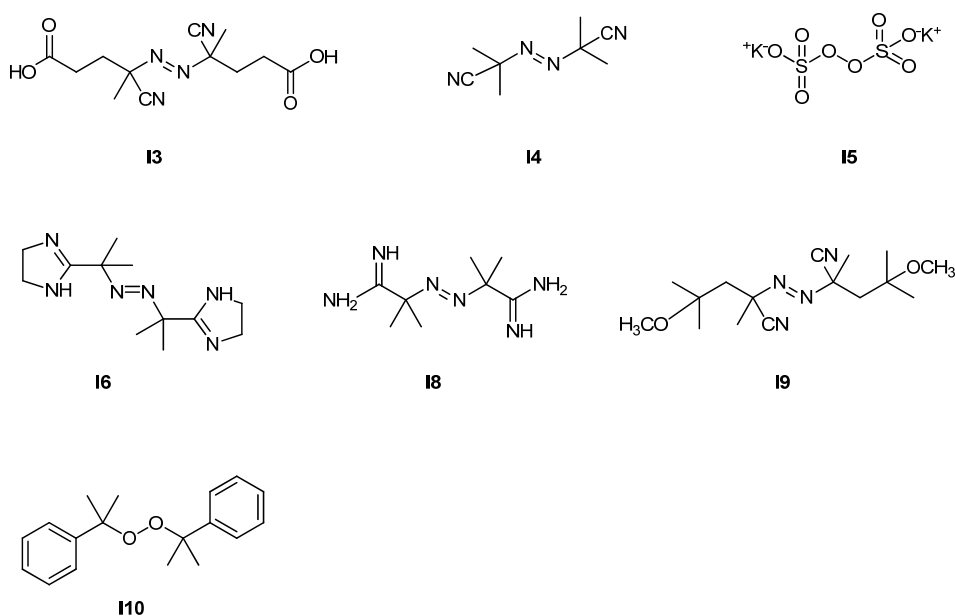
The structures of the control agents and initiators used for the synthesis of glycopolymers by RAFT are reported in Schemes 20 and 21, respectively.

**Scheme 20.** Reversible addition-fragmentation chain transfer (RAFT) agents used for the synthesis of glycopolymers.



Scheme 20. Cont.



**Scheme 21.** Initiators used in the synthesis of glycopolymers by RAFT.

### 6.1. RAFT Starting from Protected Glycomonomers/GlycoRAFT Agents

#### 6.1.1. (Meth)acrylamide Monomers

Table 3 summarizes the results obtained for the synthesis of glycopolymers by RAFT polymerization [12,158–212]. In their study on thermoresponsive glycopolymers, Voit *et al.* [161] described both the RAFT homopolymerization of glucofuranose methacrylamides **M48** and **M49** bearing a hydrophobic linker and their copolymerization with NIPAAm **M42** (Entry 145–149, Table 3). Homopolymerizations were conducted in the presence of **R10** (anisole, 80 °C or dioxane, 70 °C) and, in the case of **M48**, proceeded with pseudo-first order kinetics to afford a fairly uniform polymer ( $D = 1.34$ ). Since the initiator was AIBN and the process was run at 80 °C though, the polymerization slowed down after about 50% conversion (5 h) and reached a maximum of 60% conversion after ~8 h. Random and block copolymerizations with NiPAM were also conducted (in DMF, anisole or dioxane at 70 °C or 100 °C) and polymers with varying molar mass distributions were obtained ( $1.19 \leq D \leq 4$ ). Deprotection with 80% formic acid led to water soluble, temperature-responsive copolymers whose critical phase transition temperature ( $T_c$ ) depended on the copolymer composition and structure: In random copolymers an increase of  $T_c$  was observed with increasing glycomonomer content, while block copolymers had sharper transitions.

Gody *et al.* [158] synthesized biotinylated glycopolymers via the RAFT copolymerization of galactose acrylamide **M52** with NAM (**M53**) mediated by biotin-RAFT agent **R13** (dioxane, 90 °C; Entry 139, Table 3). Molar mass increased linearly with global conversion but above 40% the dispersity index increased substantially and a final value of  $D \cong 1.5$  was obtained at  $p = 0.80$ . The presence of the biotin ligand at the  $\alpha$ -chain end was confirmed by  $^1\text{H}$  NMR spectroscopy and MALDI-ToF MS analyses of low molar mass samples ( $M_n < 2700$  Da) obtained at conversions  $\leq 48\%$ . Finally, deprotection of the sugar residues was achieved in a  $\text{H}_2\text{O}/\text{TFA}$  (1:5 v/v) at RT.

**Table 3.** Glycopolymers by reversible addition-fragmentation chain transfer (RAFT) polymerization.

Entry	Carbohydrate	Monomer(s)	RAFT agent	Initiator	Conv. %	$M_n (\times 10^{-3})$	$M_w/M_{n,th}$	$\bar{D}$	Structure	Application sought/tested	Reference
<b>(Meth)acrylamide monomers (protected)</b>											
139	galactose ( $\alpha/\beta$ , 6- <i>N</i> )	M52/M53	R13	I4	80	~17	–	~1.5	A- <i>stat</i> -B	–	Gody <i>et al.</i> [158]
140	galactose ( $\beta$ - <i>N</i> )	M100	R26	I4	>70	11.9	1.18	–	homo	lectin recognition	Su <i>et al.</i> [159]
141 <sup>a</sup>	galactose ( $\alpha/\beta$ , 6- <i>O</i> )	M102	R5	I4	93	5.20	0.70	1.14	homo	–	Wei <i>et al.</i> [160]
142 <sup>a</sup>	galactose ( $\alpha/\beta$ , 6- <i>O</i> )	M102	R28	I4	100	28.6	1.43	1.49	hyperbranched	–	Wei <i>et al.</i> [160]
143 <sup>a</sup>	galactose ( $\alpha/\beta$ , 6- <i>O</i> )	M20	R27	I4	91	9.7	1.61	1.48	hyperbranched	–	Wei <i>et al.</i> [160]
144 <sup>b</sup>	galactose ( $\alpha/\beta$ , 6- <i>O</i> )	M20	R27	I4	82	23	1.60	1.44	hyperbranched	–	Wei <i>et al.</i> [160]
145	glucose ( $\alpha/\beta$ , 3- <i>O</i> )	M48	R10	I4	60	11.6	0.88	1.34	homo	–	Ozyurek <i>et al.</i> [161]
146	glucose ( $\alpha/\beta$ , 3- <i>O</i> )	M48/M42	R10	I4	80	20.5 <sup>c</sup>	–	1.69 <sup>c</sup>	A- <i>stat</i> -B	–	Ozyurek <i>et al.</i> [161]
147	glucose ( $\alpha/\beta$ , 3- <i>O</i> )	M49/M42	R10	I4	65	18.7 <sup>c</sup>	–	1.29 <sup>c</sup>	A- <i>stat</i> -B	–	Ozyurek <i>et al.</i> [161]
148	glucose ( $\alpha/\beta$ , 3- <i>O</i> )	M48	polyM42-R10	I4	–	15.2	–	1.57	block AB	–	Ozyurek <i>et al.</i> [161]
149	glucose ( $\alpha/\beta$ , 3- <i>O</i> )	M49	polyM42-R10	I4	–	27.0	–	1.69	block AB	–	Ozyurek <i>et al.</i> [161]
150	glucose ( $\beta$ - <i>N</i> )	M99	R26	I4	>70	11.9	1.20	–	homo	lectin recognition	Su <i>et al.</i> [159]
151	mannose ( $\alpha$ - <i>O</i> )	M53/M61	R13	I4	73	12.7	1.26	1.20	A- <i>stat</i> -B	avidin and lectin recognition	Jiang <i>et al.</i> [162]
152	mannose ( $\alpha$ - <i>O</i> )	M53/M61	R16	I4	83	9.70	1.21	1.14	A- <i>stat</i> -B	lectin recognition	Jiang <i>et al.</i> [162]
153	<i>N</i> -acetylglucosamine ( $\beta$ - <i>O</i> )	M53/M60	R13	I4	85	53.7	0.91	1.60	A- <i>stat</i> -B	avidin and lectin recognition	Jiang <i>et al.</i> [162]
154	<i>N</i> -acetylglucosamine ( $\beta$ - <i>O</i> )	M53/M60	R16	I4	93	62.3	1.02	1.46	A- <i>stat</i> -B	lectin recognition	Jiang <i>et al.</i> [162]
<b>(Meth)acrylamide monomers (unprotected)</b>											
155	cellobiose ( $\beta$ - <i>O</i> )	M108	R33	I3	98	22.5	–	1.22	homo	–	Belardi <i>et al.</i> [163]
156	galactose ( $\alpha$ - <i>O</i> )	M77b/M75	R18	I8	34	12.0	–	1.40	A- <i>stat</i> -B	lectin recognition	Toyoshima <i>et al.</i> [164]
157	gluconic acid (amide)	M69	R1	I3	93	8.9	0.82	1.18	homo	cytotoxicity tests	Deng <i>et al.</i> [165]
158	gluconic acid (amide)	M70	R1	I3	78	18.2	0.96	1.20	homo	cytotoxicity tests	Deng <i>et al.</i> [165]
159	gluconic acid (amide)	M71	polyM69-R1	I3	70	15.3	0.83	1.44	block AB	cytotoxicity tests	Deng <i>et al.</i> [165]
160	gluconic acid (amide)	M55	polyM70-R1	I3	70	18.4	1.47	1.40	block AB	cytotoxicity tests	Deng <i>et al.</i> [165]

Table 3. Cont.

Entry	Carbohydrate	Monomer(s)	RAFT agent	Initiator	Conv. %	$M_n (\times 10^{-3})$	$M_n/M_{n,th}$	$\bar{D}$	Structure	Application sought/tested	Reference
161	gluconic acid (amide)	M72	polyM69-R1	I3	70	25.0	1.05	1.39	block AB	cytotoxicity tests	Deng <i>et al.</i> [165]
162	gluconic acid (amide)	M70/M55	R1	I3	–	29.5	–	1.29	A-stat-B	gene delivery	Ahmed <i>et al.</i> [166]
163	gluconic acid (amide)	M70/M71	R1	I3	–	18.2	–	1.31	A-stat-B	gene delivery	Ahmed <i>et al.</i> [166]
164	gluconic acid (amide)	M70/M106	R1	I3	–	38.0	–	2.50	hyperbranched	biomedical	Ahmed <i>et al.</i> [167]
165	gluconic acid (amide)	M70/M71/ M106	R1	I3	–	27.0	–	2.50	hyperbranched	gene delivery	Ahmed <i>et al.</i> [168]
166	glucosamine ( $\alpha/\beta$ , 2-N)	M41	R5 <sup>d</sup>	I3	89	100.8	1.20	1.26	homo	–	Bernard <i>et al.</i> [169]
167	glucosamine ( $\alpha/\beta$ , 2-N)	M41	R5 <sup>e</sup>	I3	19	6.60	1.40	1.15	homo	–	Bernard <i>et al.</i> [169]
168	glucosamine ( $\alpha/\beta$ , 2-N)	M42	polyM41-R5	I3	88	88.4	1.07	<1.25	block AB	–	Bernard <i>et al.</i> [169]
169	glucosamine ( $\alpha/\beta$ , 2-N)	M41	R7	I3	40	72.2	1.22	1.21	star (3-arm)	–	Bernard <i>et al.</i> [169]
170	glucosamine ( $\alpha/\beta$ , 2-N)	M41	R21	I4	79	13.5	2.14	1.30	homo	–	Ting <i>et al.</i> [170]
171	glucosamine ( $\alpha/\beta$ , 2-N)	St	polyM41-R21	I3	83	38.5	1.63	1.65	lattex	lectin recognition	Ting <i>et al.</i> [170]
172	glucosamine ( $\alpha/\beta$ , 2-N)	St	polyM41-R21	I3	81	660	–	1.33	latex (cross-linked)	lectin recognition	Ting <i>et al.</i> [170]
173	glucosamine ( $\alpha/\beta$ )	M84	R24	I4	–	11.7	–	1.24	homo	–	Smith <i>et al.</i> [171]
174	glucosamine ( $\alpha/\beta$ )	M71	polyM84-R24	I4	–	14.4	–	1.15	block AB	gene delivery	Smith <i>et al.</i> [171]
175	glucosamine ( $\alpha/\beta$ )	M71	polyM84-R24	I4	–	17.8	–	1.12	block AB	gene delivery	Smith <i>et al.</i> [171]
176	glucose ( $\alpha$ -O)	M85	R5	I3	85	113	–	1.08	homo	–	Abdelkader <i>et al.</i> [172]
177	glucose ( $\beta$ -N)	M116	polyM53	I4	–	25.6	0.74	1.06	block ABA	–	Albertin <i>et al.</i> [173]
178	glucuronic acid ( $\beta$ -O)	M81/M75	R18	I8	81	73.0	–	1.7	A-stat-B	biomedical	Miura <i>et al.</i> [174]
179	lactobionic acid (amide)	M105/M106	R1	I3	–	36.0	–	2.20	hyperbranched	biomedical	Ahmed <i>et al.</i> [167]
180	lactobionic acid (amide)	M105/M71/ M106	R1	I3	–	31.0	–	2.10	hyperbranched	gene delivery	Ahmed <i>et al.</i> [168]
181	lactose ( $\beta$ -O)	M107a	R33	I3	95	20.7	–	1.21	homo	–	Belardi <i>et al.</i> [163]
182	mannose ( $\alpha$ -O)	M76	R18	I8	85	47.5	–	1.20	homo	lectin recognition	Toyoshima <i>et al.</i> [175]
183	mannose ( $\alpha$ -O)	M76/M75	R18	I8	82	9.30	–	1.50	A-stat-B	lectin recognition	Toyoshima <i>et al.</i> [175]

Table 3. Cont.

Entry	Carbohydrate	Monomer(s)	RAFT agent	Initiator	Conv. %	$M_n (\times 10^{-3})$	$M_n/M_{n,th}$	$\bar{D}$	Structure	Application sought/tested	Reference
184	mannose ( $\alpha$ -O)	M76/M75	R18	I8	–	20.0	–	1.30	A-stat-B	biosensor	Ishii <i>et al.</i> [176]
185	mannose (2-deoxy-2-azido, $\alpha$ -O)	M86	R5	I3	50	37.0	–	1.35	homo	–	Abdelkader <i>et al.</i> [172]
186	mannose (2-deoxy-2-azido, $\alpha$ -O)	M86	R5	I9	75	56.0	–	1.15	homo	–	Abdelkader <i>et al.</i> [172]
187	N-acetylglucosamine ( $\alpha$ -O)	M77/M75	R18	I8	19	8.60	–	1.50	A-stat-B	lectin recognition	Toyoshima <i>et al.</i> [175]
188	N-acetylglucosamine (6-sulfo, $\beta$ -O)	M80/M75	R18	I8	67	210	–	1.0	A-stat-B	biomedical	Miura <i>et al.</i> [174]
189	N-acetylglucosamine (6-sulfo, $\beta$ -O)	M80/M81/M75	R18	I8	16	7.60	–	1.4	A-stat-B-stat-C	biomedical	Miura <i>et al.</i> [174]
<b>(Meth)acrylate monomers (protected)</b>											
190	fructose ( $\alpha/\beta$ , 3-O)	M45	R9	I5	91	41.2	2.48	1.25	homo	–	Al-Bagoury <i>et al.</i> [177]
191	galactose ( $\alpha/\beta$ , 6-O)	M20	R9	I4	75	13.9	–	1.20	homo	–	Lowe <i>et al.</i> [178]
192	galactose ( $\alpha/\beta$ , 6-O)	M20	R10	I4	–	12.3	–	1.18	homo	–	Lowe <i>et al.</i> [178]
193	galactose ( $\alpha/\beta$ , 6-O)	M44	polyM20	I4	–	16.3	–	1.20	block AB	–	Lowe <i>et al.</i> [178]
194	galactose ( $\alpha/\beta$ , 6-O)	M74	R22	I4	86	51.0	1.11	1.17	homo	–	Ting <i>et al.</i> [179]
195	galactose ( $\alpha/\beta$ , 6-O)	M74	R17	I4	73	52.0	0.71	1.20	block AB	biomedical	Ting <i>et al.</i> [179]
196	galactose ( $\alpha/\beta$ , 3-O)	M13	R1	I3	40	4.10	0.94	1.12	homo	–	Liu <i>et al.</i> [180]
197	galactose ( $\alpha/\beta$ , 3-O)	M13	polyM79 <sub>18</sub>	I3	–	7.00	–	1.19	block AB	lectin recognition/ biomedical	Liu <i>et al.</i> [180]
198	galactose ( $\alpha/\beta$ , 6-O)	M20	R10	I4	86	13.7	–	1.22	homo	biosensor	Pfaff <i>et al.</i> [181]
199	galactose ( $\alpha/\beta$ , 6-O)	M96/M20	polyM20-R10	I4	–	14.8	–	1.18	A-block-(B-stat-C)	biosensor	Pfaff <i>et al.</i> [181]
200	galactose ( $\beta$ -O)	M101	R1	I3	50-60	6.30	0.96	1.10	homo	lectin recognition, antioxidant	Shi <i>et al.</i> [182]



Table 3. Cont.

Entry	Carbohydrate	Monomer(s)	RAFT agent	Initiator	Conv. %	$M_n (\times 10^{-3})$	$M_n/M_{n,th}$	$\bar{D}$	Structure	Application sought/tested	Reference
201	glucose ( $\alpha/\beta$ , 3- <i>O</i> )	M13	R11	I5	90	213	17.8	1.90	homo	–	Al-Bagoury <i>et al.</i> [177]
202	glucose ( $\alpha/\beta$ , 3- <i>O</i> )	M13	R11	I4	60	313	64.0	1.58	homo	–	Al-Bagoury <i>et al.</i> [177]
203	glucose ( $\alpha/\beta$ , 3- <i>O</i> )	M13	R10	I5	30	20.9	4.01	1.32	homo	–	Al-Bagoury <i>et al.</i> [177]
204	glucose ( $\alpha/\beta$ , 3- <i>O</i> )	M13	R9	I5	99	27.7	2.64	1.10	homo	–	Al-Bagoury <i>et al.</i> [177]
205	glucose ( $\alpha/\beta$ , 3- <i>O</i> )	M13	R1	I3	43	6.40	–	1.21	homo	lectin recognition	Luo <i>et al.</i> [183]
206	glucose ( $\alpha/\beta$ , 3- <i>O</i> )	M33	polyM13	I3	45	7.50	–	1.21	block AB	lectin recognition	Luo <i>et al.</i> [183]
207	glucose ( $\alpha/\beta$ , 3- <i>O</i> )	M42	poly(M13- <i>block</i> -M33)	I3	35	9.30	–	1.27	block ABA	lectin recognition	Luo <i>et al.</i> [183]
208	glucose ( $\alpha/\beta$ , 3- <i>O</i> )	M9	R32	I4	–	6.40	–	1.14	homo	–	Glassner <i>et al.</i> [184]
209	glucose ( $\alpha/\beta$ , 3- <i>O</i> )	M9	R23	I4	25	4.20	–	1.20	homo	–	Kaupp <i>et al.</i> [185]
210	glucose ( $\beta$ - <i>O</i> )	M113a	R10	I4	74 <sup>f</sup>	21.9	–	1.09	homo	lectin recognition	Dan <i>et al.</i> [186]
211	glucose ( $\beta$ - <i>O</i> )	M113b	R10	I4	46 <sup>f</sup>	13.0	–	1.12	homo	lectin recognition	Dan <i>et al.</i> [186]
212	lactose ( $\beta$ - <i>O</i> )	M43	R9	I4	31	6.29	0.87	1.09	homo	stationary phase	Guo <i>et al.</i> [187]
213	lactose ( $\beta$ - <i>O</i> )	M43	R1	I4	>90	20.0	–	1.22	homo	gene therapy	Zhou <i>et al.</i> [188]
<b>(Meth)acrylate monomers (unprotected)</b>											
214	galactose ( $\beta$ - <i>O</i> )	M38	R1	I3	80	24.0	1.01	1.09	homo	lectin recognition	Spain <i>et al.</i> [189]
215	galactose ( $\beta$ - <i>O</i> )	M38/M115	R35	I3	> 99	12.2	–	1.20	A- <i>stat</i> -B	biomedical	Song <i>et al.</i> [12]
216	gluconic acid (amide)	M23	R14	I3	> 95	14.1	–	1.19	homo	streptavidin binding	Housni <i>et al.</i> [190]
217	glucose ( $\alpha/\beta$ - <i>O</i> )	M34a	R1	I3	70	27.4	1.31	1.03	homo	–	Lowe <i>et al.</i> [191]
218	glucose ( $\alpha/\beta$ - <i>O</i> )	M34a	R1	I3	40	14.2	1.18	1.07	homo	–	Lowe <i>et al.</i> [191]
219	glucose ( $\alpha/\beta$ - <i>O</i> )	M34a	polyM34a	I3	–	33.8	0.92	1.54	block AB	–	Lowe <i>et al.</i> [191]
220	glucose ( $\alpha/\beta$ - <i>O</i> )	M35	polyM34a	I3	–	37.1	–	1.63	block AB	–	Lowe <i>et al.</i> [191]
221	glucose ( $\beta$ - <i>S</i> , 6- <i>O</i> )	M103	polyM59	I4	53	15.2	0.94	1.45	block AB	biomedical	Pearson <i>et al.</i> [192]
222	glucose ( $\alpha/\beta$ - <i>O</i> )	M34a	polyM36·R1	I3	71	52.0	0.82	1.20	block AB	–	Albertin <i>et al.</i> [193]
223	glucose/mannose ( $\alpha/\beta$ ; or $\alpha$ -methyl, 6- <i>O</i> )	M37	polyM34a·R1	I3	52	61.3	0.75	1.16	block AB	–	Albertin <i>et al.</i> [193]
224 <sup>s</sup>	glucose ( $\alpha$ -methyl, 6- <i>O</i> )	M36	R1	I3	97	327	12.5	3.67	homo	–	Albertin <i>et al.</i> [194]

Table 3. Cont.

Entry	Carbohydrate	Monomer(s)	RAFT agent	Initiator	Conv. %	$M_n (\times 10^{-3})$	$M_n/M_{n,th}$	$\bar{D}$	Structure	Application sought/tested	Reference
225 <sup>h</sup>	glucose ( $\alpha$ -methyl, 6- <i>O</i> )	M36	R1	I3	99	174	6.60	1.75	homo	–	Albertin <i>et al.</i> [194]
226 <sup>i</sup>	glucose ( $\alpha$ -methyl, 6- <i>O</i> )	M36	R1	I3	100	26.3	0.93	1.14	homo	–	Albertin <i>et al.</i> [194]
227 <sup>i</sup>	glucose ( $\alpha$ -methyl, 6- <i>O</i> )	M33	polyM36-R1	I3	–	45.0	–	1.20	block AB	–	Albertin <i>et al.</i> [195]
228	lactobionic acid (amide)	M25	R15	I3	>95	24.7	–	1.22	homo	streptavidin binding	Housni <i>et al.</i> [190]
229	mannose ( $\alpha/\beta$ , 6- <i>O</i> )	M39	R1	I4	71	42.5	–	1.23	homo	–	Pfaff <i>et al.</i> [196]
230	mannose ( $\alpha/\beta$ , 6- <i>O</i> )	M39	R1	I3	$\geq 95$	85.0	$\cong 1.13$	1.06	homo	lectin recognition	Granville <i>et al.</i> [197]
231	mannose ( $\beta$ - <i>O</i> )	M114/M115	R35	I3	>99	11.4	–	1.20	A- <i>stat</i> -B	biomedical	Song <i>et al.</i> [12]
232	N-acetylglucosamine ( $\beta$ - <i>O</i> )	M31/M115	R35	I3	>99	13.1	–	1.20	A- <i>stat</i> -B	biomedical	Song <i>et al.</i> [12]
<b>Vinyl ester monomers (unprotected)</b>											
233	glucose ( $\alpha/\beta$ , 6- <i>O</i> )	M40	R2	I3	14	17.1	–	1.10	homo	–	Albertin <i>et al.</i> [198]
234	glucose ( $\alpha/\beta$ , 6- <i>O</i> )	M40	R3	I3	27	19.6	–	1.19	homo	–	Albertin <i>et al.</i> [198]
235	glucose ( $\alpha/\beta$ , 6- <i>O</i> )	M40	R4	I3	50	~28	–	1.48	star (4-arm)	–	Bernard <i>et al.</i> [199]
<b>Diene-like monomers (unprotected)</b>											
236	mannose ( $\alpha$ - <i>O</i> )	M78	R5	I3	48	51.5	–	1.16	homo	lectin recognition	Hetzer <i>et al.</i> [200]
237	mannose ( $\alpha$ - <i>O</i> )	M42	polyM78	I4	–	32.4	–	1.12	block AB	lectin recognition	Hetzer <i>et al.</i> [200]
<b>Styrenic monomers (protected)</b>											
238	galactose ( $\alpha/\beta$ , 6- <i>O</i> )	M50	R11	I4	85	27.0	$\cong 0.6$	1.10	homo	protein bioconjugation	Xiao <i>et al.</i> [201]
239	galactose ( $\alpha/\beta$ , 6- <i>O</i> )	M50/M94	R11	I10	75	18.0	–	1.29	A- <i>stat</i> -B	drug delivery	Xiao <i>et al.</i> [202]
240	galactose ( $\alpha/\beta$ , 6- <i>O</i> )	M51	R12	I4	60	5.20	–	1.11	homo	chiral recognition	Wang <i>et al.</i> [203]
241	galactose ( $\alpha/\beta$ , 6- <i>O</i> )	M51	polySty-R12	I4	–	19.6	–	1.57	block AB	–	Wang <i>et al.</i> [203]
242	galactose ( $\alpha/\beta$ , 6- <i>O</i> )	M51	polyMMA-R12	I4	–	20.8	–	1.41	block AB	–	Wang <i>et al.</i> [203]
243	galactose ( $\alpha/\beta$ , 6- <i>O</i> )	M51	polyMA-R12	I4	–	24.6	–	1.35	block AB	–	Wang <i>et al.</i> [203]
<b>Styrenic monomers (unprotected)</b>											
244	trehalose	M104	R29	I4	77	9.40	0.98	1.07	homo	protein formulation	Mancini <i>et al.</i> [204]
245	trehalose	M104	R30	I4	73	24.5	0.95	1.20	homo	protein formulation	Mancini <i>et al.</i> [204]
246	trehalose	M104	R30	I4	81	49.5	1.10	1.47	homo	protein formulation	Mancini <i>et al.</i> [204]

Table 3. Cont.

Entry	Carbohydrate	Monomer(s)	RAFT agent	Initiator	Conv. %	$M_n (\times 10^{-3})$	$M_w/M_{n,th}$	$\bar{D}$	Structure	Application sought/tested	Reference
<b>Glycopolymers from post-polymerization reaction</b>											
247	galactose ( $\alpha/\beta$ , 6- <i>O</i> )	M57/M59	R5	I4	–	11.0	0.88	1.14	A- <i>stat</i> -B	glycoGNP	Boyer <i>et al.</i> [205]
248	galactose ( $\alpha$ - <i>N</i> ), 2-deoxy-2-amino-D-glucose ( <i>N</i> )	M68	R5	I4	–	2.80	0.84	1.20	homo	lectin recognition	Boyer <i>et al.</i> [206]
249	galactose ( $\alpha$ - <i>N</i> ), 2-deoxy-2-amino-D-glucose ( <i>N</i> )	M68, M121	R5	I4	70, 96	90.0	0.84	1.18	star (16-arm)	–	Boyer <i>et al.</i> [207]
250	galactose ( $\beta$ - <i>O</i> ), glucose ( $\beta$ - <i>S</i> )	M82/M83	R20	I4	93	29.0	–	1.90	branched	–	Semsarilar <i>et al.</i> [208]
251	glucose ( $\beta$ - <i>S</i> )	M57/M58	R5	I4	–	10.0	0.91	1.12	A- <i>stat</i> -B	glycoGNP	Boyer <i>et al.</i> [205]
252	glucose ( $\beta$ - <i>S</i> )	M58	R19	–	85	51.4	0.49	1.90	star (4-arm)	lectin recognition	Chen <i>et al.</i> [209]
253	glucose ( $\beta$ - <i>S</i> )	M82	R10	I4	25	15.4	–	11.8	branched	–	Semsarilar <i>et al.</i> [208]
254	glucose ( $\beta$ - <i>S</i> )	M57	R23	I4	–	5.60	–	1.13	homo	lectin recognition	Kumar <i>et al.</i> [210]
255	glucose ( $\beta$ - <i>S</i> )	M59	polyM57-R5	I4	–	6.10	–	1.15	homo	lectin recognition	Kumar <i>et al.</i> [210]
256	glucuronic acid (1-amino-1-deoxy alditol)	M54	R1	I6	47	33.0	0.98	1.05	homo	–	Alidedeoglu <i>et al.</i> [211]
257	glucuronic acid (1-amino-1-deoxy alditol)	M55	R1	I3	31	15.0	1.3	1.08	homo	–	Alidedeoglu <i>et al.</i> [211]
258	glucuronic acid (1-amino-1-deoxy alditol)	M56	polyM54	I3	33	48.4	0.85	1.05	block AB	–	Alidedeoglu <i>et al.</i> [211]
259	<i>N</i> -acetylglucosamine ( $\alpha$ - <i>O</i> )	M111	R34	I3	82	15	–	1.12	A- <i>stat</i> -B	biosensor	Godula <i>et al.</i> [212]

<sup>a</sup>  $[M]_0/[RAFT_{inimer}]_0 = 20$ ; <sup>b</sup>  $[M]_0/[RAFT_{inimer}]_0 = 100$ ; <sup>c</sup> after deprotection; <sup>d</sup>  $[R5]_0 = 1.78 \text{ mmol L}^{-1}$ , 7 h; <sup>e</sup>  $[R5]_0 = 7.14 \text{ mmol L}^{-1}$ , 8 h; <sup>f</sup> isolated yield; <sup>g</sup> In  $0.1 \text{ mol L}^{-1} \text{ Na}_2\text{CO}_3$ ;

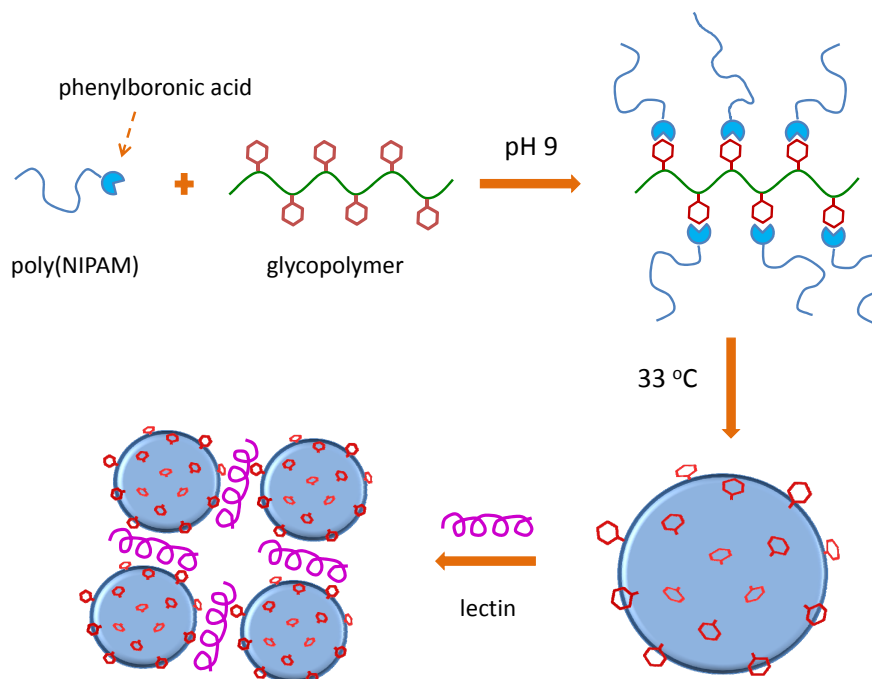
<sup>h</sup> In  $0.1 \text{ mol L}^{-1} \text{ NaHCO}_3$ ; <sup>i</sup> In  $\text{H}_2\text{O}/\text{EtOH}$  9:1.

In collaboration with Ravin Narain, the same group [213] investigated the photochemical synthesis of gold nanoparticles stabilized by hydrophilic polymer chains. To this end,  $\text{HAuCl}_4$  was reduced *in situ* by Irgacure-2959 under UV irradiation and in the presence of methoxy-PEG-SH, biotinylated glycopolymer poly(**M52-stat-M53**) (deprotected) and poly(**NIPAAm**) (both obtained by RAFT polymerization). SPR sensorgrams demonstrated that the biotin residues on the surface of the nanoparticles were still accessible for bioconjugation on a streptavidin immobilized sensor chip. In a continuation to this study, Jiang *et al.* [162] synthesized copolymers of NAM **M53** with *N*-acetyl-D-glucosaminoside- or D-mannoside-derived glycomonomers **M60** and **M61** using both biotin-derived RAFT agent **R13** and *tert*-butyl dithiobenzoate **R16** (dioxane, 75 °C or 90 °C; Entry 151–154, Table 3). Good control over the molar mass was achieved in all cases ( $0.91 \leq M_n/M_{n,th} \leq 1.26$ ) but uniform polymers were only obtained with the D-mannoside-derived glycomonomer ( $D = 1.14$ – $1.20$ ). After Zemplén deacetylation, the deprotected glycopolymers were used for the preparation of biotinylated and non-biotinylated gold glyconanoparticles via the photochemical process previously described. The former were then immobilized onto avidin-coated chips and used for the study lectin-carbohydrate interactions (ConA for  $\alpha$ -mannoside and WGA for *N*-acetyl-D-glucosaminoside).

Jiang *et al.* [159] reported the synthesis of carbohydrate-decorated artificial vesicles via the self-assembly of glycopolymers grafted with polyNIPAAm chains (Scheme 22). Firstly, NIPAAm (**M42**) was polymerized in the presence of trithiocarbonate **R25** (**I4**, 1,4-dioxane, 70 °C) to afford a phenylboronic acid-functionalized uniform polymer ( $M_n = 6400$  Da,  $D = 1.10$ ). Secondly, peracetylated *N*-acryloyl- $\beta$ -D-glucopyranosylamine **M99** and *N*-acryloyl- $\beta$ -D-galactopyranosylamine **M100** were polymerized under the same conditions (Entry 140 and 150, Table 3) and in the presence of trithiocarbonate **R26** to yield poly**M99** ( $M_n = 11,900$ ,  $D = 1.20$ ) and poly**M100** ( $M_n = 11,900$ ,  $D = 1.18$ ). After Zemplén deacetylation in DMF, poly(NIPAAm) chains were grafted to the deprotected glycopolymers via reversible boron-oxygen cyclic ester bonds formed in basic solution. Upon heating at 33 °C, the “graft-like” complex formed uniform vesicles ( $R_h = 62$  nm– $68$  nm,  $D_R \cong 1.1$ ) having a hydrophilic glycopolymer layer at the outer surface of the membrane. Finally, vesicles featuring  $\beta$ -galactose moieties bound to *Arachis hypogaea* (PNA) and *Erythrina cristagalli* (ECA) lectins, whereas those featuring  $\beta$ -glucose did not.

Wei *et al.* [160] described the synthesis of hyperbranched glycopolymers carrying galactose residues using RAFT inimers (Entry 141–144, Table 3). Galactose methacrylate **M20** and galactose acrylamide **M102** were polymerized in the presence of **R27** and **R28**, respectively (**I4**, ethyl acetate, 70 °C), to afford fairly uniform hyperbranched glycopolymers ( $D < 1.5$ ) with  $M_n = 1700$ – $29,000$  Da. Control over the molar mass was poor though and higher M/CTA ratios resulted in higher dispersity indices. Linear poly**M102** was also prepared by using **R5** as the RAFT agent under the same conditions: a uniform polymer was obtained in this case ( $M_n = 5700$  Da,  $D = 1.14$ ) but the control over molar mass was no better. Finally, water soluble glycopolymers were attained after deprotection of the sugar residues with TFA.

**Scheme 22.** Synthesis of carbohydrate-decorated polymersomes and their lectin-induced aggregation as reported by Jiang *et al.* [159].



### 6.1.2. (Meth)acrylate Monomers

Guo *et al.* [187] described the polymerization of lactoside methacrylate **M43** in the presence of cumyl dithiobenzoate **R9** as the RAFT agent (chloroform, 70 °C, 24 h; Entry 212, Table 3). Uniform polymers were obtained ( $\mathcal{D} = 1.09\text{--}1.34$ ) with good control over the molar mass ( $M_n/M_{n,\text{th}} = 0.87$ ) but a non-steady state kinetics was observed during the first 4 h of polymerization accompanied by a jump in the molar mass of the polymer (“hybrid” behavior between conventional radical and RAFT polymerization). After this initialization period, pseudo-first order kinetics was followed together with a linear increase of molar mass with conversion. Increasing the  $[\mathbf{R9}]_0/[\mathbf{I4}]_0$  ratio resulted in slower kinetics but a better control over the molar mass. The obtained glycopolymer was then grafted onto silica particles via radical addition to immobilized methacrylate groups, and a grafting density or  $\sim 0.1$  chain  $\text{nm}^{-2}$  was achieved. Finally, the acetate groups were removed with  $\text{CH}_3\text{ONa}/\text{CH}_3\text{OH}$ .

Lowe and Wang [178] studied the RAFT polymerization of galactose methacrylate **M20** using dithiobenzoate-type RAFT agents **R9** and **R10** (DMF, 60 °C; Entry 191–192, Table 3). With cumyl dithiobenzoate **R9**, an induction period of 50 min. was observed at the beginning of polymerization that was followed by pseudo-first order kinetics. This kind of behavior had already been observed in the CDB-mediated polymerization of methacrylates [214] and its origin is the subject of a lively debate [215–218]. Fairly uniform polymers ( $\mathcal{D} \leq 1.20$ ) with  $M_n$  up to 14,000 Da were obtained that were chain extended with 2-(dimethylamino)ethyl methacrylate **M44** (Entry 193, Table 3) to give double hydrophilic-hydrophilic AB diblock glycopolymers after deprotection of the sugar moieties (TFA/ $\text{H}_2\text{O}$  5:1 v/v, RT, 1 h). It is noteworthy that these deprotection conditions effectively removed isopropylidene groups without affecting the ester bonds.

Al-Bagoury *et al.* [177] reported the RAFT polymerization of isopropylidene protected D-glucofuranose methacrylate **M13** and D-fructopyranose methacrylate **M45** in mini-emulsion. Polymerizations were conducted at 70 °C in a mixture of hexadecane/H<sub>2</sub>O/SDS/NaHCO<sub>3</sub> using three different dithiobenzoate-type RAFT agents (**R9**, **R10** and **R11**; Entry 190, 201–204, Table 3). Big deviations of molar masses with respect to their theoretical values were observed in all cases and the best results were obtained using **R9** ( $D \leq 1.25$ ,  $M_n/M_{n,th} < 2.7$ ). A few examples of chain extension with butyl methacrylate **M46** and butyl acrylate **M47** were also reported.

Stenzel *et al.* [179] synthesized hollow nanospheres featuring D-galactose glycopolymer chains on their surface. First the efficacy of a benzyl trithiocarbonate RAFT agent in the homopolymerization of 6-*O*-acryloyl-D-galactose **M74** was proved using **R22** ( $\alpha,\alpha,\alpha$ -trifluorotoluene, 70 °C, 8 h,  $M_n/M_{n,th} = 1.11$ ,  $D = 1.15$ ). Then an amphiphilic block copolymer was synthesized by chain extending the poly(lactide) macroRAFT agent **R17** with **M74** (6 h; Entry 195, Table 3). A uniform glycopolymer was obtained ( $D = 1.20$ ) whose molar mass significantly deviated from its theoretical value ( $M_n/M_{n,th} = 0.71$ ). After deprotection of the sugar moieties, the glycopolymer self-assembled in aqueous solution to form spherical micelles that were cross-linked at the polymer nexus by radical reaction with hexandiol diacrylate. Finally glycopolymer nanocages were obtained by aminolysis of the poly(lactide) core.

Liu *et al.* [180] described the synthesis of pH responsive copolymers and their self-assembly in basic solution (Entry 196–197, Table 3). First, the homopolymerization of protected glucofuranose methacrylate **M13** was studied in the presence of 4-cyano-4-[(phenylcarbonothioyl)sulfanyl]pentanoic acid **R1** (dioxane, 70 °C, 8 h): After an induction period of 3 h, the reaction proceeded with pseudo-first order kinetics to afford uniform polymers ( $D \leq 1.12$ ) with a controlled molar mass. As previously seen for similar systems, a jump in the molar mass of the polymer was observed at low conversion (“hybrid” behavior between conventional radical and RAFT polymerization). The same protocol was then applied to the synthesis of a poly(2-(diethylamino)ethyl methacrylate) macroRAFT agent ( $M_n = 3800$  Da,  $D = 1.06$ ) that was chain extended with protected glucofuranose methacrylate **M13**. In this case neither an induction period nor a molar mass jump was observed in the early stages of the reaction. Fairly uniform poly**M79**<sub>18</sub>-*block*-poly**M13**<sub>19–44</sub> were obtained ( $D = 1.19–1.41$ ) that, after deprotection with aqueous TFA, self-assembled into spherical micelles at pH > 7.5. Finally, the obtained micelles showed specific recognition towards ConA.

Pfaff *et al.* [196] described the synthesis of mannose- and galactose-decorated PDVB particles ( $d = 2.4$   $\mu\text{m}$ ) with a high density of grafting (0.20–0.43 chains nm<sup>-2</sup>). Three different strategies were explored: (i) 6-*O*-methacryloyl-D-mannose **M39** and isopropylidene protected galactose methacrylate **M20** were grafted through the surface styrenyl moieties of PDVB particles in the presence of **R1** and **R9**, respectively (DMF, 70 °C; poly**M39**  $M_n = 42,300$ ; poly**M20**  $M_n = 110,000$  Da,  $D = 1.14$ ); (ii) alternatively, the radical addition of cumyl dithiobenzoate to the surface styrenyl moieties of PDVB particles was carried out first (DMF, **I4**, 60 °C, 2 d) and poly**M20** was grafted from the surface in the presence of **R9** as sacrificial chain transfer agent ( $M_n = 68,500$  Da,  $D = 1.17$ ); (iii) poly**M20**-SH was prepared by aminolysis of the corresponding RAFT polymer ( $M_n = 94,700$  Da,  $D = 1.14$ ) and grafted to PDVB particles via thiol-ene radical addition. Unsurprisingly, PDVB-*graft*-poly**M39** did not show any interaction with ConA, *Lens culinaris* agglutinin or Pealectin-I, because of the 6-*O*-linked mannose units. By contrast, after deprotection with TFA/H<sub>2</sub>O, PDVB-*graft*-poly**M20** microspheres could bind RCA120.

The same group investigated the synthesis of magnetic and fluorescent nanoparticles covered with a glycopolymer brush for biosensing and diagnostic applications (Entry 198–199, Table 3) [181]. To this end, poly**M20** ( $M_n = 13,700$  Da,  $D = 1.22$ ) was obtained by the polymerization of **M20** in the presence of **R10** (DMF, 70 °C) and used as macroRAFT agent for the copolymerization of 4-(pyrenyl)butyl methacrylate **M96** and **M20**. A fluorescent glycopolymer poly**M20-block-poly(M20-stat-M96)** with  $M_n = 14,800$  Da and  $D = 1.18$  was thus obtained that was deprotected in acidic conditions and subjected to aminolysis. The resulting thiol-terminated polymer was then grafted to silica-encapsulated magnetic particles via thiol-ene radical addition. Interestingly, neither the encapsulation of iron oxide in silica nor the grafting of the glycopolymer did influence the magnetic properties of the particles. The sugar-covered nanoparticles were found to be non-cytotoxic and were uptaken into the nucleus and cytoplasm of adenocarcinomic human alveolar basal epithelial cells within 24 h.

Yang *et al.* [219] reported the preparation of BSA-imprinted polymer beads displaying surface glycopolymer graft chains. To this end,  $\beta$ -lactoside methacrylate **M43** was polymerized in the presence of **R1** as the control agent ( $\text{CHCl}_3$ , 70 °C) to afford a uniform polymer ( $M_n = 4070$  Da,  $D = 1.07$ ). Subsequently, the glycopolymer was used as macroCTA in the suspension copolymerization of methyl methacrylate and ethylene glycol dimethacrylate in the presence of bovine serum albumin (BSA). After deprotection of the lactose moieties, rebinding tests showed that the glycopolymer-functionalized imprinted polymer beads presented a higher selectivity than the unmodified analogues.

Shi *et al.* [182] prepared glycopolymer-peptide bioconjugates with anti-oxidant activity. Thus,  $\beta$ -glucoside methacrylate **M101** was polymerized in the presence of 4-cyano-4-[(phenylcarbonothioyl)sulfanyl]pentanoic acid **R1** (dioxane, 70 °C) to afford a uniform glycopolymer carrying a dithiobenzoate group at the  $\omega$ -chain end ( $M_n = 6300$  Da,  $D = 1.10$ , Entry 200, Table 3). The latter was replaced with a pyridyldisulfide by concomitant aminolysis (with ethanolamine) and thiol-disulfide exchange (with 2,2'-dithiodipyridine). After Zemplén deacetylation of the glucoside residues ( $\text{MeONa/MeOH/CHCl}_3$ ), reduced L-glutathione (an antioxidant tripeptide) was conjugated to the glycopolymer via a thiol-disulfide exchange reaction with release of 2-mercaptopyridine in solution. Conjugation of the peptide to the glycopolymer enhanced its affinity for ConA (3-fold increase in  $K_a$  compared to the pyridyldisulfide modified glycopolymer) and conferred antioxidant properties to the adduct, thus expanding its biomedical potential.

Zhou *et al.* [188] described the synthesis of glycopolymer-modified with poly(L-lysine) and studied its condensation with plasmid DNA for gene therapy applications. To this end,  $\beta$ -lactoside methacrylate **M43** was polymerized in the presence of **R1** ( $\text{CHCl}_3$ , 70 °C) to afford glycopolymers with various chain lengths ( $M_n = 5500$ – $20,000$  Da,  $D = 1.14$ – $1.22$ , Entry 213, Table 3). After Zemplén deacetylation of the lactoside moieties, glycopolymer chains were grafted to poly(L-lysine) ( $M_w = 150$ – $300$  kDa) via the carboxylic group at their  $\alpha$ -chain end (EDC/NHS, water). The resulting conjugate was less cytotoxic than the starting poly(L-Lysine), possibly due to reduced number of charges, and could condense plasmid DNA. Successful transfection trials were conducted with mouse embryonic fibroblast (NIH3T3) and human hepatoma (HepG2) cell lines

Luo *et al.* [183] synthesized thermoresponsive glycopolymer architectures by a combination of RAFT and ROP (Entry 205–207, Table 3). To this aim, glucofuranose methacrylate **M13** was polymerized in the presence of **R1** (1,4-dioxane, 70 °C, 7 h) and the resulting macroRAFT agent ( $M_n = 6400$  Da,  $D = 1.21$ ) was consecutively chain extended with 2-hydroxyethyl methacrylate **M33**

and NIPAAm **M42** (DMF, 70 °C) to afford fairly uniform triblock glycopolymers (e.g.,  $M_n = 9,300$  Da,  $D = 1.27$ ). After removal of the thiocarbonylthio end-group with AIBN (**I4**), the former was used to initiate the polymerization of  $\epsilon$ -caprolactone **M19** in the presence of  $\text{Sn}(\text{Oct})_2$  (DMF/toluene, 110 °C, 48 h) to afford uniform “coil-comb-coil” poly**M13**-*block*-poly(**M33**-*graft*-**M19**)-*block*-poly**M42** (e.g.,  $M_n = 13,000$  Da,  $D = 1.21$ ). After removal of protecting groups (80% formic acid, 60 °C), the amphiphilic glycopolymer self-assembled into spherical micelles with temperature dependent size and featuring a hydrophobic poly(**M33**-*graft*-poly**M19**) core and a hydrophilic poly**M13**/poly**M42** shell. The micelles bound to ConA and a longer polyNIPAAm segment resulted in a lower association constant  $K_a$ . This effect was attributed to the steric hindrance of the polyNIPAAm block in the shell.

Glassner *et al.* [184] reported the synthesis of block copolymers via hetero-Diels-Alder (HDA) coupling of end-of-chain diene- (cyclic or open chain) and dienophile-functionalized polymers obtained by RAFT polymerization. Hence glucofuranose acrylate **M9** was polymerized in the presence of dithioester chain transfer agent **R32** (toluene, 75 °C) to afford, after deprotection in formic acid 70%, a polymer with  $M_n = 6400$  Da and  $D = 1.14$  (Entry 208, Table 3). The thiocarbonyl group at the  $\omega$ -chain-end was then used as dienophile in the reaction with a stoichiometric amount of cyclopentadiene-terminated PEG (water, RT, 15 min) to afford a double hydrophilic diblock glycopolymer ( $M_n = 13,600$  Da,  $D = 1.11$ ). Interestingly, the possibility to use open-chain dienes in HDA reactions in water at ambient temperature was also demonstrated.

The same group [185] described the decoration of poly(glycidyl methacrylate) microspheres with glycopolymer chains by HDA addition. Thus, glucofuranose acrylate **M9** was polymerized using dithioester RAFT agent **R23** (toluene, 75 °C) to obtain a fairly uniform polymer with  $M_n = 4200$  Da and  $D = 1.20$  ( $p = 25\%$ , Entry 209, Table 3). Subsequently, the dienophilic dithioester end-group of the glycopolymer was reacted with cyclopentadiene-functionalized poly(glycidyl methacrylate) microspheres (TFA,  $\text{CHCl}_3$ , 50 °C) to afford, after deprotection of the sugar residues, glycopolymer-decorated microspheres with a loading capacity of  $2.63 \times 10^{19}$  chains/g and  $0.16$  chains/ $\text{nm}^2$ . These values are comparable to those obtained from other grafting “from” or “to” methods.

Dan *et al.* [186] described the polymerization of an amphiphilic glycomonomer and the pH-dependent self-assembly of the resulting polymer.  $\beta$ -Glucoside methacrylate **M113a-b** carrying a hydrophobic alkyl chain (C6 or C8) was polymerized in the presence of dithiobenzoate **R10** ( $\text{CHCl}_3$ , 65 °C; Entry 210–211, Table 3) to afford uniform polymers ( $D = 1.09$ – $1.12$ ) with  $M_n = 13,000$ – $22,000$  Da. After Zemplén deacetylation of the carbohydrate residues, the amphiphilic homoglycopolymer self-assembled in aqueous solution to give multimicellar assemblies such as spherical aggregates, fractals, and swelled micellar clusters, depending upon the solution pH. The binding efficiency of these clusters to ConA was nevertheless moderate.

### 6.1.3. Styrenic Monomers

The RAFT polymerization of aldehydo-glycomonomer **M50** and the self-organization of the resulting polymer into micelles was the subject of a paper by Xiao *et al.* [201] The reaction was mediated by **R11** (THF, 60 °C, 50 h; Entry 238, Table 3) and proceeded with pseudo-first order kinetics and a linear increase of molar mass with conversion. Uniform polymers were thus obtained ( $D_d = 0.10$ ) whose molar mass substantially deviated from the theoretical value though ( $M_n/M_{n,\text{th}} \cong 0.6$ ).



Deprotection of the sugar moieties (88% formic acid) afforded amphiphilic glycopolymers that, in aqueous solution, auto-assembled into micelles with diameter in the range 80–205 nm depending on the molar mass of the polymer. Protein-bioconjugated nanoparticles were then prepared by the immobilization of BSA onto the aldehyde-functionalized micelles, presumably with formation of imine bonds.

This work was later extended to the synthesis of biodegradable glycopolymers micelles loaded with Doxorubicin (an anticancer drug) [202]. To this end, **M50** was copolymerized with dioxepane derivative **M94** in the presence of **R11** (**I10**, anisole, 130 °C) to afford a fairly uniform copolymer with  $M_n = 18,000$  Da and  $D = 1.29$  (Entry 239, Table 3). Deprotection of the corresponding copolymer was performed under acid conditions (90% formic acid, RT, 2 h) but the extent of any concomitant hydrolysis of ester linkages was not investigated. Doxorubicin was then conjugated to the deprotected glycopolymer (via an imine bond formed in DMSO) and micelles loaded with up to 14% w/w of drug were obtained by dialysis against water. These micelles had average hydrodynamic diameter of 125 nm, narrow size distribution ( $D_d < 0.2$ ) and proved to be cytotoxic for HeLa cancer cells.

Wang *et al.* [203] studied the optical activity of homopolymers and block copolymers obtained from the RAFT polymerization of protected glycomonomer **M51**. Homopolymerizations of **M51** were carried out in the presence of **R12** (toluene, 90 °C, 50 h) and showed a hybrid evolution of molar mass with conversion, with  $M_n$  reaching a plateau at ~40% conversion (Entry 240, Table 3). Here it should be noted that under the condition used all initiator was actually consumed in the first few hours of reaction. The same monomer was also polymerized using polySty, polyMMA and polyMA macro-chain transfer agents under the same conditions (Entry 241–243, Table 3). Unsurprisingly, the optical rotatory power of poly**M51** in THF was found to depend on its molar mass (for homopolymers) and on the mass content of glycomonomer (for the copolymers). Also, preliminary tests suggested that poly**M51** can selectively adsorb one enantiomer from a solution of racemate into which it was suspended.

## 6.2. RAFT Starting from Unprotected Glycomonomers/GlycoRAFT Agents

### 6.2.1. Diene-Like Monomers

Stenzel *et al.* [200] synthesized thermoresponsive glycopolymers bearing  $\alpha$ -mannoside residues and studied their interaction with ConA. Thus, homo- and block copolymers of 4-ethenyl-1*H*-1,2,3-triazole derivative **M78** with NIPAAm **M42** were synthesized (Entry 236–237, Table 3): The homopolymerization of **M78** was mediated by **R5** ( $H_2O/MeOH = 2:1$ , 60 °C) and afforded a series of fairly uniform glycopolymers ( $M_n = 8900$ – $51,500$  Da,  $D = 1.16$ – $1.24$ ). One of them was then used as macroCTA for the polymerization of NIPAAm (DMAc, 60 °C) to afford a thermoresponsive glycopolymer with  $M_n = 32,400$  Da and  $D = 1.12$ . Interestingly, the avidity of block copolymer micelles for ConA exceeded that for the linear glycopolymer at the same temperature.

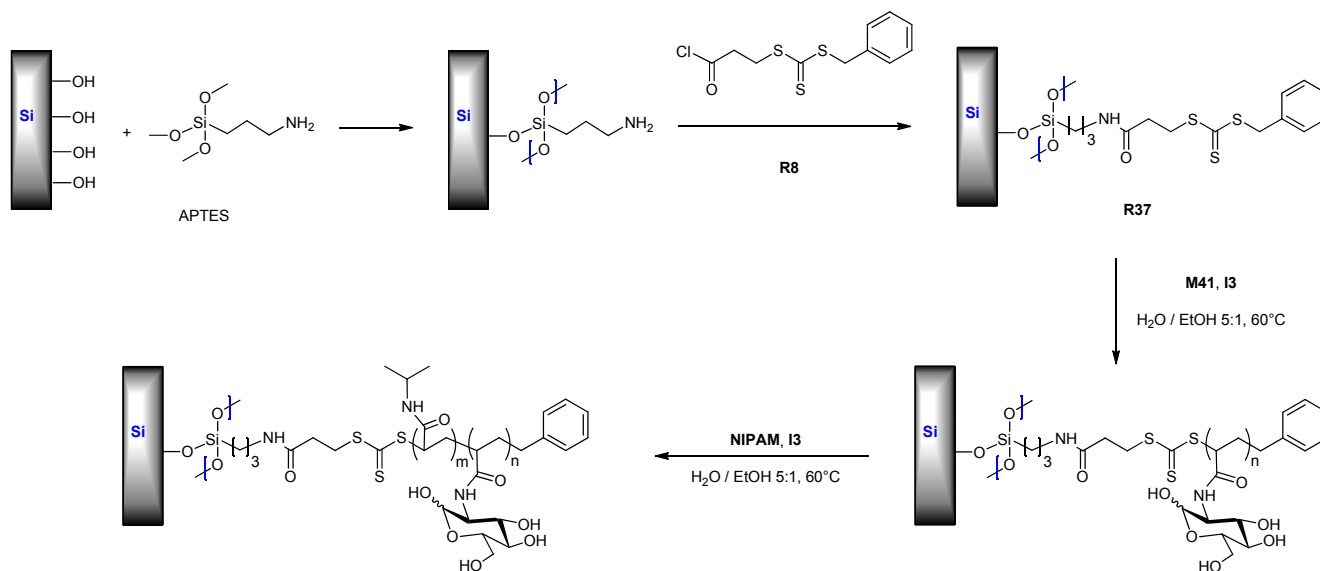
### 6.2.2. (Meth)acrylamide Monomers

Stenzel *et al.* [169] studied the polymerization of glucosamine acrylamide **M41** in aqueous medium with monofunctional trithiocarbonate **R5** and with trifunctional trithiocarbonate **R7** ( $H_2O/EtOH$  5:1,

60 °C). In the case of **R5**, increasing the amount of RAFT agent while keeping constant the amount of initiator resulted in a longer induction period (up to 3 h), a slower rate of polymerization and narrower molar mass distributions (Entry 166–167, Table 3). Furthermore, a poly**M41**·**R5** macroRAFT agent was chain extended with NIPAAm **M42** in order to obtain a thermoresponsive block copolymer (DMSO/H<sub>2</sub>O 1:1, 60 °C; Entry 168, Table 3). SEC traces indicated a non-quantitative re-initiation of the macroRAFT agent together with significant bimolecular termination above ~80% conversion. The possibility to generate 3-arm poly**M41** stars from Z-designed trifunctional RAFT agent **R7** was also investigated: First the macroRAFT agent was prepared by the polymerization of 2-hydroethyl acrylate with **R6** ( $M_n = 4500 \text{ g mol}^{-1}$ ,  $D = 1.07$ ); the latter was then used for the polymerization of **M41** under the conditions previously described (Entry 169, Table 3). Monomer consumption did not obey a first order kinetics but, contrary to what was seen with **R5**, no induction period was observed at the beginning of polymerization and similar reaction rates were observed for two different monomer/CTA<sub>0</sub> ratios. Fairly uniform polymers ( $D = 1.21$ ) and good control over molar mass ( $M_n/M_{n,th} = 1.22$ ) were observed at low monomer conversion for a monomer/CTA<sub>0</sub> ratio of 200, but higher conversions and/or the targeting of longer chains resulted in a marked loss of control, possibly due to increasing steric crowding around star core.

The same monomers (**M41** and **M42**) were also used for grafting glycopolymers and thermosensitive block copolymers brushes onto silica wafers [220]. To this aim, RAFT agent **R8** was immobilized on a silica surface previously modified with (3-aminopropyl)triethoxysilane (Scheme 23) and **R5** was added as sacrificial CTA to better control the polymerization. The homopolymerizations of **M41** (monomer<sub>0</sub>/CTA<sub>0</sub> = 200) and NIPAAm (monomer<sub>0</sub>/CTA<sub>0</sub> = 400) were carried out under the conditions previously described by Bernard *et al.* [169]. A linear increase of the brush thickness was observed with conversion and in fairly uniform polymer chains ( $D \leq 1.25$ ). Chain extension of Si-brush-poly**M41** with NIPAAm had a similar effect on the brush layer thickness and contact angle measurement confirmed that the second block had grown between the first block and the silicon surface as depicted in Scheme 23.

**Scheme 23.** Immobilization of a RAFT agent on silica wafer followed by the synthesis of a thermo-responsive glyco-block copolymer as described by Stenzel *et al.* [220].



Narain *et al.* [165] described the polymerization of unprotected methacrylamide derivatives **M69** and **M70** in H<sub>2</sub>O/DMF mixtures (14%–20% DMF, 70 °C) in the presence of **R1** as the RAFT agent (Entry 157–158, Table 3). After an induction period of 60 min, reactions proceeded with pseudo-first order kinetics and a linear evolution of  $M_n$  with conversion. Fairly uniform glycopolymers ( $D \leq 1.2$ ) were thus obtained which possessed monomodal molar mass distributions and a predetermined molar mass ( $0.82 \leq M_n/M_{n,th} \leq 0.96$ ). MacroRAFT agents were then prepared by stopping the polymerizations at 60%–75% conversion; they were chain extended with three different monomers (**M55**, **M71** and **M72**) in aqueous solution (at pH 4 in the case of **M72**; 70–80 °C) to afford double hydrophilic cationic block glycopolymers with  $1.39 \leq D \leq 1.44$  (Entry 159–161, Table 3). Toxicity studies showed that neither the glycopolymers nor the derived cationic-copolymers were cytotoxic in the concentration range  $2 \mu\text{mol L}^{-1}$  to  $6 \mu\text{mol L}^{-1}$ . Finally, complexation of the cationic glyco-copolymers with plasmid DNA resulted in the formation of well-defined nanostructures ( $d = 30\text{--}35 \text{ nm}$ ).

The same group [221], successfully modified fluorescent quantum dots (QDs) with biotinylated glycopolymers via carbodiimide coupling. To this aim, a statistical copolymer of **M69**, **M71** and biotinylated methacrylamide **M73** was synthesized by RAFT polymerization mediated by **R14** (water, 70 °C). QDs featuring carboxylic groups at their surface were then activated with EDC and coupled with the pendant amino groups of the glycopolymer: The resulting QDs showed excellent optical properties and colloidal stability together with an improvement in biocompatibility (*i.e.*, lowered cytotoxicity) compared to the original QDs.

Miura *et al.* [164,175] synthesized sugar-decorated gold nanoparticles (GNPs) and gold substrates from thiol-terminated glycopolymers obtained by RAFT. Hence, acrylamide derivatives of  $\alpha$ -D-mannoside **M76** and 2-acetamido-2-deoxy- $\alpha$ -D-glucoside **M77** were both homopolymerized and copolymerized with acrylamide (**M75**) in the presence of dithiobenzoate **R18** (DMSO/H<sub>2</sub>O, 60 °C; Entry 182–183, 187, Table 3) [175]. Under these conditions a partial hydrolysis of the RAFT agent was observed that negatively affected control over the molar mass ( $1.2 \leq D \leq 1.5$ ). The end-of-chain dithiobenzoate group was then reduced with NaBH<sub>4</sub> and the resulting thiol-terminated glycopolymers were grafted to pre-formed GNPs ( $d = 40 \text{ nm}$ ) to yield glycoparticles of various diameters ( $d = 15\text{--}100 \text{ nm}$ ). The latter showed specific recognition of lectins and of selected strains of *E. coli* (*i.e.*, ORN178, an  $\alpha$ -Man binding strain, and ORN208, a mutant strain with no  $\alpha$ -Man binding ability).

In a separate study [164], the same chemistry was applied to the synthesis of gold substrates covered with a glycopolymer thin layer ( $\sim 2.5 \text{ nm}$ ) of poly(**M76-stat-AM**) and poly(**M77b-stat-AM**) which were then used for SPR experiments (Entry 156, Table 3): A specific interaction with lectins (ConA and PNA) and Shiga toxins was observed. Furthermore, glycopolymer-substituted GNPs were shown to amplify the SPR signal observed during the detection of lectins.

GNPs functionalized with poly(**M76-stat-AM**) were also employed in a lateral flow assay for the detection of proteins: A test solution of ConA at  $0.01 \mu\text{g mL}^{-1}$  was readily detectable with the glycopolymer-modified GNPs with a sugar ratio of 6% (Entry 184, Table 3) [176]. Finally, the same type of GNPs were used in an electrochemical assay for the detection of ConA [222]. Under optimal conditions, a linear relationship between a differential pulse voltammetry peak current intensity and ConA concentration was found within the range  $10\text{--}10,000 \text{ ng mL}^{-1}$ .

The same group [174,223] investigated the synthesis and biological activity of glycosaminoglycan-mimic polymers capable of inhibiting the association of amyloid  $\beta$ -peptide (a

process associated with Alzheimer's disease). To this end, charged glycomonomers derived from 6-sulfo- $\beta$ -D-GlcNAc (**M80**) and  $\beta$ -D-glucuronic acid (**M81**) were copolymerized either together or with acrylamide (**M75**) in the presence of **R18** as the control agent (H<sub>2</sub>O/DMSO, 60 °C; Entry 178, 188–189, Table 3). Polymers with molar masses up to 100,000 Da were obtained with  $D$  in the range 1.3–1.7, the sole improbable exception being a poly(**M80-stat-M75**) copolymer with  $M_n = 210,000$  Da and  $D = 1.0$ . The interaction between these glycopolymers and A $\beta$ (1-40) peptide was investigated by AFM, Circular Dichroism and Thioflavin T fluorescence assay (for the inhibition of protein aggregation) and polymers containing **M80** units were found to have the highest inhibition activity for peptide aggregate.

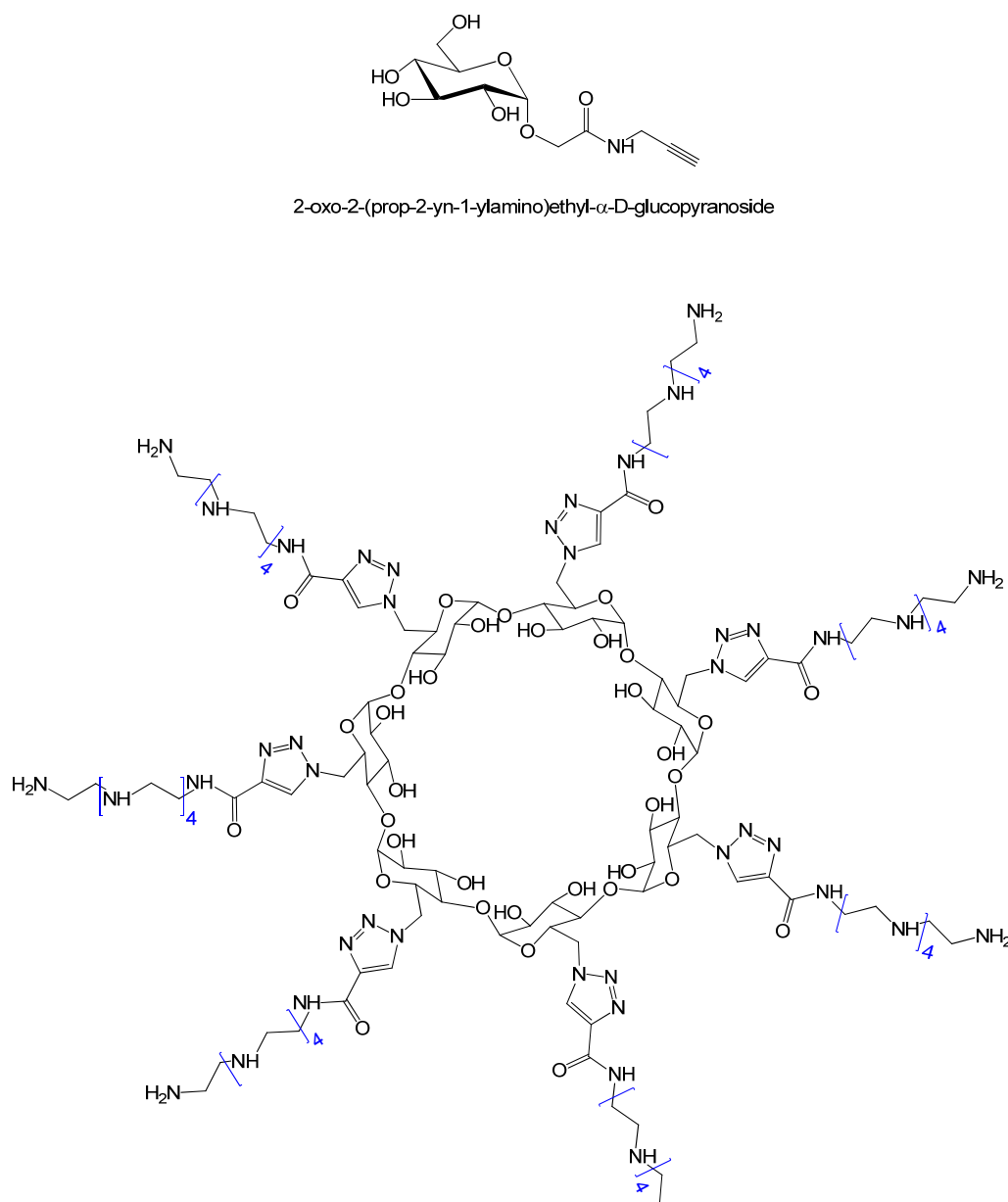
The one-pot synthesis of glycopolymers by *ab initio* RAFT emulsion polymerization was described by Stenzel *et al.* [170]. To this end, a RAFT colloidal stabilizer (RAFT*stab*) was obtained by the polymerization of 2-acrylamido-2-deoxy-D-glucosamine **M41** in the presence of **R21** (DMAc, 70 °C; Entry 170, Table 3). The RAFT*stab* was then dissolved in water at a concentration higher than its cac ( $>14.5$  mmol L<sup>-1</sup>) and was used for the emulsion polymerization of styrene with and without a disulfide-derived crosslinker (80 °C; Entry 171–172, Table 3). TEM images showed that spherical particles were obtained with and without the added crosslinker, although more uniform particle size distributions were obtained in the first case. Also, following reduction of the disulfide bonds with DTT, cross-linked glycoparticles could be re-dissolved in DMAc. Finally, the functionalized latexes were clustered by ConA and formed aggregates with *E. Coli*, thus confirming the availability of carbohydrate residues.

The same group [224] investigated the surface grafting of poly(**M41-stat-NIPAAm**) statistical copolymers to honeycomb structured porous films via a grafting-to approach. To this end, a cross-linked film of poly(**St-stat-MAnh**) was reacted with a diamine and **R8** was attached to the resulting amino-groups on the surface. The same film was then exposed to the copolymerization of **M41** and **NIPAAm** in the presence of **R5** as sacrificial control agent (H<sub>2</sub>O/acetone 1:1, 60 °C). As a result, thermoresponsive glycopolymer chains were grafted to the film surface and their molar mass was found to be 3 times that of the free chains in solution (for which  $M_n/M_{n,th}$  was close to unity). Interestingly, above LCST the surface glycopolymer could bind ConA but the same interaction was turned off below LCST.

Abdelkader *et al.* [172] described the synthesis of three acrylamide glycomonomers (**M85**, **M86** and **M87**) and their polymerization in the presence of **R5**. After an induction period of one hour, the polymerization of  $\alpha$ -D-glucoside **M85** (H<sub>2</sub>O/MeOH 5:1, 70 °C) proceeded with first order kinetics to afford uniform polymers ( $D \leq 1.13$ ) with  $M_n$  in the range 15,600–113,000 Da (Entry 176, Table 3). Also, a poly**M85-R5** macroRAFT agent was prepared in the same way and successfully chain extended with NIPAAm **M42** (DMSO/H<sub>2</sub>O 1:1, 70 °C). By contrast, the polymerizations of azido-functionalized glycomonomers **M86** and **M87** was more complicated (Entry 185–186, Table 3): When the same conditions used for **M85** were applied to 2-azido-2-deoxy- $\alpha$ -D-mannoside **M86**, a fairly uniform polymer was obtained ( $D = 1.35$ ) that could not be chain extended though. However, conducting the polymerization at a lower temperature (30 °C, **I9**) lead to a uniform glycopolymer ( $D = 1.15$ ,  $M_n = 56,000$  Da) that could be chain extended with NIPAAm (always at 30 °C) to give a fairly uniform block copolymer ( $D = 1.18$ ). Finally, starting with 6-azido-6-deoxy- $\alpha$ -D-mannoside **M87** no polymerization was observed at either 30 °C or 70 °C. Poly**M86** was further functionalized by

Huisgen 1,3-dipolar Cycloaddition with 2-oxo-2-(prop-2-yn-1-ylamino)ethyl- $\alpha$ -D-glucopyranoside (Scheme 24).

**Scheme 24.** Propargyl glucoside used by Abdelkader *et al.* [172] for the post polymerization functionalization of azido-containing glycopolymers (top) and polycationic cyclodextrin cluster used by Buckwalter *et al.* for the preparation of pDNA polyplexes (bottom) [225].



Smith *et al.* [171] reported the synthesis of positively charged diblock glycopolymers and their use in cell transfection. The rationale was that these macromolecules would form interpolyelectrolyte nanoparticle complexes (“polyplexes”) with a core of nucleic acid complexed to a poly(amine) block and a shell of hydrophilic glycopolymer chains. The latter would ensure the water solubility of the complex and provide steric stabilization against aggregation in the presence of salts and negatively charged serum proteins. Thus, 2-deoxy-2-methacrylamido-D-glucose **M84** was polymerized in the presence of **R24** (acetate buffer/EtOH 4:1, pH 5.2, 70 °C) and the resulting macroRAFT agent

(poly**M84**<sub>46</sub>,  $M_n = 11,700$  Da,  $D = 1.24$ ) was chain extended with 2-aminoethyl methacrylamide **M71** to yield uniform block glycopolymers with a varying length of the second block (Entry 173–175, Table 3). From these, stable polyplexes with plasmid DNA (pDNA) and small interfering RNA (siRNA) were prepared whose cytotoxicity and transfection efficiency was found to depend on the length of the poly**M71** block: Shorter **M71** blocks resulted in lower toxicity and better transfection results in the case of pDNA polyplexes, whereas the opposite was observed for siRNA delivery from siRNA polyplexes, with significant gene knockdown with a longer poly**M71** block.

The use of polycationic glycopolymers as non-viral gene delivery carriers was also investigated by Ahmed and Narain [166]. To this aim they synthesized both homopolymers and statistical and block copolymers of gluconic acid derivative **M70** with 2-aminoalkyl methacrylamides **M55** and **M71** in the presence of dithiobenzoate **R1** (H<sub>2</sub>O/DMF 5:1, 70 °C; Entry 162–163, Table 3). It was found that statistical copolymers poly(**M70**<sub>25-stat-M55</sub><sub>34</sub>) and poly(**M70**<sub>36-stat-M71</sub><sub>40</sub>) had the lower cytotoxicity and the higher gene expression after transfection among the polymers tested.

The same authors [167] synthesized hyperbranched glycopolymers carrying propyl-D-gluconamide and ethyl-D-lactonamide residues and examined their blood compatibility (Entry 164 and 179; Table 3). To this end, methacrylamides **M70** and **M105** were copolymerized with *N,N'*-methylenebisacrylamide **M106** (the crosslinker) in the presence of dithiobenzoate **R1** (DMF/water, 70 °C) to afford hyperbranched glycopolymers with molar mass in the range 19,000–38,000 Da and  $D = 1.74$ – $2.5$ . The synthesized materials showed good blood compatibility as tested by blood coagulation assays, hemolysis assays, and platelet and complement activation analysis in the concentration range 0.1–5 g L<sup>-1</sup>. Nevertheless, their cytotoxicity proved to be cell- and concentration-dependent, with human dermal fibroblasts and leukemia cells remaining more viable than malignant hepatoma cells (Hep G2 cells) after exposure the glycopolymers. The aforementioned strategy was also applied to the synthesis of cationic branched copolymers of **M70** and **M105** with 2-aminoethyl methacrylamide **M71** that were then used for DNA complexation (Entry 165, 180; Table 3) [168]. This study confirmed that in addition to the composition and molar mass of the polymers, their molecular architecture has an influence on the stability of the derived polyplexes and thus on the level of transfection. Indeed, linear glycopolymers appear to be more effective than hyperbranched ones [166].

Buckwalter *et al.* [225] reported a comparative study between two adamantine-terminated polymers for their ability to stabilize plasmid DNA (pDNA) polyplexes once complexed by a polycationic cyclodextrin cluster. To this end, 2-deoxy-2-methacrylamido-D-glucose **M84** was polymerized in the presence of adamantyl-derivative **R31** (acetate buffer, 70 °C) to afford poly**M84** with  $M_n \cong 13,000$  Da. A complex was then formed between the adamantyl group at the  $\alpha$ -chain end of the glycopolymer and the cyclodextrin-derived cluster in Scheme 24. Said complex was subsequently used to form polyplexes with pDNA ( $d = 90$ – $110$  nm) at different N/P ratios (N = number of protonatable amines on the cluster, P = phosphate groups on the DNA chain). As a result, the novel glycopolymer-based polyplexes had better colloidal stability than their AD-PEG analogues under physiological salt conditions, whereas comparable stability was observed in serum-containing medium but only at high N/P ratios. Yet, the intake of glycopolymer-polyplexes by cells depended on the cell type: It was efficient with human glioblastoma cells but poor in the case of human adenocervical carcinoma cells (HeLa).

Galectins are the most widely expressed class of lectins in all organisms, typically bind glycans containing  $\beta$ -galactoside residues and share primary structural homology in their carbohydrate binding domain [24]. Bertozzi *et al.* [163] probed the galectin-mediated ligand cross-linking directly on live cells incorporating fluorescently labeled glycopolymers in their cellular membrane. To this aim,  $\beta$ -lactoside acrylamide **M107a** and  $\beta$ -cellobioside acrylamide **M108** were homopolymerized in the presence of a RAFT agent (**R33**) featuring a phospholipid-derived leaving group (DMF/H<sub>2</sub>O 1:4, 70 °C) to afford fairly uniform polymers with  $M_n \cong 21,000$ – $23,000$  Da (Entry 155 and 181, Table 3). The trithiocarbonate group of the polymers was reduced with NaBH<sub>4</sub> and the resulting thiols were conjugated to a maleimide functionalized fluorescent dye (either Alexa fluor 488 or Alexa fluor 555). The fluorescent glycopolymers were then incorporated into the cell membrane of *ldld* Chinese Hamster Ovary (CHO) cell mutant (a cell line that is deficient in galactosides) and their fluorescence lifetime and diffusion time were measured by FRET imaging and fluorescence correlation spectroscopy in the presence and in the absence of galectin-1. As a result, evidence was gathered for the galectin-1-mediated glycopolymer cross-linking on the surface of the engineered cells.

Albertin *et al.* [173] described the synthesis and self-assembly of a triblock glycopolymer bearing  $\beta$ -D-glucopyranosylamine and *N*-acryloylmorpholine residues. First, symmetrical trithiocarbonate **R36** was used for the synthesis of a poly**M53** macroRAFT agent (D<sub>2</sub>O, 60 °C,  $M_n = 16,800$  Da,  $D = 1.04$ ); second, the former was chain extended with *N*-acryloyl- $\beta$ -D-glucopyranosylamine **M116** (H<sub>2</sub>O, 60 °C) to afford a uniform ABA triblock glycopolymer ( $M_n = 26,000$  Da,  $D = 1.06$ , Entry 177). Even though the polymer was highly hydrophilic, AFM and DLS analysis showed that a small fraction of it associated in water to give hollow structures that were fairly uniform in size ( $d \cong 320$  nm) and possessed a very thin wall (1.5–3 nm). By contrast, in THF/water 91:9 v/v the same polymer self-organized into spherical unilamellar polymersomes with a diameter of about 380 nm and polyNAM external layer.

### 6.2.3. (Meth)acrylate Monomers

The first report on the synthesis of a well-defined glycopolymer by RAFT was published by Lowe *et al.* in 2003 [191]. Remarkably, this was also the first example of RDRP of an unprotected glycomonomer directly in aqueous solution. 2-Methacryloxyethyl-D-glucopyranoside **M34a** was polymerized in the presence of **R1** as the chain transfer agent and **I3** as the initiator (water, 70 °C; Entry 217–218, Table 3): No induction period was observed at the beginning of the process and monomer consumption followed pseudo first order kinetics. The increase of molar mass with conversion was linear up to 40% but accelerated afterwards, and a 30% deviation from the theoretical value was attained at  $p = 70\%$ . Here it should be noted that NaHCO<sub>3</sub> was used to help the solubilization of **I3** in water. A poly**M34a**·**R1** macroCTA was then prepared by stopping the polymerization at 40% conversion and it was used for a self-blocking experiment and for chain extension with 3-sulfopropyl methacrylate **M35** (Entry 219–220, Table 3). In the two cases a good agreement between experimental and theoretical molar mass was observed, but the dispersity index was somewhat high ( $D = 1.54$ – $1.63$ ).

The same chain transfer agent was used by Albertin *et al.* [194] for a comprehensive study of the RAFT polymerization of model glucoside methacrylate **M36** in aqueous solution. Since the solubility

of **R1** and **I3** in straight neutral water is low, three different protocols were tested for polymerizations at 70 °C. In the three cases the initiator and CTA were dissolved separately before being added to the monomer solution in water: In protocol 1, **R1** and **I3** were dissolved in Na<sub>2</sub>CO<sub>3</sub> 0.1 mol L<sup>-1</sup> (pH ≅ 11), in protocol 2 they were dissolved in NaHCO<sub>3</sub> 0.1 mol L<sup>-1</sup> (pH ≅ 8.3) and in protocol 3 they were dissolved in EtOH (Entry 224–226, Table 3). Substitution of a base by EtOH eliminated the hydrolysis of the RAFT agent throughout the polymerization and lead to a uniform polymer ( $\bar{D} = 1.14$ ) and a good control over molar mass ( $M_n/M_{n,th} = 0.93$ ) event at complete conversion. The conditions found in this study were then applied to synthesis of uniform poly**M36** samples of varying  $DP$  [195] and to the synthesis of double-hydrophilic block copolymers with 2-hydroxyethyl methacrylate **M33** (60 °C) and 2-methacryloxyethyl-D-glucopyranoside **M34a** (Entry 222 and 227, Table 3) [193]. The kinetics for the two chain extension experiments were first order and fairly uniform water soluble polymers ( $\bar{D} = 1.20$ ) with reasonably controlled molar masses were obtained ( $M_n/M_{n,th} \cong 0.82$ ). The same protocol was applied to the homopolymerization of **M34** and to the synthesis of a uniform diblock glycopolymer with mannoside methacrylate **M37** ( $\bar{D} = 1.16$ ; Entry 223, Table 3). The polymerization kinetics for the second step was slower than what observed for the chain extension of poly**M36** with **M34a**: The authors attributed this difference to the higher steric hindrance around the propagating radicals of **M37** compared to **M34a**. A detailed kinetic study of the radical polymerization of **M36** mediated by **R1** and initiated by **I3** in D<sub>2</sub>O/DMSO-*d*<sub>6</sub> was also performed [226]. In their paper, Albertin and Cameron used *in situ* <sup>1</sup>H NMR spectroscopy to probe the influence of temperature, initiator and chain transfer agent concentration, molecular mass of the CTA leaving group, as well as the presence of residual oxygen on polymerization kinetics. In general, RAFT processes were slower than the corresponding conventional radical polymerizations and for a given **R1/I3** ratio, a lower initial concentration of chain transfer agent resulted in lesser rate retardation. Under all tested conditions, an initial non-steady-state period was observed for RAFT polymerization whose duration was inversely proportional to the ratio between the initial amount of CTA and the flux of primary radicals. Attainment of steady-state coincided with complete consumption of the initial CTA, but when **R1** was replaced by a macroCTA the time needed to reach steady state was shortened but not eliminated and its duration proved to still depend on the CTA/initiator ratio. The presence of residual oxygen induced a short induction period (~4 min) and a rate retardation of ~37% in conventional radical polymerization and resulted in a 40 min inhibition period followed by much retarded polymerization in the analogous RAFT experiment. Finally, findings of this study were applied to the synthesis of well-defined oligo**M36** in high yield ( $DP_n = 15\text{--}66$ ;  $\bar{D} = 1.05\text{--}1.12$ ;  $p = 0.93\text{--}1.00$ ).

Spain *et al.* [189] described the synthesis of multivalent glyco-nanoparticles based on poly(β-D-galactoside methacrylate) poly**M38**. First, the polymerization of **M38** was carried out under the same conditions described by Albertin *et al.* [195] to afford a uniform polymer ( $\bar{D} = 1.09$ ) with excellent control over molar mass ( $M_n/M_{n,th} = 1.01$ ; Entry 214, Table 3). From this, glycopolymer-stabilized gold nanoparticles ( $d = 11.5$  nm from DLS) were synthesized by the direct reduction of HAuCl<sub>4</sub> with NaBH<sub>4</sub> in the presence of poly**M38**. These multivalent particles were capable to agglutinate PNA-coated agarose beads in solution.

The strategy described by Albertin *et al.* [195] was used by Stenzel *et al.* [197] for the polymerization of mannose methacrylate **M39** (Entry 230, Table 3). Experiments with different monomer/CTA ratios but a constant initiator concentration were conducted: They all followed



pseudo-first order kinetics and led to uniform polymers ( $D \leq 1.14$ ). As already observed by Albertin and Cameron [226], higher CTA/initiator ratios resulted in longer induction periods. Unsurprisingly, the 6-*O*-linked mannoside residues were unable to bind ConA.

After reporting the atom transfer radical polymerization of **M23** and **M25**, [124] Narain *et al.* investigated their RAFT polymerization (DMF, H<sub>2</sub>O/DMF or H<sub>2</sub>O/MeOH, 60 °C) with the aim of synthesizing multivalent gold nanoparticles (Entry 216 and 228, Table 3) [190]. Two RAFT agents were used in this study (**R14** and **R15**). Fairly uniform polymers were obtained ( $D = 1.19$ – $1.48$ ) at high conversion with  $M_n$  in the range 14,000 Da–51,500 Da. Stable multifunctional glyconanoparticles were synthesized by the *in situ* reduction of H<sub>2</sub>AuCl<sub>4</sub> in the presence of trithiocarbonate-containing glycopolymer and of biotinylated-polyethylene glycol thiol (*bio*-PEG-SH) and their aggregation in the presence of streptavidin was studied.

In their attempt to design nanoparticles for the controlled release of insulin, Cheng *et al.* [227] synthesized an amphiphilic glycopolymer carrying phenylboronic acid residues. To this end, lactobionic acid derivative **M25** was homopolymerized in the presence of **R1** (H<sub>2</sub>O/DMSO 1:1 v/v, 70 °C, 12 h). The resultant polymer was then chain extended with 3-acrylamidophenylboronic acid **M95** under the same conditions (5 h) to yield the target glycopolymer, for which no molecular characterization was provided. The latter self-assembled in water to give nanoparticles with non-uniform size in the range of 50–200 nm, most probably due to inter and intra-molecular interactions of the carbohydrate moieties with phenylboronic acid residues. In fact addition of glucose resulted in the reorganization of the chains into relatively uniform nanoparticles ~160 nm in diameter. Interestingly, their size decreased with increasing glucose concentration.

Pearson *et al.* [192] described the synthesis of a polymeric auranofin mimic via RAFT (auranofin is 1-thio- $\beta$ -D-glucopyranosatotriethylphosphine gold-2,3,4,6-tetraacetate). To this aim, poly(**M59**)-**R5** ( $M_n = 18,800$  Da,  $M_w/M_{n,th} = 2.9$ ,  $D = 1.19$ ) was chain extended with 6-*O*-acryloyl-1-thio- $\beta$ -D-glucoside derivative **M103** (DMF, 70 °C) to afford a non-uniform block glycopolymer ( $M_n = 15,200$  Da,  $M_w/M_{n,th} = 0.94$ ,  $D = 1.45$ , Entry 221, Table 3). The pyridyl disulfide group was then reduced with D,L-dithiothreitol and complexed with AuPEt<sub>3</sub>Cl to yield an amphiphilic copolymer ( $M_n = 28,800$  Da,  $D = 1.29$ ) that self-assembled in aqueous solution to give micelles with  $d = 75$  nm. The latter showed slightly higher anti-proliferation activity against OVCAR-3 human ovarian carcinoma cells than deacetylated auranofin.

Song *et al.* [12] synthesized a series of glycopolymers capable of specifically targeting macrophages for intracellular drug delivery. To this end, three monomers based on *N*-acetyl- $\beta$ -D-glucosamine (**M31**),  $\beta$ -D-galactoside (**M38**), and  $\beta$ -D-mannoside (**M114**) were copolymerized with methacrylamide derivative **M115** carrying a pyridyl-disulfide group (10% molar feed) in the presence of trithiocarbonate **R35** (water/ethanol 3:1, 70 °C). Uniform polymers ( $D = 1.2$ ) with monomodal molar mass distributions and  $M_n$  up to 13,000 Da were obtained with complete monomer conversion (Entry 215, 231–232, Table 3). The specific targeting of these glycopolymers to macrophages was sugar and dose dependent: For instance *in vitro* studies revealed that  $\beta$ -D-mannoside- and *N*-acetyl- $\beta$ -D-glucosamine containing glycopolymers specifically targeted mouse bone marrow-derived macrophages, whereas  $\beta$ -D-galactoside-containing glycopolymer did not. This result was confirmed by *in vivo* studies, which demonstrated that the uptake of the mannoside glycopolymer by alveolar macrophages was up to 6 fold higher than of the galactoside analogue.

#### 6.2.4. Styrenic Monomers

Mancini *et al.* [204] conjugated a trehalose-derived glycopolymer to hen egg white lysozyme to protect it from environmental stresses. Thus, trehalose glycomonomer **M104** was polymerized in the presence of pyridyl-disulfide RAFT agent **R29** or **R30** (DMF, 80 °C; Entry 244–246, Table 3) to afford fairly uniform polymers with  $M_n$  in the range 4200–24,500 Da. A higher molar dispersity index was instead obtained when a higher molar mass was targeted with **R30** ( $M_n = 49,500$  Da,  $D = 1.47$ ). Glycopolymers obtained with **R30** were then conjugated to thiopropionyl lysozyme and the stability of the resulting glyco-conjugates was studied: Compared to the wild-type protein, they retained a higher fraction of activity when stressed with repeated lyophilization cycles (no loss of activity after 10 cycles) and heating (81% activity retained after 1 h at 90 °C).

#### 6.2.5. Vinyl Ester Monomers

The first example of uniform, poly(vinyl ester)-like glycopolymer was reported by Albertin *et al.*, in 2004 [198]. The interest in this type of materials lies in the distinctive advantages that they can offer in terms of environmental biodegradability [228] and, whenever *in vivo* applications are sought after, biocompatibility of the polymer backbone. In fact, hydrolytic cleavage of the pendant groups leaves a poly(vinyl alcohol) main chain, that is a material already used in a number of medical applications [229,230] and that does not seem to interact with cellular blood components [231]. Hence, 6-*O*-vinyladipoyl-D-glucopyranose **M40** was synthesized via enzymatic catalysis and homopolymerized in the presence of either xanthate **R2** (MeOH) or dithiocarbamate **R3** (H<sub>2</sub>O) as the chain transfer agents (**I3**, 60 °C, 48 h). Fairly uniform polymers were obtained ( $D \leq 1.19$ ) at low monomer conversion having  $M_n = 17,000$ – $20,000$  Da (Entry 233–234, Table 3). A higher conversion was obtained in water. The same monomer was subsequently used for the synthesis of star glycopolymers with a grafting-from strategy by using tetra-xanthate **R4** (**I3**, DMAc, 70 °C, 24 h; Entry 235, Table 3) [199]. In spite of the higher temperature and monomer concentration used (70 °C *vs.* 60 °C and 2 mol L<sup>-1</sup> *vs.* 0.5 mol L<sup>-1</sup> of the previous study), a limiting conversion of 50% was achieved after 9 h, probably because 98% of the starting initiator had been consumed by that time.

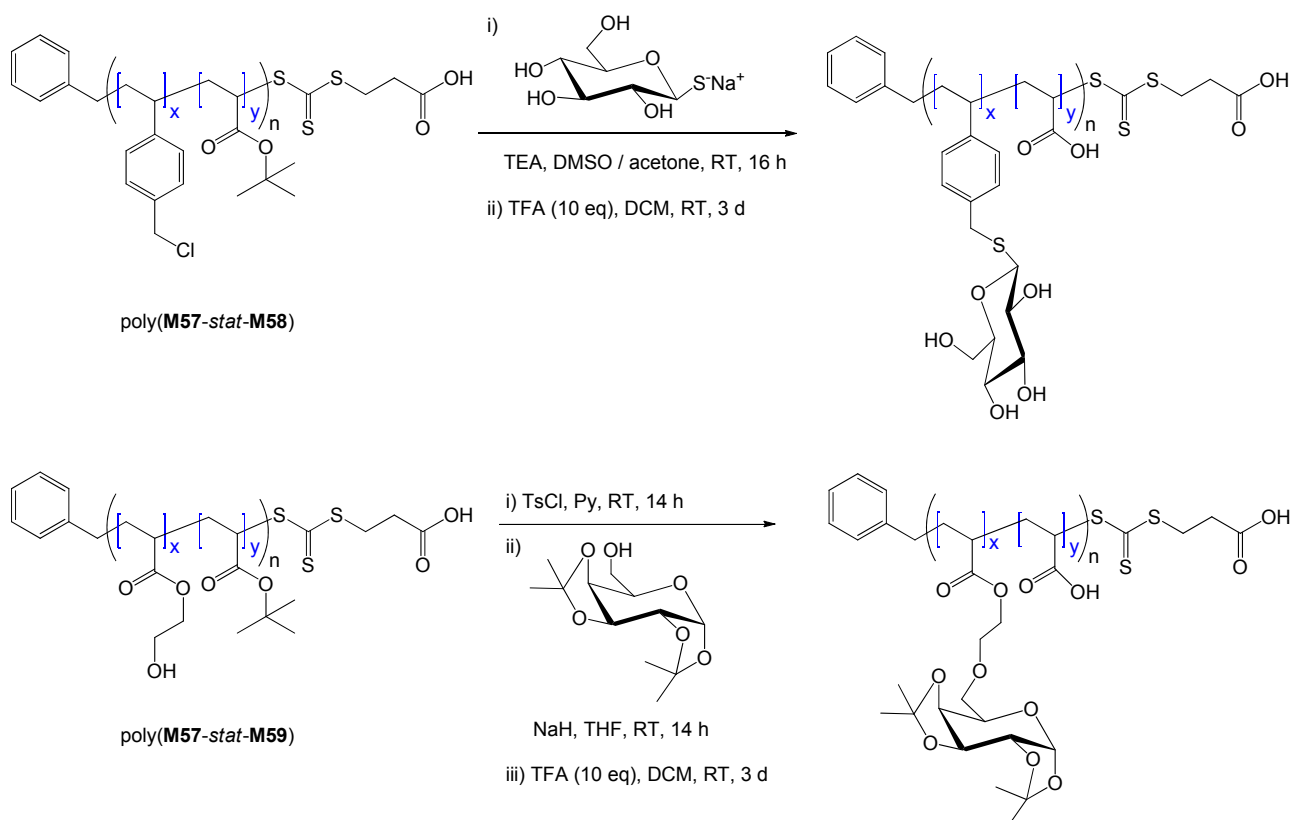
### 6.3. Glycopolymers from Post-Polymerization Reaction

Davis *et al.* [206] reported a versatile one-pot synthesis of end-of-chain biotinylated glycopolymers that is adapted to any amino-sugar (Entry 248, Table 3). Activated acrylate ester **M68** was polymerized in the presence of **R5** (benzene, 70 °C) to afford fairly uniform polymer precursors ( $M_n = 2800$ – $16,000$  Da). The polymers were then isolated and reacted with 2-deoxy-2-amino-D-galactose or 2-deoxy-2-amino-D-glucose firstly (DMF/H<sub>2</sub>O, 3 h; this reaction also cleaves the trithiocarbonate end-group) and to biotin-modified maleimide secondly [Please note that Scheme 1 in the paper by Boyer and Davis contains a mistake: It suggests the use of  $\alpha$ -D-galactopyranosylamine when the equilibrium mixture of D-galactopyranosylamine consists almost entirely of the  $\beta$  form (which is what can be purchased commercially) [232]. Also, the supplementary information to the same paper indicates the use of D-galactose amine hydrochloride from Aldrich, which led us to conclude that the compound used was actually 2-deoxy-2-amino-D-galactose hydrochloride]. In accordance with

previous literature, D-glucose-functionalized glycopolymers were capable of precipitating ConA, whereas their D-galactose analogues were not. The above described strategy was also adapted to the synthesis of star polymers via an arm-first approach (for an example see Entry 249, Table 3) [207]. To this end, poly**M68-R5** was crosslinked with a bis-acrylamide (e.g., **M121**) to afford fairly uniform star polymers that were post-functionalized by nucleophilic displacement with a number of amino-compounds (2-deoxy-2-amino-D-galactose and 2-deoxy-2-amino-D-glucose, among others) or by thiol-ene reaction (e.g., with fluorescein acrylate).

The same group [205] investigated the synthesis of gold nanoparticles decorated by glycopolymers using a layer by layer approach: Two types of copolymers were synthesized starting from *tert*-butyl acrylate **M57**, chloromethylstyrene **M58** and 2-hydroxyethyl acrylate **M59** and by using **R5** as the RAFT agent either in acetonitrile at 60 °C (for poly(**M57-stat-M58**)) or in toluene at 70 °C (for poly(**M57-stat-M59**)) for 12 h (Entry 247, 251, Table 3). The isolated polymers were then functionalized with 1-thio- $\beta$ -D-glucopyranose or 1,2:3,4-di-*O*-isopropylidene- $\alpha$ -D-galactopyranose as depicted in Scheme 25 (Please note that in the original paper there are several mistakes in the representation of the carbohydrate molecules and residues. Here we have reported a corrected version), and following deprotection of the *tert*-butyl and isopropylidene groups with TFA, the negatively charged glycopolymers were assembled layer-by-layer with polyethylenimine onto positively charged gold nanoparticle (GNPs). Finally, the presence of accessible sugar moieties on the surface of the GNPs was confirmed by a binding assay with ConA.

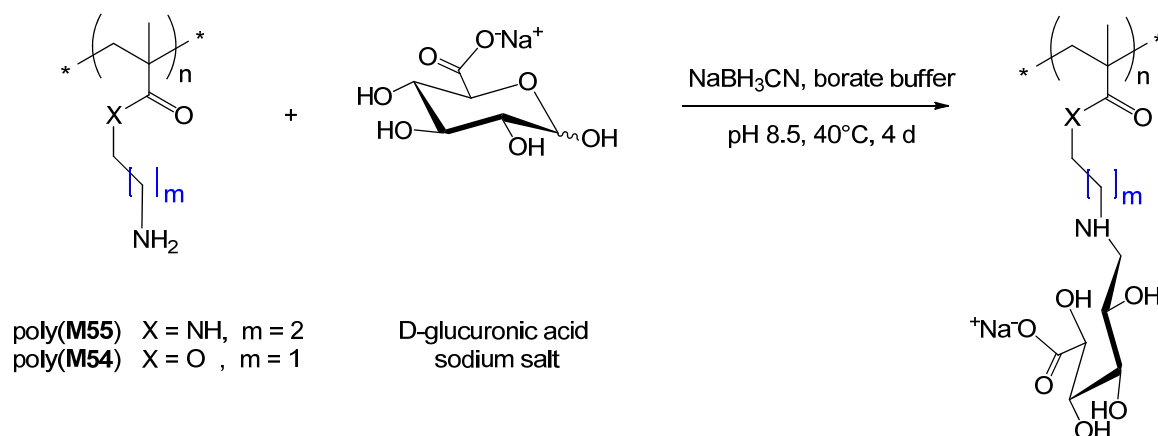
**Scheme 25.** Strategy reported by Boyer *et al.* for the post-polymerization synthesis of negatively charged glycopolymers [205].



Chen *et al.* [209] reported the synthesis of 4-arm star styrenic glycopolymers by post-polymerization reaction (Entry 252, Table 3). First, star polymers were synthesized by the R-group approach: Chloromethylstyrene (**M58**) was polymerized in the presence of tetra functional RAFT agent **R19** (bulk, 120 °C, self-initiation) and fairly uniform polymers were obtained up to 65% conversion ( $\mathcal{D} < 1.35$ ), after which the molar mass distribution was substantially broadened by the presence of linear chains. A series of star polymers was then prepared with  $M_n$  in the range 6000–51,000 Da and reacted with stoichiometric amounts of 1-thio- $\beta$ -D-glucopyranose sodium salt (DMSO, 40 °C, 110 h) to afford star-shaped glycopolymers. Finally, the ability of the later to cluster ConA was tested using turbidity assays and it was found to be equivalent to that of a linear analogue.

Alidedeoglu *et al.* [211] synthesized well-defined glycopolymers carrying 1-amino-1-deoxy-alditol residues derived from D-glucuronic acid directly in water (Entry 256–258, Table 3). To this end, 2-aminoethyl methacrylate **M54** and 2-aminopropyl methacrylamide **M55** were homopolymerized in acetic buffer (pH 5) at 50 °C and 70 °C, respectively, for around an hour in the presence of RAFT agent **R1**; the double hydrophilic copolymer poly(**M54**)-*block*-poly(**M56**) was also prepared under similar conditions. Uniform polymers ( $\mathcal{D} \leq 1.08$ ) with a predetermined molar mass ( $0.85 \leq M_n/M_{n,th} \leq 1.30$ ) were obtained in all cases, although only moderate monomer conversions were achieved ( $p < 0.5$ ). The primary amino functions of these polymers were then used for the reductive amination of D-glucuronic acid (10 eq.) in order to obtain carboxylic acid functionalized glycopolymers (Scheme 26). Higher yields of conjugation were achieved in all cases (>94%), but poly(**M54**) sequences probably underwent side-reactions under the alkaline conditions used.

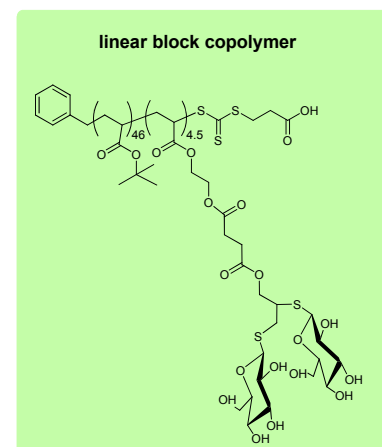
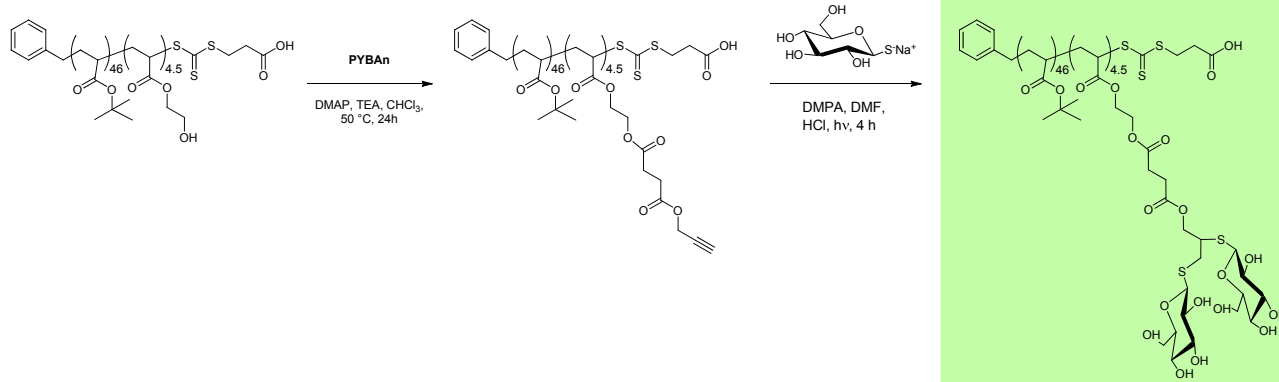
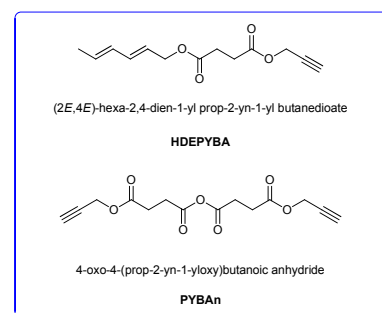
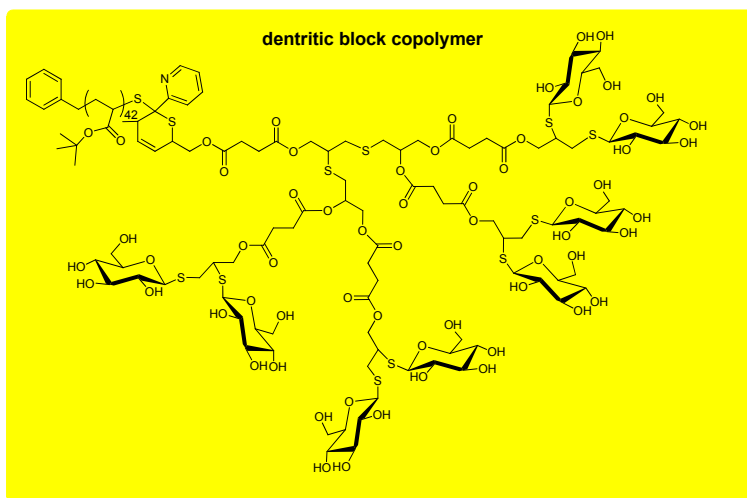
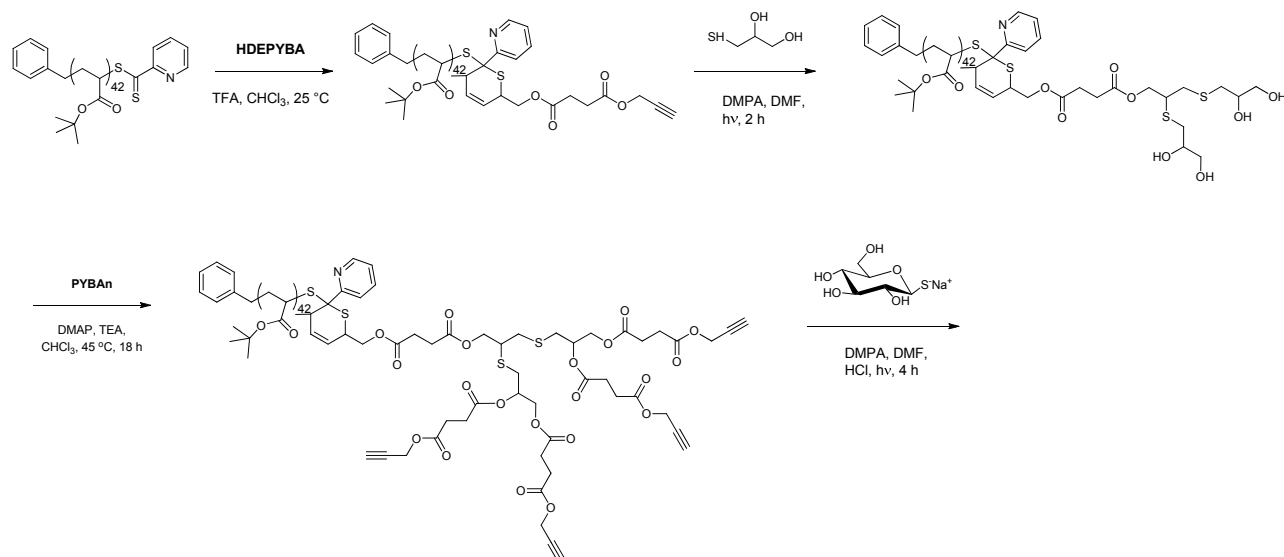
**Scheme 26.** Post-polymerization conjugation of D-glucuronic acid to water soluble polymer featuring primary amino functions as reported by Alidedeoglu *et al.* [211].



The synthesis of highly branched glycopolymers featuring  $\beta$ -D-galactopyranoside and 1-thio- $\beta$ -D-glucopyranoside residues was reported by Semsarilar *et al.* [208] Hence, ethylene glycol dimethacrylate **M82** was either homopolymerized or copolymerized with trimethylsilylpropyne acrylate **M83** (toluene, 60 °C) in the presence of **R10** and **R20**, respectively (Entry 250, 253, Table 3). Non-uniform polymers were obtained in all cases ( $\mathcal{D} \geq 1.6$ ) with  $M_n$  in the range 55,500–182,000 Da. After deprotection of the alkyne groups with TFA, poly(**M82**-*stat*-**M83**) was functionalized either with 1-thio- $\beta$ -D-glucopyranose via thiol-yne radical addition or with azidoethyl- $\beta$ -D-galactopyranose via

Cu(I)-catalyzed dipolar cycloaddition. By contrast, the homopolymer polyM83 was only functionalized with 1-thio-β-D-glucopyranose via phosphine-catalyzed Michael addition.

**Scheme 27.** Synthetic strategies followed by Stenzel *et al.* [210] for the synthesis of amphiphilic glycopolymers.





of the trithiocarbonate group with cysteamine liberated an end-of-chain sulfhydryl that was conjugated to a maleimide-functionalized fluorescent dye (Cy3). 2-(Acetylamino)-1-*O*-amino-2-deoxy- $\alpha$ -D-glucopyranose ( $\alpha$ -aminoxy-GalNAc) residues were then grafted to the polymer backbone in varying density via acid catalyzed oxime ligation. The resulting glycopolymers were anchored to streptavidin coated microarray substrates to generate arrays with variable glycopolymer densities. It was thus found that (i) the binding of the glycopolymer to Soybean agglutinin (SBA), Wisteria floribunda lectin (WFL), and Vicia villosa-B-4 agglutinin (VVA) was dependent on the GalNAc valency, whereas the binding to Helix pomatia agglutinin (HPA) was not; (ii) only SBA cross-linked valency glycopolymers, as indicated by the decreasing dissociation constant observed with increasing average spacing of the surface-bound ligands.

## 7. Conclusion and Perspectives

Well defined glycopolymers architectures have been successfully synthesized with four major reversible-deactivation radical polymerization techniques: Nitroxide-mediated radical polymerization (NMP), cyanoxyl-mediated radical polymerization (CMRP), atom transfer radical polymerization (ATRP) and reversible addition-fragmentation chain transfer polymerization (RAFT). NMP has been mostly applied to protected styrenic monomers and glycoNMP initiators in organic solvent, although Hawker *et al.* also succeeded in polymerizing a protected glucose acrylate using a second-generation alkoxyamine [87,233]. This is mostly the result of the historical period during which those studies were realized (1998–2002): It took several years for scientists to develop new nitroxides and alkoxyamines effective in the polymerization of monomers other than styrenics, and then reaction temperatures remained too high for some carbohydrate derivatives ( $>90$  °C). To date, NMP has been extended to almost all monomers with the exception of vinyl esters and vinyl chloride. Also, SG1 and SG1-derived initiators (essentially BlocBuilder MA) have been applied to the polymerization of acrylamide- [234–236], styrenic- [234], acrylate- [234] and methacrylate-monomers [233,237], directly in homogeneous aqueous solution. Nevertheless, the use of a small fraction of comonomer (typically 8% of acrylonitrile for methacrylates, or sodium 4-styrenesulfonate for methacrylic acid) proved essential for the system to work at  $T < 100$  °C and even then the dispersity index was systematically higher than 1.20.

In spite of these and other limitations, NMP has few advantages over other RDRP techniques: Most monomers can be polymerized with a single nitroxide [53] such as SG1 (and the derived alkoxyamine BlocBuilder MA) or TIPNO, which are now easily accessible; when an alkoxyamine is used the polymerization system requires this sole molecule as both the initiator and the control agent and the system is metal-free; in the synthesis of block copolymers, if no additional radical initiator is used, the system is free of homopolymer chains of the second block. Finally, according to the manufacturer the lethal dose 50 (LD50) of BlocBuilder MA is extremely high, at about  $2000 \text{ g kg}^{-1}$ , and the SG1 that composes the alkoxyamine is not cytotoxic up to  $0.3 \text{ mg mL}^{-1}$  on different cell lines [53]; It can therefore be maintained at the polymer chain-end for most biomedical applications.

Alternatively, cyanoxyl persistent radicals have been successfully used with dienes, acrylamides and acrylates in aqueous solution at temperatures as low as 50 °C. This technique has the added advantage of producing polymers with a cyanate group at the  $\omega$ -chain end that can be easily coupled to

a primary amine for bioconjugation or surface functionalization. Control over the molar mass and molar mass dispersity is limited though, and high monomer conversions are virtually unattainable.

ATRP has proven a more versatile technique for the synthesis of glycopolymer architectures with poly(acrylate) and poly(methacrylate) backbone: Multi-block copolymers, graft copolymers, multi-arm stars, hyperbranched polymers as well as cylindrical brushes have been successfully prepared by ATRP. Furthermore, Armes *et al.* extended its applicability to unprotected monomers in aqueous or aqueous/alcoholic media [123,124,126], while Fukuda and co. successfully grafted well-defined glycopolymer brushes onto a silicon substrate [110]. In spite of this, several drawbacks to the use of ATRP in glycopolymer synthesis persist:

- i. functional groups likely to deactivate the catalyst (e.g., acid functions) need to be protected during the polymerization process [238];
- ii. achieving a good degree of control in aqueous media is challenging due to the occurrence of several side reactions involving the catalytic system [239]. For instance, in water the  $\text{Cu}^{\text{I}}$ -based ATRP activator may disproportionate; the  $\text{Cu}^{\text{II}}$ -based deactivator is likely to lose its halide ligand; and the alkyl halide initiator may hydrolyze or react with the monomer if it contains basic or nucleophilic groups. In this case, better results are obtained by adding an organic co-solvent (e.g., methanol or DMF) and (or) a  $\text{Cu}^{\text{II}}$  halide complex to the catalyst;
- iii. between 1000 ppm and 10,000 ppm of copper are present in a polymer prepared by classic ATRP and its removal adds to the complexity of the process.

Concerning this last point, huge progress has been recently made thanks to a number of modified ATRP processes: In 2006, Matyjaszewski *et al.* [240] reported an ATRP variation called ARGET (Activators ReGenerated by Electron Transfer), in which the catalyst is continuously regenerated by non-toxic reducing agents like ascorbic acid. They also reported another variation called ICAR (Initiators for Continuous Activator Regeneration), in which radical initiators are used for the same purpose [241]. Both strategies reduce the concentration of copper catalyst needed to 10–50 ppm, *i.e.*, several orders of magnitude lower than in conventional ATRP. The results disclosed by Rosen and Percec [242] in 2006 were even more spectacular: In their Single-Electron Transfer Living Radical Polymerization technique (SET-LRP) elemental copper activates the polymerization and is converted to a  $\text{Cu}^{\text{I}}$  intermediate in the process. A spontaneous disproportionation of the intermediate, mediated by environmentally friendly solvents such as water or alcohols, then generates the  $\text{Cu}^{\text{II}}$  deactivator. Thanks to the higher activity of  $\text{Cu}^0$  in SET-LRP (when compared to the  $\text{Cu}^{\text{I}}$  species used in classic ATRP) only tens-of-ppm of it is needed, about the same range as in ARGET and ICAR. With respect to the latter, SET-LRP offers a number of advantages though: It takes place at room temperature, side reactions are minimized, reaction times are fast, ultra-high molecular weight ( $>10^6 \text{ g mol}^{-1}$ ) polymers can be accessed, both non-activated monomers such as vinyl chloride and activated monomers such as acrylates and methacrylates can be polymerized [243]. Finally, it is amenable to function in aqueous solution [244,245].

RAFT polymerization is a robust and versatile technique that is particularly adapted to the synthesis of glycopolymers: It can be carried out in homogeneous aqueous media, at moderate to ambient temperature, and with monomers carrying complex functional groups. Also, by carefully matching the RAFT agent to the monomer to be polymerized, the RAFT process can control the polymerization of



virtually all monomers amenable to polymerize via a radical chain mechanism. Finally, the RAFT process can be easily conducted under heterogeneous conditions and lead to the preparation of surface-functionalized glyco-nanoparticles [246]. The main problem with polymers synthesized by RAFT is that they bear a thiocarbonylthio-group at their  $\omega$ -end. Since the latter can degrade over time and release some malodorous and toxic sulphur compounds, it should be removed before using the material in its final application. This can be accomplished by radical-induced reduction (e.g., with non-toxic *N*-ethylpiperidine hypophosphite), addition–fragmentation coupling (*i.e.*, heating the RAFT-synthesized polymer with a large excess of a radical initiator) or aminolysis/hydrolysis/ionic reduction, with the latter producing thiol-terminated chains that can be further functionalized/conjugated.

In perspective, RDRP will enable the application of well-defined glycopolymers both *in vitro* and *in vivo*. Materials covered with a suitable glycopolymer have improved biocompatibility [97,99] and, in the case of nanoparticles, can be targeted to a specific organ [10,247,248]. Examples have already emerged of glycopolymer decorated quantum dots [221], and superparamagnetic iron oxide nanoparticles which may be used for *in vivo* imaging and hyperthermia treatment [249]. Magnetic beads featuring glycopolymer grafts on their surface might be used for specific biocapture applications while glycosylated latex particles [122,196] could be used in protein separation and precipitation or, in the case of fluorescent nanoparticles, for cell imaging [181]. The use of glycopolymers from RDRP as free entities *in vivo* shall heed the lessons learned by the development of the first polymer therapeutics [250,251]: More hydrophilic polymers are less likely to bind blood proteins and to be immunogenic; with a few exceptions (copolymerization with a ketene acetal, poly(vinyl ester)s) polymers obtained by radical polymerization are non-biodegradable and molar masses  $\leq 30,000$  Da shall be targeted to ensure renal elimination; a narrow molar mass distribution is essential to establish robust structure-property relationships. Examples in this field include the use of positively charged glycopolymers for the preparation of polyplexes for cell transfection [166,171,225] and GlycoPol™, possibly the first glycopolymer synthesized by RDRP to reach commercial status. Originally based on the work of Haddleton *et al.* [135,143] on the post-polymerization functionalization of well-defined polymethacrylates carrying alkyne groups and, eventually, an  $\alpha$ -chain end group suitable for conjugation, GlycoPol™ is now being developed by PolyTherics as a modular platform for targeted delivery of therapeutics. According to the company website, mono- and polysaccharides as well as fluorescent labels can be attached to the starting polymer backbone in varying density, and the resulting polymer can be conjugated to a therapeutic entity.

## References

1. Horejsi, V.; Smolek, P.; Kocourek, J. Studies on lectins. XXXV. Water-soluble *O*-glycosyl polyacrylamide derivatives for specific precipitation of lectins. *Biochim. Biophys. Acta Gen. Subj.* **1978**, *538*, 293–298.
2. Choi, S.K.; Mammen, M.; Whitesides, G.M. Generation and *in situ* evaluation of libraries of poly(acrylic acid) presenting sialosides as side chains as polyvalent inhibitors of influenza-mediated hemagglutination. *J. Am. Chem. Soc.* **1997**, *119*, 4103–4111.
3. Gordon, E.J.; Strong, L.E.; Kiessling, L.L. Glycoprotein-inspired materials promote the proteolytic release of cell surface l-selectin. *Bioorg. Med. Chem.* **1998**, *6*, 1293–1299.

4. Kiessling, L.L.; Gestwicki, J.E.; Strong, L.E. Synthetic multivalent ligands in the exploration of cell-surface interactions. *Curr. Opin. Chem. Biol.* **2000**, *4*, 696–703.
5. David, A.; Kopeckova, P.; Kopecek, J.; Rubinstein, A. The role of galactose, lactose, and galactose valency in the biorecognition of *N*-(2-hydroxypropyl)methacrylamide copolymers by human colon adenocarcinoma cells. *Pharm. Res.* **2002**, *19*, 1114–1122.
6. Roy, R.; Baek, M.G. Glycodendrimers: Novel glycotopes isosteres unmasking sugar coding. Case study with T-antigen markers from breast cancer MUC1 glycoprotein. *Rev. Mol. Biotechnol.* **2002**, *90*, 291–309.
7. Gambaryan, A.S.; Boravleva, E.Y.; Matrosovich, T.Y.; Matrosovich, M.N.; Klenk, H.D.; Moiseeva, E.V.; Tuzikov, A.B.; Chinarev, A.A.; Pazynina, G.V.; Bovin, N.V. Polymer-bound 6' sialyl-*N*-acetylactosamine protects mice infected by influenza virus. *Antivir. Res.* **2005**, *68*, 116–123.
8. Fleming, C.; Maldjian, A.; Da Costa, D.; Rullay, A.K.; Haddleton, D.M.; John, J.St.; Penny, P.; Noble, R.C.; Cameron, N.R.; Davis, B.G. A carbohydrate-antioxidant hybrid polymer reduces oxidative damage in spermatozoa and enhances fertility. *Nat. Chem. Biol.* **2005**, *1*, 270–274.
9. Palomino, E. Carbohydrate handles as natural resources in drug delivery. *Adv. Drug Deliv. Rev.* **1994**, *13*, 311–323.
10. Wadhwa, M.S.; Rice, K.G. Receptor mediated glycotargeting. *J. Drug Target.* **1995**, *3*, 111–127.
11. Wang, Y.; Zhang, X.; Han, Y.; Cheng, C.; Li, C. pH- and glucose-sensitive glycopolymer nanoparticles based on phenylboronic acid for triggered release of insulin. *Carbohydr. Polym.* **2012**, *89*, 124–131.
12. Song, E.-H.; Manganiello, M.J.; Chow, Y.-H.; Ghosn, B.; Convertine, A.J.; Stayton, P.S.; Schnapp, L.M.; Ratner, D.M. *In vivo* targeting of alveolar macrophages via RAFT-based glycopolymers. *Biomaterials* **2012**, *33*, 6889–6897.
13. Karamuk, E.; Mayer, J.; Wintermantel, E.; Akaike, T. Partially degradable film/fabric composites: Textile scaffolds for liver cell culture. *Artif. Organs* **1999**, *23*, 881–884.
14. Chaikof, E.L.; Grande, D.; Baskaran, S. Glycopolymers and Free Radical Polymerization Methods. U.S. Patent 7,244,830 B2, 17 July 2007.
15. Liu, X.C.; Dordick, J.S. Sugar acrylate-based polymers as chiral molecularly imprintable hydrogels. *J. Polym. Sci. A Polym. Chem.* **1999**, *37*, 1665–1671.
16. Gruber, H.; Knaus, S. Synthetic polymers based on carbohydrates: Preparation, properties and applications. *Macromol. Symp.* **2000**, *152*, 95–105.
17. Baek, M.G.; Roy, R. Design and synthesis of water-soluble glycopolymers bearing breast tumor marker and enhanced lipophilicity for solid-phase assays. *Biomacromolecules* **2000**, *1*, 768–770.
18. Miyata, T.; Urugami, T.; Nakamae, K. Biomolecule-sensitive hydrogels. *Adv. Drug Deliv. Rev.* **2002**, *54*, 79–98.
19. Novick, S.J.; Dordick, J.S. Preparation of active and stable biocatalytic hydrogels for use in selective transformations. *Chem. Mater.* **1998**, *10*, 955–958.
20. Wulff, G.; Schmid, J.; Venhoff, T.P. The preparation of new types of polymerizable vinyl sugars with C–C bonds between sugar and double bond. *Macromol. Chem. Phys.* **1996**, *197*, 1285–1299.

21. Wulff, G.; Zhu, L.; Schmidt, H. Investigations on surface-modified bulk polymers. 1. copolymers of styrene with a styrene moiety containing a sugar monomer. *Macromolecules* **1997**, *30*, 4533–4539.
22. Miyata, T.; Nakamae, K. Polymers with pendent saccharides: “glycopolymers”. *Trends Polym. Sci.* **1997**, *5*, 198–206.
23. Wulff, G.; Schmidt, H.; Zhu, L.M. Generating hydrophilic surfaces on standard polymers after copolymerization with low amounts of protected vinyl sugars. *Macromol. Chem. Phys.* **1999**, *200*, 774–782.
24. Varki, A.; Cummings, R.; Esko, J.; Freeze, H.; Hart, G.; Marth, J. *Essentials of Glycobiology*, 2nd ed.; Cold Spring Harbor Laboratory Press: Cold Spring Harbor, NY, USA, 2009.
25. Whittaker, G.R. Intracellular trafficking of influenza virus: Clinical implications for molecular medicine. *Expert Rev. Mol. Med.* **2001**, *3*, 1–13.
26. Weis, W.; Brown, J.H.; Cusack, S.; Paulson, J.C.; Skehel, J.J.; Wiley, D.C. Structure of the influenza-virus haemagglutinin complexed with its receptor, sialic-acid. *Nature* **1988**, *333*, 426–431.
27. Bertozzi, C.R.; Kiessling, L.L. Chemical glycobiology. *Science* **2001**, *291*, 2357–2364.
28. Vandamme, E.J.; de Baets, S.; Steinbüchel, A. *Polysaccharides I: Polysaccharides from Prokaryotes*; Wiley-VCH: Weinheim, Germany, 2002.
29. Vandamme, E.J.; de Baets, S.; Steinbüchel, A. *Polysaccharides II: Polysaccharides from Eukaryotes*; Wiley-VCH: Weinheim, Germany, 2002.
30. Haddleton, D.M.; Ohno, K. Well-Defined oligosaccharide-terminated polymers from living radical polymerization. *Biomacromolecules* **2000**, *1*, 152–156.
31. Halila, S.; Manguian, M.; Fort, S.; Cottaz, S.; Hamaide, T.; Fleury, E.; Driguez, H. Syntheses of well-defined glyco-polyorganosiloxanes by “click” chemistry and their surfactant properties. *Macromol. Chem. Phys.* **2008**, *209*, 1282–1290.
32. Chiron, S.; Labeau, M.-P.; Fleury, E.; Viet, D.; Cottaz, S.; Driguez, H.; Halila, S. Novel Glycopolymers, Uses Thereof, and Monomers Useful for Preparation Thereof. WO Patent 2006016063 A1, 13 November 2008.
33. Narumi, A.; Miura, Y.; Otsuka, I.; Yamane, S.; Kitajyo, Y.; Satoh, T.; Hirao, A.; Kaneko, N.; Kaga, H.; Kakuchi, T. End-functionalization of polystyrene by malto-oligosaccharide generating aggregation-tunable polymeric reverse micelle. *J. Polym. Sci. A Polym. Chem.* **2006**, *44*, 4864–4879.
34. Houga, C.; Le Meins, J.-F.; Borsali, R.; Taton, D.; Gnanou, Y. Synthesis of ATRP-induced dextran-*b*-polystyrene diblock copolymers and preliminary investigation of their self-assembly in water. *Chem. Commun.* **2007**, 3063–3065.
35. Aissou, K.; Otsuka, I.; Rochas, C.; Fort, S.; Halila, S.; Borsali, R. Nano-Organization of Amylose-*b*-polystyrene block copolymer films doped with bipyridine. *Langmuir* **2011**, *27*, 4098–4103.
36. Bernard, J.; Save, M.; Arathoon, B.; Charleux, B. Preparation of a xanthate-terminated dextran by click chemistry: Application to the synthesis of polysaccharide-coated nanoparticles via surfactant-free ab initio emulsion polymerization of vinyl acetate. *J. Polym. Sci. A Polym. Chem.* **2008**, *46*, 2845–2857.

37. Ghadban, A.; Albertin, L.; Rinaudo, M.; Heyraud, A. Biohybrid glycopolymer capable of ionotropic gelation. *Biomacromolecules* **2012**, *13*, 3108–3119.
38. Sigal, G.B.; Mammen, M.; Dahmann, G.; Whitesides, G.M. Polyacrylamides bearing pendant alpha-sialoside groups strongly inhibit agglutination of erythrocytes by influenza virus—The strong inhibition reflects enhanced binding through cooperative polyvalent interactions. *J. Am. Chem. Soc.* **1996**, *118*, 3789–3800.
39. Kanai, M.; Mortell, K.H.; Kiessling, L.L. Varying the size of multivalent ligands—The dependence of concanavalin A binding on neoglycopolymer length. *J. Am. Chem. Soc.* **1997**, *119*, 9931–9932.
40. Georges, M.K.; Veregin, R.P.N.; Kazmaier, P.M.; Hamer, G.K. Narrow molecular weight resins by a free-radical polymerization process. *Macromolecules* **1993**, *26*, 2987–2988.
41. Kato, M.; Kamigaito, M.; Sawamoto, M.; Higashimura, T. Polymerization of methyl methacrylate with the carbon tetrachloride/dichlorotris- (triphenylphosphine)ruthenium(II)/Methylaluminum Bis(2,6-di-tert-butylphenoxide) initiating System: Possibility of living radical polymerization. *Macromolecules* **1995**, *28*, 1721–1723.
42. Chiefari, J.; Chong, Y.K.; Ercole, F.; Krstina, J.; Jeffery, J.; Le, T.P.T.; Mayadunne, R.T.A.; Meijs, G.F.; Moad, C.L.; Moad, G.; *et al.* Living free-radical polymerization by reversible addition-fragmentation chain transfer—The RAFT process. *Macromolecules* **1998**, *31*, 5559–5562.
43. Matyjaszewski, K.; Davis, T.P. *Handbook of radical polymerization*; John Wiley and Sons, Inc.: Hoboken, NJ, USA, 2002.
44. Lowe, A.B.; McCormick, C.L. Homogeneous controlled free radical polymerization in aqueous media. *Aust. J. Chem.* **2002**, *55*, 367–379.
45. Xia, J.H.; Gaynor, S.G.; Matyjaszewski, K. Controlled/“living” radical polymerization. Atom transfer radical polymerization of acrylates at ambient temperature. *Macromolecules* **1998**, *31*, 5958–5959.
46. Robinson, K.L.; Khan, M.A.; Banez, M.V.D.; Wang, X.S.; Armes, S.P. Controlled polymerization of 2-hydroxyethyl methacrylate by ATRP at ambient temperature. *Macromolecules* **2001**, *34*, 3155–3158.
47. Quinn, J.F.; Rizzardo, E.; Davis, T.P. Ambient temperature reversible addition-fragmentation chain transfer polymerisation. *Chem. Commun.* **2001**, 1044–1045.
48. Moad, G.; Rizzardo, E.; Thang, S.H. Living radical polymerization by the RAFT process. *Aust. J. Chem.* **2005**, *58*, 379–410.
49. Moad, G.; Rizzardo, E.; Thang, S.H. Living radical polymerization by the RAFT process—A first update. *Aust. J. Chem.* **2006**, *59*, 669–692.
50. Moad, G.; Rizzardo, E.; Thang, S.H. Living radical polymerization by the RAFT process—A second update. *Aust. J. Chem.* **2009**, *62*, 1402–1472.
51. Matyjaszewski, K. Atom Transfer Radical Polymerization (ATRP): Current status and future perspectives. *Macromolecules* **2012**, *45*, 4015–4039.
52. Grubbs, R.B. Nitroxide-Mediated radical polymerization: Limitations and versatility. *Polym. Rev.* **2011**, *51*, 104–137.

53. Nicolas, J.; Guillaneuf, Y.; Lefay, C.; Bertin, D.; Gigmes, D.; Charleux, B. Nitroxide-mediated polymerization. *Prog. Polym. Sci.* **2013**, *63*–235.
54. Jenkins, A.D.; Jones, R.G.; Moad, G. Terminology for reversible-deactivation radical polymerization previously called “controlled” radical or “living” radical polymerization (IUPAC Recommendations 2010). *Pure Appl. Chem.* **2010**, *82*, 483–491.
55. Fukuda, T.; Goto, A.; Tsujii, Y. Kinetics of Living Radical Polymerisation. In *Handbook of Radical Polymerization*; Matyjaszewski, K., Davis, T.P., Eds.; John Wiley and Sons, Inc.: Hoboken, NJ, USA, 2002; pp. 407–462.
56. Matyjaszewski, K. General Concepts and History of Living Radical Polymerisation. In *Handbook of Radical Polymerization*; Matyjaszewski, K., Davis, T.P., Eds.; John Wiley and Sons, Inc.: Hoboken, NJ, USA, 2002; pp. 361–406.
57. Miura, Y. Design and synthesis of well-defined glycopolymers for the control of biological functionalities. *Polym. J.* **2012**, *44*, 679–689.
58. Becer, C.R. The glycopolymer code: Synthesis of glycopolymers and multivalent carbohydrate-lectin interactions. *Macromol. Rapid Commun.* **2012**, *33*, 742–752.
59. Spain, S.G.; Cameron, N.R. A spoonful of sugar: The application of glycopolymers in therapeutics. *Polym. Chem.* **2011**, *2*, 60–68.
60. Pearson, S.; Chen, G.; Stenzel, M.H. Synthesis of Glycopolymers. In *Engineered Carbohydrate-Based Materials for Biomedical Applications*; John Wiley & Sons, Inc.: Hoboken, NJ, USA, 2011; pp. 1–118.
61. Voit, B.; Appelhans, D. Glycopolymers of various architectures-more than mimicking nature. *Macromol. Chem. Phys.* **2010**, *211*, 727–735.
62. Ting, S.R.S.; Chen, G.; Stenzel, M.H. Synthesis of glycopolymers and their multivalent recognitions with lectins. *Polym. Chem.* **2010**, *1*, 1392–1412.
63. Zhang, Y.; Wang, J.; Xia, C.; Wang, P.G. Glycopolymers: The Future Antiadhesion Drugs. In *Polymer Biocatalysis and Biomaterials II*; American Chemical Society: Washington, DC, USA, 2008; Volume 999, pp. 342–361.
64. Spain, S.G.; Gibson, M.I.; Cameron, N.R. Recent advances in the synthesis of well-defined glycopolymers. *J. Polym. Sci. A Polym. Chem.* **2007**, *45*, 2059–2072.
65. Rice, K.G.; Kim, J.-S.; Liu, D. Glycopolymer Tools for Studying Targeted Nonviral Gene Delivery. In *Polymeric Gene Delivery Principles and Applications*; Amiji, M.M., Ed.; CRC Press: Punta Gorda, FL, USA, 2005; pp. 509–521.
66. Ladmiraal, V.; Melia, E.; Haddleton, D.M. Synthetic glycopolymers: An overview. *Eur. Polym. J.* **2004**, *40*, 431–449.
67. Okada, M. Molecular design and syntheses of glycopolymers. *Prog. Polym. Sci.* **2001**, *26*, 67–104.
68. Roy, R. Blue-prints, synthesis and applications of glycopolymers. *Trends Glycosci. Glycotechnol.* **1996**, *8*, 79–99.
69. Druliner, J.D. Living radical polymerization involving oxygen-centered species attached to propagating chain ends. *Macromolecules* **1991**, *24*, 6079–6082.
70. Gnanou, Y.; Grande, D.; Guerrero, R. (Meth)Acrylate-based graft copolymers via cyanoxyl-mediated free-radical polymerization. *Polym. Prepr.* **1999**, *40*, 99–100.

71. Grande, D.; Guerrero, R.; Gnanou, Y. Cyanoxy-mediated free-radical polymerization of acrylic acid: Its scope and limitations. *J. Polym. Sci. A Polym. Chem.* **2005**, *43*, 519–533.
72. David, G.; Boyer, C.; Tonnar, J.; Ameduri, B.; Lacroix-Desmazes, P.; Boutevin, B. Use of iodocompounds in radical polymerization. *Chem. Rev.* **2006**, *106*, 3936–3962.
73. Yamago, S. Development of organotellurium-mediated and organostibine-mediated living radical polymerization reactions. *J. Polym. Sci. A Polym. Chem.* **2006**, *44*, 1–12.
74. Goto, A.; Hirai, N.; Nagasawa, K.; Tsujii, Y.; Fukuda, T.; Kaji, H. Phenols and carbon compounds as efficient organic catalysts for reversible chain transfer catalyzed living radical polymerization (RTCP). *Macromolecules* **2010**, *43*, 7971–7978.
75. Kickelbick, G.; Pintauer, T.; Matyjaszewski, K. Structural comparison of Cu-II complexes in atom transfer radical polymerization. *New J. Chem.* **2002**, *26*, 462–468.
76. Baskaran, S.; Grande, D.; Sun, X.L.; Yayon, A.; Chaikof, E.L. Glycosaminoglycan-Mimetic biomaterials. 3. Glycopolymers prepared from alkene-derivatized mono- and disaccharide-based glycomonomers. *Bioconjug. Chem.* **2002**, *13*, 1309–1313.
77. Grande, D.; Baskaran, S.; Baskaran, C.; Gnanou, Y.; Chaikof, E.L. Glycosaminoglycan-mimetic biomaterials. 1. Nonsulfated and sulfated glycopolymers by cyanoxy-mediated free-radical polymerization. *Macromolecules* **2000**, *33*, 1123–1125.
78. Grande, D.; Baskaran, S.; Chaikof, E.L. Glycosaminoglycan mimetic biomaterials. 2. Alkene- and acrylate-derivatized glycopolymers via cyanoxy-mediated free-radical polymerization. *Macromolecules* **2001**, *34*, 1640–1646.
79. Sun, X.L.; Grande, D.; Baskaran, S.; Hanson, S.R.; Chaikof, E.L. Glycosaminoglycan mimetic biomaterials. 4. Synthesis of sulfated lactose-based glycopolymers that exhibit anticoagulant activity. *Biomacromolecules* **2002**, *3*, 1065–1070.
80. Guan, R.; Sun, X.L.; Hou, S.; Wu, P.; Chaikof, E.L. A glycopolymer chaperone for fibroblast growth factor-2. *Bioconjug. Chem.* **2004**, *15*, 145–151.
81. Narla, S.N.; Sun, X.-L. Orientated glyco-macroligand formation based on site-specific immobilization of O-cyanate chain-end functionalized glycopolymer. *Org. Biomol. Chem.* **2011**, *9*, 845–850.
82. Sun, X.-L.; Cui, W.; Haller, C.; Chaikof, E.L. Site-Specific multivalent carbohydrate labeling of quantum dots and magnetic beads. *ChemBioChem* **2004**, *5*, 1593–1596.
83. Hou, S.; Sun, X.-L.; Dong, C.-M.; Chaikof, E.L. Facile synthesis of chain-end functionalized glycopolymers for site-specific bioconjugation. *Bioconjug. Chem.* **2004**, *15*, 954–959.
84. Faucher, K.M.; Sun, X.L.; Chaikof, E.L. Fabrication and characterization of glycocalyx-mimetic surfaces. *Langmuir* **2003**, *19*, 1664–1670.
85. Sun, X.L.; Faucher, K.M.; Houston, M.; Grande, D.; Chaikof, E.L. Design and synthesis of biotin chain-terminated glycopolymers for surface glycoengineering. *J. Am. Chem. Soc.* **2002**, *124*, 7258–7259.
86. Ting, S.R.S.; Min, E.-H.; Escale, P.; Save, M.; Billon, L.; Stenzel, M.H. Lectin recognizable biomaterials synthesized via nitroxide-mediated polymerization of a methacryloyl galactose monomer. *Macromolecules* **2009**, *42*, 9422–9434.

87. Gotz, H.; Harth, E.; Schiller, S.M.; Frank, C.W.; Knoll, W.; Hawker, C.J. Synthesis of lipo-glycopolymer amphiphiles by nitroxide-mediated living free-radical polymerization. *J. Polym. Sci. A Polym. Chem.* **2002**, *40*, 3379–3391.
88. Chen, Y.M.; Wulff, G. Synthesis of poly(styryl sugar)s by TEMPO mediated free radical polymerization. *Macromol. Chem. Phys.* **2001**, *202*, 3426–3431.
89. Chen, Y.M.; Wulff, G. Amphiphilic block copolymers with pendent sugar as hydrophilic segments and their surface properties. *Macromol. Chem. Phys.* **2001**, *202*, 3273–3278.
90. Narumi, A.; Matsuda, T.; Kaga, H.; Satoh, T.; Kakuchi, T. Glycoconjugated polymer II. Synthesis of polystyrene-block-poly(4-vinylbenzyl glucoside) and polystyrene-block-poly(4-vinylbenzyl maltohexaoside) via 2,2,6,6-tetramethylpiperidine-1-oxyl-mediated living radical polymerization. *Polym. J.* **2001**, *33*, 939–945.
91. Narumi, A.; Matsuda, T.; Kaga, H.; Satoh, T.; Kakuchi, T. Synthesis of amphiphilic triblock copolymer of polystyrene and poly(4-vinylbenzyl glucoside) via TEMPO-mediated living radical polymerization. *Polymer* **2002**, *43*, 4835–4840.
92. Narumi, A.; Otsuka, I.; Matsuda, T.; Miura, Y.; Satoh, T.; Kaneko, N.; Kaga, H.; Kakuchi, T. Glycoconjugated polymer: synthesis and characterization of poly(vinyl saccharide)-block-polystyrene-block-poly(vinyl saccharide) as an amphiphilic ABA triblock copolymer. *J. Polym. Sci. A Polym. Chem.* **2006**, *44*, 3978–3985.
93. Ohno, K.; Tsujii, Y.; Miyamoto, T.; Fukuda, T.; Goto, M.; Kobayashi, K.; Akaike, T. Synthesis of a well-defined glycopolymer by nitroxide-controlled free radical polymerization. *Macromolecules* **1998**, *31*, 1064–1069.
94. Ohno, K.; Fukuda, T.; Kitano, H. Free radical polymerization of a sugar residue-carrying styryl monomer with a lipophilic alkoxyamine initiator: Synthesis of a well-defined novel glycolipid. *Macromol. Chem. Phys.* **1998**, *199*, 2193–2197.
95. Miura, Y.; Koketsu, D.; Kobayashi, K. Synthesis and properties of a well-defined glycopolymer via living radical polymerization. *Polym. Adv. Technol.* **2007**, *18*, 647–651.
96. Babiuch, K.; Wyrwa, R.; Wagner, K.; Seemann, T.; Hoepfener, S.; Becer, C.R.; Linke, R.; Gottschaldt, M.; Weisser, J.; Schnabelrauch, M.; *et al.* Functionalized, biocompatible coating for superparamagnetic nanoparticles by controlled polymerization of a thioglycosidic monomer. *Biomacromolecules* **2011**, *12*, 681–691.
97. Babiuch, K.; Becer, C.R.; Gottschaldt, M.; Delaney, J.T.; Weisser, J.; Beer, B.; Wyrwa, R.; Schnabelrauch, M.; Schubert, U.S. Adhesion of Preosteoblasts and fibroblasts onto Poly(pentafluorostyrene)-based glycopolymeric films and their biocompatibility. *Macromol. Biosci.* **2011**, *11*, 535–548.
98. Wild, A.; Babiuch, K.; Konig, M.; Winter, A.; Hager, M.D.; Gottschaldt, M.; Prokop, A.; Schubert, U.S. Synthesis of a glycopolymeric Pt<sup>II</sup> carrier and its induction of apoptosis in resistant cancer cells. *Chem. Commun.* **2012**, *48*, 6357–6359.
99. Becer, C.R.; Babiuch, K.; Pilz, D.; Hornig, S.; Heinze, T.; Gottschaldt, M.; Schubert, U.S. Clicking pentafluorostyrene copolymers: Synthesis, nanoprecipitation, and glycosylation. *Macromolecules* **2009**, *42*, 2387–2394.
100. Narla, S.N.; Sun, X.-L. Immobilized sialyloligo-macroligand and its protein binding specificity. *Biomacromolecules* **2012**, *13*, 1675–1682.

101. Mammen, M.; Choi, S.K.; Whitesides, G.M. Polyvalent interactions in biological systems: Implications for design and use of multivalent ligands and inhibitors. *Angew. Chem. Int. Ed.* **1998**, *37*, 2755–2794.
102. Chaikof, E.L.; Sun, X.L. Multivalent Polymers with Chain-Terminating Binding Groups. WO Patent 2003099835 A1, 4 December 2003.
103. Grande, D.; Baskaran, S.; Chaikof, E.L. Mono- and disaccharide-based glycopolymers by free-radical polymerization processes. *Polym. Mater. Sci. Eng.* **2001**, *84*, 141–142.
104. Yu, K.; Kizhakkedathu, J.N. Synthesis of functional polymer brushes containing carbohydrate residues in the pyranose form and their specific and nonspecific interactions with proteins. *Biomacromolecules* **2010**, *11*, 3073–3085.
105. Chen, Y.M.; Wulff, G. ABA and star amphiphilic block copolymers composed of polymethacrylate bearing a galactose fragment and poly( $\epsilon$ -caprolactone). *Macromol. Rapid Commun.* **2002**, *23*, 59–63.
106. Ke, B.-B.; Wan, L.-S.; Zhang, W.-X.; Xu, Z.-K. Controlled synthesis of linear and comb-like glycopolymers for preparation of honeycomb-patterned films. *Polymer* **2010**, *51*, 2168–2176.
107. Ladmiral, V.; Monaghan, L.; Mantovani, G.; Haddleton, D.M.  $\hat{\pm}$ -Functional glycopolymers: New materials for (poly)peptide conjugation. *Polymer* **2005**, *46*, 8536–8545.
108. Bes, L.; Angot, S.; Limer, A.; Haddleton, D.M. Sugar-coated amphiphilic block copolymer micelles from living radical polymerization: Recognition by immobilized lectins. *Macromolecules* **2003**, *36*, 2493–2499.
109. Ohno, K.; Tsujii, Y.; Fukuda, T. Synthesis of a well-defined glycopolymer by atom transfer radical polymerization. *J. Polym. Sci. A Polym. Chem.* **1998**, *36*, 2473–2481.
110. Ejaz, M.; Ohno, K.; Tsujii, Y.; Fukuda, T. Controlled grafting of a well-defined glycopolymer on a solid surface by surface-initiated atom transfer radical polymerization. *Macromolecules* **2000**, *33*, 2870–2874.
111. Muthukrishnan, S.; Plamper, F.; Mori, H.; Muller, A.H.E. Synthesis and characterization of glycomethacrylate hybrid stars from silsesquioxane nanoparticles. *Macromolecules* **2005**, *38*, 10631–10642.
112. Muthukrishnan, S.; Jutz, G.; Andre, X.; Mori, H.; Muller, A.H.E. Synthesis of hyperbranched glycopolymers via self-condensing atom transfer radical copolymerization of a sugar-carrying acrylate. *Macromolecules* **2005**, *38*, 9–18.
113. Muthukrishnan, S.; Mori, H.; Muller, A.H.E. Synthesis and characterization of methacrylate-type hyperbranched glycopolymers via self-condensing atom transfer radical copolymerization. *Macromolecules* **2005**, *38*, 3108–3119.
114. Muthukrishnan, S.; Zhang, M.; Burkhardt, M.; Drechsler, M.; Mori, H.; Muller, A.H.E. Molecular sugar sticks: Cylindrical glycopolymer brushes. *Macromolecules* **2005**, *38*, 7926–7934.
115. Gao, C.; Muthukrishnan, S.; Li, W.W.; Yuan, J.Y.; Xu, Y.Y.; Muller, A.H.E. Linear and hyperbranched glycopolymer-functionalized carbon nanotubes: Synthesis, kinetics, and characterization. *Macromolecules* **2007**, *40*, 1803–1815.



116. Wang, J.; Qian, Y.; Zhang, F.; Zhu, B.; Xu, Y. Synthesis and self-assembly of amphiphilic ABA type triblock copolymer with well-defined glycopolymer segments. *Chin. Sci. Bull.* **2008**, *53*, 1343–1351.
117. Liang, Y.-Z.; Li, Z.-C.; Chen, G.-Q.; Li, F.-M. Synthesis of well-defined poly[(2- $\beta$ -D-glucopyranosyloxy)ethyl acrylate] by atom transfer radical polymerization. *Polym. Int.* **1999**, *48*, 739–742.
118. You, L.-C.; Lu, F.-Z.; Li, Z.-C.; Zhang, W.; Li, F.-M. Glucose-Sensitive aggregates formed by Poly(ethylene oxide)-block-poly(2-glucosyloxyethyl acrylate) with concanavalin A in dilute aqueous medium. *Macromolecules* **2003**, *36*, 1–4.
119. Dong, C.-M.; Sun, X.-L.; Faucher, K.M.; Apkarian, R.P.; Chaikof, E.L. Synthesis and characterization of glycopolymer-polypeptide triblock copolymers. *Biomacromolecules* **2004**, *5*, 224–231.
120. Dong, C.-M.; Faucher, K.M.; Chaikof, E.L. Synthesis and properties of biomimetic poly(L-glutamate)-b-poly(2-acryloyloxyethyl lactoside)-b-poly(L-glutamate) triblock copolymers. *J. Polym. Sci. A Polym. Chem.* **2004**, *42*, 5754–5765.
121. Pfaff, A.; Muller, A.H.E. Hyperbranched glycopolymer grafted microspheres. *Macromolecules* **2011**, *44*, 1266–1272.
122. Pfaff, A.; Shinde, V.S.; Lu, Y.; Wittmann, A.; Ballauff, M.; Muller, A.H.E. Glycopolymer-grafted polystyrene nanospheres. *Macromol. Biosci.* **2011**, *11*, 199–210.
123. Narain, R.; Armes, S.P. Direct synthesis and aqueous solution properties of well-defined cyclic sugar methacrylate polymers. *Macromolecules* **2003**, *36*, 4675–4678.
124. Narain, R.; Armes, S.P. Synthesis of low polydispersity, controlled-structure sugar methacrylate polymers under mild conditions without protecting group chemistry. *Chem. Commun.* **2002**, 2776–2777.
125. Qiu, S.; Huang, H.; Dai, X.-H.; Zhou, W.; Dong, C.-M. Star-shaped polypeptide/glycopolymer biohybrids: Synthesis, self-assembly, biomolecular recognition, and controlled drug release behavior. *J. Polym. Sci. A Polym. Chem.* **2009**, *47*, 2009–2023.
126. Narain, R.; Armes, S.P. Synthesis and aqueous solution properties of novel sugar methacrylate-based homopolymers and block copolymers. *Biomacromolecules* **2003**, *4*, 1746–1758.
127. Mateescu, A.; Ye, J.; Narain, R.; Vamvakaki, M. Synthesis and characterization of novel glycosurfaces by ATRP. *Soft Matter* **2009**, *5*, 1621–1629.
128. Kitano, H.; Saito, D.; Kamada, T.; Gemmei-Ide, M. Binding of  $\beta$ -amyloid to sulfated sugar residues in a polymer brush. *Colloids Surf. B* **2012**, *93*, 219–225.
129. Fleet, R.; van den Dungen, E.T.A.; Klumperman, B. Novel glycopolymer brushes via ATRP: 1. synthesis and characterization. *Macromol. Chem. Phys.* **2011**, *212*, 2191–2208.
130. Narain, R. Tailor-made protein-glycopolymer bioconjugates. *React. Funct. Polym.* **2006**, *66*, 1589–1595.
131. Yang, Q.; Ulbricht, M. Cylindrical membrane pores with well-defined grafted linear and comblike glycopolymer layers for lectin binding. *Macromolecules* **2011**, *44*, 1303–1310.

132. O'Connell, M.A.; de Cuendias, A.; Gayet, F.; Shirley, I.M.; Mackenzie, S.R.; Haddleton, D.M.; Unwin, P.R. Evanescent Wave Cavity Ring-Down Spectroscopy (EW-CRDS) as a probe of macromolecule adsorption kinetics at functionalized interfaces. *Langmuir* **2012**, *28*, 6902–6910.
133. Xu, L.Q.; Huang, C.; Wang, R.; Neoh, K.-G.; Kang, E.-T.; Fu, G.D. Synthesis and characterization of fluorescent perylene bisimide-containing glycopolymers for Escherichia coli conjugation and cell imaging. *Polymer* **2011**, *52*, 5764–5771.
134. Kitano, H.; Takahashi, Y.; Mizukami, K.; Matsuura, K. Kinetic study on the binding of lectin to mannose residues in a polymer brush. *Colloids Surf. B* **2009**, *70*, 91–97.
135. Geng, J.; Mantovani, G.; Tao, L.; Nicolas, J.; Chen, G.; Wallis, R.; Mitchell, D.A.; Johnson, B.R.G.; Evans, S.D.; Haddleton, D.M. Site-Directed conjugation of “clicked” glycopolymers to form glycoprotein mimics: Binding to mammalian lectin and induction of immunological function. *J. Am. Chem. Soc.* **2007**, *129*, 15156–15163.
136. Vazquez-Dorbatt, V.; Maynard, H.D. Biotinylated glycopolymers synthesized by atom transfer radical polymerization. *Biomacromolecules* **2006**, *7*, 2297–2302.
137. Vazquez-Dorbatt, V.; Tolstyka, Z.P.; Chang, C.-W.; Maynard, H.D. Synthesis of a pyridyl disulfide end-functionalized glycopolymer for conjugation to biomolecules and patterning on gold surfaces. *Biomacromolecules* **2009**, *10*, 2207–2212.
138. Leon, O.; Bordege, V.; Munoz-Bonilla, A.; Sanchez-Chaves, M.; Fernandez-Garcia, M. Well-controlled amphiphilic block glycopolymers and their molecular recognition with lectins. *J. Polym. Sci. A Polym. Chem.* **2010**, *48*, 3623–3631.
139. Leon, O.; Munoz-Bonilla, A.; Bordege, V.; Sanchez-Chaves, M.; Fernandez-Garcia, M. Amphiphilic block glycopolymers via atom transfer radical polymerization: Synthesis, self-assembly and biomolecular recognition. *J. Polym. Sci. A Polym. Chem.* **2011**, *49*, 2627–2635.
140. Munoz-Bonilla, A.; Heuts, J.P.A.; Fernandez-Garcia, M. Glycoparticles and bioactive films prepared by emulsion polymerization using a well-defined block glycopolymer stabilizer. *Soft Matter* **2011**, *7*, 2493–2499.
141. De, L.A.S.; Munoz-Bonilla, A.; Fernandez-Garcia, M.; Rodriguez-Hernandez, J. Breath figures method to control the topography and the functionality of polymeric surfaces in porous films and microspheres. *J. Polym. Sci. A Polym. Chem.* **2012**, *50*, 851–859.
142. Menon, S.; Das, S. A photoresponsive fluorescent glycopolymer. *Polym. Chem.* **2012**, *3*, 2619–2624.
143. Ladmiral, V.; Mantovani, G.; Clarkson, G.J.; Cauet, S.; Irwin, J.L.; Haddleton, D.M. Synthesis of neoglycopolymers by a combination of “click chemistry” and living radical polymerization. *J. Am. Chem. Soc.* **2006**, *128*, 4823–4830.
144. Richards, S.-J.; Jones, M.W.; Hunaban, M.; Haddleton, D.M.; Gibson, M.I. Probing bacterial-toxin inhibition with synthetic glycopolymers prepared by tandem post-polymerization modification: Role of linker length and carbohydrate density. *Angew. Chem. Int. Ed.* **2012**, *51*, 7812–7816.
145. Gou, Y.; Slavin, S.; Geng, J.; Voorhaar, L.; Haddleton, D.M.; Becer, C.R. Controlled alternate layer-by-layer assembly of lectins and glycopolymers using QCM-D. *ACS Macro Lett.* **2011**, *1*, 180–183.

146. Houga, C.; Giermanska, J.; Lecommandoux, S.; Borsali, R.; Taton, D.; Gnanou, Y.; Le, M.J.-F. Micelles and polymersomes obtained by self-assembly of dextran and polystyrene based block copolymers. *Biomacromolecules* **2009**, *10*, 32–40.
147. Yu, K.; Lai, B.F.L.; Kizhakkedathu, J.N. Carbohydrate structure dependent hemocompatibility of biomimetic functional polymer brushes on surfaces. *Adv. Healthc. Mater.* **2012**, *1*, 199–213.
148. Fleet, R.; van den Dungen, E.T.A.; Klumperman, B. Novel glycopolymer brushes via ATRP: 2. thermal and mechanical properties. *Macromol. Chem. Phys.* **2011**, *212*, 2209–2216.
149. Fleet, R.; van den Dungen, E.T.A.; Klumperman, B. Synthesis of novel glycopolymer brushes via a combination of RAFT-mediated polymerization and ATRP. *S. Afr. J. Sci.* **2011**, *107*, 101–111.
150. Yuan, J.; Meng, J.-Q.; Kang, Y.-L.; Du, Q.-Y.; Zhang, Y.-F. Facile surface glycosylation of PVDF microporous membrane via direct surface-initiated AGET ATRP and improvement of antifouling property and biocompatibility. *Appl. Surf. Sci.* **2012**, *258*, 2856–2863.
151. Meng, J.; Yuan, J.; Kang, Y.; Zhang, Y.; Du, Q. Surface glycosylation of polysulfone membrane towards a novel complexing membrane for boron removal. *J. Colloid Interface Sci.* **2012**, *368*, 197–207.
152. Hardy, J.; Selkoe, D.J. The amyloid hypothesis of Alzheimer's disease: Progress and problems on the Road to therapeutics. *Science* **2002**, *297*, 353–356.
153. Kohri, M.; Sato, M.; Abo, F.; Inada, T.; Kasuya, M.; Taniguchi, T.; Nakahira, T. Preparation and lectin binding specificity of polystyrene particles grafted with glycopolymers bearing S-linked carbohydrates. *Eur. Polym. J.* **2011**, *47*, 2351–2360.
154. Becer, C.R.; Gibson, M.I.; Geng, J.; Ilyas, R.; Wallis, R.; Mitchell, D.A.; Haddleton, D.M. High-Affinity glycopolymer binding to human DC-SIGN and disruption of DC-SIGN interactions with HIV envelope glycoprotein. *J. Am. Chem. Soc.* **2010**, *132*, 15130–15132.
155. Gou, Y.; Richards, S.-J.; Haddleton, D.M.; Gibson, M.I. Investigation of glycopolymer-lectin interactions using QCM-d: Comparison of surface binding with inhibitory activity. *Polym. Chem.* **2012**, *3*, 1634–1640.
156. Geng, J.; Biedermann, F.; Zayed, J.M.; Tian, F.; Scherman, O.A. Supramolecular glycopolymers in water: A reversible route toward multivalent carbohydrate-lectin conjugates using Cucurbit[8]uril. *Macromolecules* **2011**, *44*, 4276–4281.
157. Muñoz-Bonilla, A.; León, O.; Cerrada, M.L.; Rodríguez-Hernández, J.; Sánchez-Chaves, M.; Fernández-García, M. Glycopolymers obtained by chemical modification of well-defined block copolymers. *J. Polym. Sci. A Polym. Chem.* **2012**, *50*, 2565–2577.
158. Gody, G.; Boullanger, P.; Ladaviere, C.; Charreyre, M.T.; Delair, T. Biotin alpha-end-functionalized gradient glycopolymers synthesized by RAFT copolymerization. *Macromol. Rapid Commun.* **2008**, *29*, 511–519.
159. Su, L.; Zhao, Y.; Chen, G.; Jiang, M. Polymeric vesicles mimicking glycocalyx (PV-Gx) for studying carbohydrate-protein interactions in solution. *Polym. Chem.* **2012**, *3*, 1560–1566.
160. Wei, Z.; Hao, X.; Gan, Z.; Hughes, T.C. One-pot synthesis of hyperbranched glycopolymers by RAFT polymerization. *J. Polym. Sci. A Polym. Chem.* **2012**, *50*, 2378–2388.
161. Ozyurek, Z.; Komber, H.; Gramm, S.; Schmaljohann, D.; Muller, A.H.E.; Voit, B. Thermoresponsive glycopolymers via controlled radical polymerization. *Macromol. Chem. Phys.* **2007**, *208*, 1035–1049.

162. Jiang, X.; Housni, A.; Gody, G.; Boullanger, P.; Charreyre, M.-T.; Delair, T.; Narain, R. Synthesis of Biotinylated  $\alpha$ -d-Mannoside or *N*-Acetyl  $\beta$ -D-Glucosaminoside decorated gold nanoparticles: Study of their biomolecular recognition with ConA and WGA lectins. *Bioconjug. Chem.* **2010**, *21*, 521–530.
163. Belardi, B.; O'Donoghue Geoff, P.; Smith Adam, W.; Groves Jay, T.; Bertozzi Carolyn, R. Investigating cell surface galectin-mediated cross-linking on glycoengineered cells. *J. Am. Chem. Soc.* **2012**, *134*, 9594–9552.
164. Toyoshima, M.; Oura, T.; Fukuda, T.; Matsumoto, E.; Miura, Y. Biological specific recognition of glycopolymer- modified interfaces by RAFT living radical polymerization. *Polym. J.* **2009**, *42*, 172–178.
165. Deng, Z.; Ahmed, M.; Narain, R. Novel well-defined glycopolymers synthesized via the reversible addition fragmentation chain transfer process in aqueous media. *J. Polym. Sci. A Polym. Chem.* **2009**, *47*, 614–627.
166. Ahmed, M.; Narain, R. The effect of polymer architecture, composition, and molecular weight on the properties of glycopolymer-based non-viral gene delivery systems. *Biomaterials* **2011**, *32*, 5279–5290.
167. Ahmed, M.; Lai, B.F.L.; Kizhakkedathu, J.N.; Narain, R. Hyperbranched glycopolymers for blood biocompatibility. *Bioconjug. Chem.* **2012**, *23*, 1050–1058.
168. Ahmed, M.; Narain, R. The effect of molecular weight, compositions and lectin type on the properties of hyperbranched glycopolymers as non-viral gene delivery systems. *Biomaterials* **2012**, *33*, 3990–4001.
169. Bernard, J.; Hao, X.J.; Davis, T.P.; Barner-Kowollik, C.; Stenzel, M.H. Synthesis of various glycopolymer architectures via RAFT polymerization: From block copolymers to stars. *Biomacromolecules* **2006**, *7*, 232–238.
170. Ting, S.R.S.; Min, E.H.; Zetterlund, P.B.; Stenzel, M.H. Controlled/Living *ab initio* emulsion polymerization via a glucose RAFTstab: degradable cross-linked glyco-particles for concanavalin A/FimH conjugations to cluster *E. coli* bacteria. *Macromolecules* **2010**, *43*, 5211–5221.
171. Smith, A.E.; Sizovs, A.; Grandinetti, G.; Xue, L.; Reineke, T.M. Diblock glycopolymers promote colloidal stability of polyplexes and effective pDNA and siRNA delivery under physiological salt and serum conditions. *Biomacromolecules* **2011**, *12*, 3015–3022.
172. Abdelkader, O.; Moebis-Sanchez, S.; Queneau, Y.; Bernard, J.; Fleury, E. Generation of well-defined clickable glycopolymers from aqueous RAFT polymerization of isomaltulose-derived acrylamides. *J. Polym. Sci. A Polym. Chem.* **2011**, *49*, 1309–1318.
173. Albertin, L.; Wolnik, A.; Ghadban, A.; Dubreuil, F. Aqueous RAFT Polymerization of *N*-Acryloylmorpholine, synthesis of an ABA triblock glycopolymer and study of its self-association behavior. *Macromol. Chem. Phys.* **2012**, *213*, 1768–1782.
174. Miura, Y.; Mizuno, H. Interaction analyses of amyloid  $\beta$  peptide (1–40) with glycosaminoglycan model polymers. *Bull. Chem. Soc. Jpn.* **2010**, *83*, 1004–1009.
175. Toyoshima, M.; Miura, Y. Preparation of glycopolymer-substituted gold nanoparticles and their molecular recognition. *J. Polym. Sci. A Polym. Chem.* **2009**, *47*, 1412–1421.

176. Ishii, J.; Toyoshima, M.; Chikae, M.; Takamura, Y.; Miura, Y. Preparation of glycopolymer-modified gold nanoparticles and a new approach for a lateral flow assay. *Bull. Chem. Soc. Jpn.* **2011**, *84*, 466–470.
177. Al-Bagoury, M.; Buchholz, K.; Yaacoub, E.J. Synthesis of well-designed polymers carrying saccharide moieties via RAFT miniemulsion polymerization. *Polym. Adv. Technol.* **2007**, *18*, 313–322.
178. Lowe, A.B.; Wang, R. Synthesis of controlled-structure AB diblock copolymers of 3-*O*-methacryloyl-1,2:3,4-di-*O*-isopropylidene-D-galactopyranose and 2-(dimethylamino)ethyl methacrylate. *Polymer* **2007**, *48*, 2221–2230.
179. Ting, S.R.S.; Gregory, A.M.; Stenzel, M.H. Polygalactose containing nanocages: The RAFT process for the synthesis of hollow sugar balls. *Biomacromolecules* **2009**, *10*, 342–352.
180. Liu, L.; Zhang, J.; Lv, W.; Luo, Y.; Wang, X. Well-defined pH-sensitive block glycopolymers via reversible addition-fragmentation chain transfer radical polymerization: Synthesis, characterization, and recognition with lectin. *J. Polym. Sci. A Polym. Chem.* **2010**, *48*, 3350–3361.
181. Pfaff, A.; Schallon, A.; Ruhland, T.M.; Majewski, A.P.; Schmalz, H.; Freitag, R.; Muller, A.H.E. Magnetic and fluorescent glycopolymer hybrid nanoparticles for intranuclear optical imaging. *Biomacromolecules* **2011**, *12*, 3805–3811.
182. Shi, H.; Liu, L.; Wang, X.; Li, J. Glycopolymer-peptide bioconjugates with antioxidant activity via RAFT polymerization. *Polym. Chem.* **2012**, *3*, 1182–1188.
183. Luo, Y.; Liu, L.; Wang, X.; Shi, H.; Lv, W.; Li, J. Sugar-installed thermoresponsive micellar aggregates self-assembled from “coil-comb-coil” triblock glycopolymers: Preparation and recognition with Concanavalin A. *Soft Matter* **2012**, *8*, 1634–1642.
184. Glassner, M.; Delaittre, G.; Kaupp, M.; Blinco, J.P.; Barner-Kowollik, C. (Ultra)Fast catalyst-free macromolecular conjugation in aqueous environment at ambient temperature. *J. Am. Chem. Soc.* **2012**, *134*, 7274–7277.
185. Kaupp, M.; Vogt, A.P.; Natterodt, J.C.; Trouillet, V.; Gruending, T.; Hofe, T.; Barner, L.; Barner-Kowollik, C. Modular design of glyco-microspheres via mild pericyclic reactions and their quantitative analysis. *Polym. Chem.* **2012**, *3*, 2605–2614.
186. Dan, K.; Ghosh, S. pH-Responsive Aggregation of amphiphilic glyco-homopolymer. *Macromol. Rapid Commun.* **2012**, *33*, 127–132.
187. Guo, T.Y.; Liu, P.; Zhu, J.W.; Song, M.D.; Zhang, B.H. Well-Defined lactose-containing polymer grafted onto silica particles. *Biomacromolecules* **2006**, *7*, 1196–1202.
188. Zhou, D.; Li, C.; Hu, Y.; Zhou, H.; Chen, J.; Zhang, Z.; Guo, T. Glycopolymer modification on physicochemical and biological properties of poly(l-lysine) for gene delivery. *Int. J. Biol. Macromol.* **2012**, *50*, 965–973.
189. Spain, S.G.; Albertin, L.; Cameron, N.R. Facile *in situ* preparation of biologically active multivalent glyconanoparticles. *Chem. Commun.* **2006**, 4198–4200.
190. Housni, A.; Cai, H.J.; Liu, S.Y.; Pun, S.H.; Narain, R. Facile preparation of glyconanoparticles and their bioconjugation to streptavidin. *Langmuir* **2007**, *23*, 5056–5061.
191. Lowe, A.B.; Sumerlin, B.S.; McCormick, C.L. The direct polymerization of 2-methacryloxyethyl glucoside via aqueous reversible addition-fragmentation chain transfer (RAFT) polymerization. *Polymer* **2003**, *44*, 6761–6765.

192. Pearson, S.; Scarano, W.; Stenzel, M.H. Micelles based on gold-glycopolymer complexes as new chemotherapy drug delivery agents. *Chem. Commun.* **2012**, *48*, 4695–4697.
193. Albertin, L.; Stenzel, M.H.; Barner-Kowollik, C.; Foster, L.J.R.; Davis, T.P. Well-defined diblock glycopolymers from RAFT polymerization in homogeneous aqueous medium. *Macromolecules* **2005**, *38*, 9075–9084.
194. Albertin, L.; Stenzel, M.H.; Barner-Kowollik, C.; Davis, T.P. Effect of an added base on (4-cyanopentanoic acid)-4-dithiobenzoate mediated RAFT polymerization in water. *Polymer* **2006**, *47*, 1011–1019.
195. Albertin, L.; Stenzel, M.; Barner-Kowollik, C.; Foster, L.J.R.; Davis, T.P. Well-defined glycopolymers from RAFT polymerization: Poly(methyl 6-*O*-methacryloyl- $\alpha$ -D-glucoside) and its block copolymer with 2-hydroxyethyl methacrylate. *Macromolecules* **2004**, *37*, 7530–7537.
196. Pfaff, A.; Barner, L.; Muller, A.H.E.; Granville, A.M. Surface modification of polymeric microspheres using glycopolymers for biorecognition. *Eur. Polym. J.* **2011**, *47*, 805–815.
197. Granville, A.M.; Quemener, D.; Davis, T.P.; Barner-Kowollik, C.; Stenzel, M.H. Chemo-enzymatic synthesis and RAFT polymerization of 6-*O*-methacryloyl mannose: a suitable glycopolymer for binding to the tetrameric lectin concanavalin A? *Macromol. Symp.* **2007**, *255*, 81–89.
198. Albertin, L.; Kohlert, C.; Stenzel, M.; Foster, L.J.R.; Davis, T.P. Chemoenzymatic synthesis of narrow-polydispersity glycopolymers: Poly(6-*O*-vinyladipoyl-D-glucopyranose). *Biomacromolecules* **2004**, *5*, 255–260.
199. Bernard, J.; Favier, A.; Zhang, L.; Nilasaroya, A.; Davis, T.P.; Barner-Kowollik, C.; Stenzel, M.H. Poly(vinyl ester) star polymers via xanthate-mediated living radical polymerization: From poly(vinyl alcohol) to glycopolymer stars. *Macromolecules* **2005**, *38*, 5475–5484.
200. Hetzer, M.; Chen, G.; Barner-Kowollik, C.; Stenzel, M.H. Neoglycopolymers based on 4-vinyl-1,2,3-triazole monomers prepared by click chemistry. *Macromol. Biosci.* **2010**, *10*, 119–126.
201. Xiao, N.-Y.; Li, A.-L.; Liang, H.; Lu, J. A Well-defined novel aldehyde-functionalized glycopolymer: synthesis, micelle formation, and its protein immobilization. *Macromolecules* **2008**, *41*, 2374–2380.
202. Xiao, N.; Liang, H.; Lu, J. Degradable and biocompatible aldehyde-functionalized glycopolymer conjugated with doxorubicin via acid-labile Schiff base linkage for pH-triggered drug release. *Soft Matter* **2011**, *7*, 10834–10840.
203. Wang, J.; Zhu, X.; Cheng, Z.; Zhang, Z.; Zhu, J. Preparation, characterization, and chiral recognition of optically active polymers containing pendent chiral units via reversible addition-fragmentation chain transfer polymerization. *J. Polym. Sci. A Polym. Chem.* **2007**, *45*, 3788–3797.
204. Mancini, R.J.; Lee, J.; Maynard, H.D. Trehalose glycopolymers for stabilization of protein conjugates to environmental stressors. *J. Am. Chem. Soc.* **2012**, *134*, 8474–8479.
205. Boyer, C.; Bousquet, A.; Rondolo, J.; Whittaker, M.R.; Stenzel, M.H.; Davis, T.P. Glycopolymer decoration of gold nanoparticles using a lbl approach. *Macromolecules* **2010**, *43*, 3775–3784.
206. Boyer, C.; Davis, T.P. One-pot synthesis and biofunctionalization of glycopolymers via RAFT polymerization and thiol-ene reactions. *Chem. Commun.* **2009**, 6029–6031.
207. Boyer, C.; Whittaker, M.; Davis, T.P. Synthesis and postfunctionalization of well-defined star polymers via “double” click chemistry. *J. Polym. Sci. A Polym. Chem.* **2011**, *49*, 5245–5256.

208. Semsarilar, M.; Ladmiral, V.; Perrier, S. Highly branched and hyperbranched glycopolymers via reversible addition-fragmentation chain transfer polymerization and click chemistry. *Macromolecules* **2010**, *43*, 1438–1443.
209. Chen, Y.; Chen, G.; Stenzel, M.H. Synthesis and lectin recognition of glyco star polymers prepared by “Clicking” thiocarbohydrates onto a reactive scaffold. *Macromolecules* **2010**, *43*, 8109–8114.
210. Kumar, J.; Bousquet, A.; Stenzel, M.H. Thiol-alkyne chemistry for the preparation of micelles with glycopolymer corona: Dendritic surfaces versus linear glycopolymer in their ability to bind to lectins. *Macromol. Rapid Commun.* **2011**, *32*, 1620–1626.
211. Alidedeoglu, A.H.; York, A.W.; Rosado, D.A.; McCormick, C.L.; Morgan, S.E. Bioconjugation of -glucuronic acid sodium salt to well-defined primary amine-containing homopolymers and block copolymers. *J. Polym. Sci. A Polym. Chem.* **2010**, *48*, 3052–3061.
212. Godula, K.; Bertozzi, C.R. Density variant glycan microarray for evaluating cross-linking of mucin-like glycoconjugates by lectins. *J. Am. Chem. Soc.* **2012**, *134*, 15732–15742.
213. Narain, R.; Housni, A.; Gody, G.; Boullanger, P.; Charreyre, M.-T.; Delair, T. Preparation of biotinylated glyconanoparticles via a photochemical process and study of their bioconjugation to streptavidin. *Langmuir* **2007**, *23*, 12835–12841.
214. Saricilar, S.; Knott, R.; Barner-Kowollik, C.; Davis, T.P.; Heuts, J.P.A. Reversible addition fragmentation chain transfer polymerization of 3-[tris(trimethylsilyloxy) silyl] propyl methacrylate. *Polymer* **2003**, *44*, 5169–5176.
215. Barner-Kowollik, C.; Buback, M.; Charleux, B.; Coote, M.L.; Drache, M.; Fukuda, T.; Goto, A.; Klumperman, B.; Lowe, A.B.; McLeary, J.B.; *et al.* Mechanism and kinetics of dithiobenzoate-mediated RAFT polymerization. I. The current situation. *J. Polym. Sci. A Polym. Chem.* **2006**, *44*, 5809–5831.
216. Konkolewicz, D.; Hawket, B.S.; Gray-Weale, A.; Perrier, S. RAFT polymerization kinetics: Combination of Apparently conflicting models. *Macromolecules* **2008**, *41*, 6400–6412.
217. Konkolewicz, D.; Hawket, B.S.; Gray-Weale, A.; Perrier, S. RAFT polymerization kinetics: How long are the cross-terminating oligomers? *J. Polym. Sci. A Polym. Chem.* **2009**, *47*, 3455–3466.
218. Ting, S.R.S.; Davis, T.P.; Zetterlund, P.B. Retardation in RAFT polymerization: Does cross-termination occur with short radicals only? *Macromolecules* **2011**, *44*, 4187–4193.
219. Yang, H.; Guo, T.-Y.; Zhou, D. Surface hydrophilic modification with well-defined glycopolymer for protein imprinting matrix. *Int. J. Biol. Macromol.* **2011**, *48*, 432–438.
220. Stenzel, M.H.; Zhang, L.; Huck, W.T.S. Temperature-responsive glycopolymer brushes synthesized via RAFT polymerization using the Z-group approach. *Macromol. Rapid Commun.* **2006**, *27*, 1121–1126.
221. Jiang, X.; Ahmed, M.; Deng, Z.; Narain, R. Biotinylated glyco-functionalized quantum dots: Synthesis, characterization, and cytotoxicity studies. *Bioconjug. Chem.* **2009**, *20*, 994–1001.
222. Ishii, J.; Chikae, M.; Toyoshima, M.; Ukita, Y.; Miura, Y.; Takamura, Y. Electrochemical assay for saccharide-protein interactions using glycopolymer-modified gold nanoparticles. *Electrochem. Commun.* **2011**, *13*, 830–833.

223. Miura, Y.; Yasuda, K.; Yamamoto, K.; Koike, M.; Nishida, Y.; Kobayashi, K. Inhibition of alzheimer amyloid aggregation with sulfated glycopolymers. *Biomacromolecules* **2007**, *8*, 2129–2134.
224. Min, E.H.; Ting, S.R.S.; Billon, L.; Stenzel, M.H. Thermo-responsive glycopolymer chains grafted onto honeycomb structured porous films via RAFT polymerization as a thermo-dependent switcher for lectin Concanavalin a conjugation. *J. Polym. Sci. A Polym. Chem.* **2010**, *48*, 3440–3455.
225. Buckwalter, D.J.; Sizovs, A.; Ingle, N.P.; Reineke, T.M. MAG versus PEG: Incorporating a Poly(MAG) layer to promote colloidal stability of nucleic acid/“click cluster” complexes. *ACS Macro Lett.* **2012**, *1*, 609–613.
226. Albertin, L.; Cameron, N.R. RAFT Polymerization of Methyl 6-*O*-Methacryloyl- $\alpha$ -D-glucoside in homogeneous aqueous medium. A detailed kinetic study at the low molecular weight limit of the process. *Macromolecules* **2007**, *40*, 6082–6093.
227. Cheng, C.; Zhang, X.; Wang, Y.; Li, C. Synthesis of glucose-sensitive block glycopolymers based on phenylboronic acid via raft polymerization. *J. Control. Release* **2011**, *152*, e267–e269.
228. Chiellini, E.; Corti, A.; D’Antone, S.; Solaro, R. Biodegradation of poly (vinyl alcohol) based materials. *Prog. Polym. Sci.* **2003**, *28*, 963–1014.
229. DeMerlis, C.C.; Schoneker, D.R. Review of the oral toxicity of polyvinyl alcohol (PVA). *Food Chem. Toxicol.* **2003**, *41*, 319–326.
230. Nikolaev, A.F.; Mosyagina, L.P. Poly(vinyl alcohol) and vinyl alcohol copolymers in medicine. *Int. Polym. Sci. Technol.* **2000**, *27*, T/47–T/58.
231. Yamaoka, T.; Tabata, Y.; Ikada, Y. Comparison of body distribution of poly(vinyl alcohol) with other water-soluble polymers after intravenous administration. *J. Pharm. Pharmacol.* **1995**, *47*, 479–486.
232. Frush, H.L.; Isbell, H.S. Mutorotation, hydrolysis, and structure of D-galactosamine. *J. Res. Natl. Bur. Stand.* **1951**, *47*, 239–247.
233. Brusseau, S.; D’Agosto, F.; Magnet, S.; Couvreur, L.; Chamignon, C.; Charleux, B. Nitroxide-Mediated copolymerization of methacrylic acid and sodium 4-styrenesulfonate in water solution and one-pot synthesis of amphiphilic block copolymer nanoparticles. *Macromolecules* **2011**, *44*, 5590–5598.
234. Phan, T.N.T.; Bertin, D. Synthesis of water-soluble homopolymers and block copolymers in homogeneous aqueous solution via nitroxide-mediated polymerization. *Macromolecules* **2008**, *41*, 1886–1895.
235. Rigolini, J.; Grassl, B.; Billon, L.; Reynaud, S.; Donard, O.F.X. Microwave-assisted nitroxide-mediated radical polymerization of acrylamide in aqueous solution. *J. Polym. Sci. A Polym. Chem.* **2009**, *47*, 6919–6931.
236. Rigolini, J.; Grassl, B.; Reynaud, S.; Billon, L. Microwave-assisted nitroxide-mediated polymerization for water-soluble homopolymers and block copolymers synthesis in homogeneous aqueous solution. *J. Polym. Sci. A Polym. Chem.* **2010**, *48*, 5775–5782.
237. Chenal, M.; Mura, S.; Marchal, C.; Gimes, D.; Charleux, B.; Fattal, E.; Couvreur, P.; Nicolas, J. Facile synthesis of innocuous comb-shaped polymethacrylates with PEG side chains by nitroxide-mediated radical polymerization in hydroalcoholic solutions. *Macromolecules* **2010**, *43*, 9291–9303.



238. Ashford, E.J.; Naldi, V.; O'Dell, R.; Billingham, N.C.; Armes, S.P. First example of the atom transfer radical polymerisation of an acidic monomer: Direct synthesis of methacrylic acid copolymers in aqueous media. *Chem. Commun.* **1999**, *14*, 1285–1286.
239. Tsarevsky, N.V.; Matyjaszewski, K. “Green” atom transfer radical polymerization: From process design to preparation of well-defined environmentally friendly polymeric materials. *Chem. Rev.* **2007**, *107*, 2270–2299.
240. Jakubowski, W.; Matyjaszewski, K. Activators regenerated by electron transfer for atom-transfer radical polymerization of (meth)acrylates and related block copolymers. *Angew. Chem. Int. Ed.* **2006**, *45*, 4482–4486.
241. Matyjaszewski, K.; Jakubowski, W.; Min, K.; Tang, W.; Huang, J.; Braunecker, W.A.; Tsarevsky, N.V. Diminishing catalyst concentration in atom transfer radical polymerization with reducing agents. *Proc. Natl. Acad. Sci. USA* **2006**, *103*, 15309–15314.
242. Rosen, B.M.; Percec, V. Single-Electron transfer and single-electron transfer degenerative chain transfer living radical polymerization. *Chem. Rev.* **2009**, *109*, 5069–5119.
243. Percec, V.; Guliashvili, T.; Ladislaw, J.S.; Wistrand, A.; Stjern Dahl, A.; Sienkowska, M.J.; Monteiro, M.J.; Sahoo, S. Ultrafast synthesis of ultrahigh molar mass polymers by metal-catalyzed living radical polymerization of acrylates, methacrylates, and vinyl chloride mediated by SET at 25 °C. *J. Am. Chem. Soc.* **2006**, *128*, 14156–14165.
244. Nicol, E.; Derouineau, T.; Puaud, F.; Zaitsev, A. Synthesis of double hydrophilic poly(ethylene oxide)-b-poly(2-hydroxyethyl acrylate) by single-electron transfer-living radical polymerization. *J. Polym. Sci. A Polym. Chem.* **2012**, *50*, 3885–3894.
245. Voepel, J.; Edlund, U.; Albertsson, A.C. A versatile single-electron-transfer mediated living radical polymerization route to galactoglucomannan graft-copolymers with tunable hydrophilicity. *J. Polym. Sci. A Polym. Chem.* **2011**, *49*, 2366–2372.
246. Zetterlund, P.B.; Kagawa, Y.; Okubo, M. Controlled/Living radical polymerization in dispersed systems. *Chem. Rev.* **2008**, *108*, 3747–3794.
247. Vyas, S.P.; Singh, A.; Sihorkar, V. Ligand-receptor-mediated drug delivery: An emerging paradigm in cellular drug targeting. *Crit. Rev. Ther. Drug Carrier Syst.* **2001**, *18*, 1–76.
248. Jones, M.N. Carbohydrate-mediated liposomal targeting and drug delivery. *Adv. Drug Deliv. Rev.* **1994**, *13*, 215–249.
249. Muñoz-Bonilla, A.; Marcelo, G.; Casado, C.; Teran, F.J.; Fernández-García, M. Preparation of glycopolymer-coated magnetite nanoparticles for hyperthermia treatment. *J. Polym. Sci. A Polym. Chem.* **2012**, *50*, 5087–5096.
250. Duncan, R. Development of HPMA copolymer-anticancer conjugates: Clinical experience and lessons learnt. *Adv. Drug Deliv. Rev.* **2009**, *61*, 1131–1148.
251. Duncan, R. The dawning era of polymer therapeutics. *Nat. Rev. Drug Discov.* **2003**, *2*, 347–360.